Polymer Testing 121 (2023) 107995

Contents lists available at ScienceDirect

Polymer Testing

journal homepage: www.elsevier.com/locate/polytest

Crystallization, morphology and self-assembly of double, triple and tetra crystalline block polymers

Jordana K. Palacios [a,**], Rose Mary Michell [b,c,***], Alejandro J. Müller [d,e,*]

[a] Fundación Centro Tecnológico Miranda de Ebro (CTME), Departamento de I+D Materiales, Miranda de Ebro, 09200, Burgos, Spain
[b] School of Chemical Sciences & Engineering, Yachay Tech University, Urcuquí, 100119, Ecuador
[c] Institut für Physik, Martin-Luther-Universität Halle-Wittenberg, 06099, Halle, Germany
[d] POLYMAT and Department of Advanced Polymers and Materials: Physics, Chemistry and Technology, Faculty of Chemistry, University of the Basque Country UPV/EHU, Paseo Manuel de Lardizabal 3, 20018, Donostia-San Sebastián, Spain
[e] IKERBASQUE, Basque Foundation for Science, Plaza Euskadi 5, Bilbao, 48009, Spain

ARTICLE INFO

Keywords:
Block copolymer
Polymer crystallization
Multiple crystalline phases

ABSTRACT

This review compiles a comprehensive analysis of the crystallization behaviour and self-assembly of block copolymers with up to four potentially crystallizable phases. It covers the recent advances in block copolymer crystallization, focusing on several factors that affect the development of crystalline structures: melt strength, thermal transitions, cooling conditions, chemical nature, composition, and molecular architectures, such as linear, multiblocks, stars, and combs, as well as nanofillers and other additives. Block copolymers with different blocks can exhibit double, triple, and tetra crystalline structures. Following the crystallization behaviour of four different crystalline phases is very complex and relays on the interplay of the different blocks and the crystallization conditions. The self-assembly of four lamellar crystals is a unique structure with featured properties at the nanoscale. Depending on the segregation strength, the crystalline morphology can be either driven by phase separation resulting from polymer crystallization or set by a microdomain melt structure. Mixed lamellar arrangement in 3D spherulitic microscale structures or well-separated crystalline microdomains can be developed. The crystallization phenomena in block copolymers include enhanced nucleation, plasticizing and antiplasticizing effects, fractionation, and soft and hard confinement. The crystallization kinetics is highly influenced by the chain dynamics of each block. Star block copolymers exhibit either enhanced or retarded crystallization rates depending on block position. Other external compounds, such as plasticizers and nanofillers, may enhance the crystallizability of block copolymers.

1. Introduction

Polymer crystallization is a complex process [1–6], and it is determined by both thermodynamics and kinetics. The polymer chain has to accomplish the minimum thermodynamics requirements, that is to say, stereoregularity, the existence of equivalent points within the structure, as well as the ability to crystallize during the corresponding time scale. In some cases, the polymer architecture, like in copolymers, stars, and dendrites, among others, could increase the complexity of polymer crystallization. For example, in block copolymers, the presence of a chemically different phase could lead to an increase or even suppression of the crystallization, all depending on the relation between the crystalline behaviour of the samples and their transition temperatures [7–12].

In the case of linear diblock copolymers with only one crystallizable block, the crystallization will be affected by the following:

1. Miscibility in the melt state
2. The glass transition temperature of the amorphous block
3. Molecular architecture
4. The presence of a third component, for example, a nucleating agent, filler, or reinforcement.

* Corresponding author. POLYMAT and Department of Advanced Polymers and Materials: Physics, Chemistry and Technology, Faculty of Chemistry, University of the Basque Country UPV/EHU, Paseo Manuel de Lardizabal 3, 20018, Donostia-San Sebastián, Spain.
** Corresponding author.
*** Corresponding author. School of Chemical Sciences & Engineering, Yachay Tech University, Urcuquí, 100119, Ecuador.
E-mail addresses: jordanapalacios@ctme.es (J.K. Palacios), rose.michell-uribe@physik.uni-halle.de (R.M. Michell), alejandrojesus.muller@ehu.es (A.J. Müller).

https://doi.org/10.1016/j.polymertesting.2023.107995
Received 17 January 2023; Received in revised form 27 February 2023; Accepted 10 March 2023
Available online 13 March 2023

5. The crystallization conditions and the crystallization kinetics of the crystallizable block.

The miscibility in the melt is one of the most influential factors that affect the crystallization of copolymers, depending on the relationship between the order-disorder transition temperature (T_{ODT}), the crystallization temperature (especially of the block with the highest crystallization temperature) and the glass transition (of the amorphous block) the crystallization could progress within microdomains (MD) or in a single phase melt.

A diblock copolymer system will develop different specific morphologies according to five possibilities [12–20]:

1. Homogeneous melt, $T_{ODT} < T_c > T_g$. In this case, during cooling, the crystallization happens before the phase separation, and the amorphous block is rubbery, so typically, the crystallization occurs without restriction, and the amorphous block is trapped between the crystalline lamellae. Spherulites of the semi-crystalline block are typically observed.
2. Weakly segregated systems, $T_{ODT} > T_c > T_g$ with soft confinement. For this system, phase separation happens before crystallization, but the strength of the repulsion between phases is low. Also, the amorphous block is rubbery, the crystallization process overcomes the phase separation, and the block morphology is similar to that obtained upon cooling from a homogeneous melt (i.e., spherulites or axialites).
3. Weakly segregated systems, $T_{ODT} > T_c < T_g$ with hard confinement. For this system, phase separation happens before crystallization, but the strength of the repulsion between phases is low. The amorphous block is a glassy block; nevertheless, as the segregation strength is weak, the crystal growth will break the segregated MDs [21]. This phenomenon is called break-out. It occurs because crystallization overrides the phase-segregated morphology that existed previously in the melt. Once again, crystalline superstructures could be observed, like spherulite or axialites, although they may be distorted, depending on the segregation strength.
4. Strongly segregated systems, $T_{ODT} > T_c > T_g$ with soft confinement. In this case, and when the segregation strength is very high, even with a rubbery block, the crystallization will happen inside the MDs. No crystalline superstructures like spherulites or axialites will be observed as the crystallization occurs confined within the micro phase segregated MDs.
5. Strongly segregated systems, $T_{ODT} > T_c < T_g$ with hard confinement. In this case, the crystallization will always take place inside the MDs.

The aforementioned factors influence the crystallization of block copolymers with more than one crystallizable block. However, other features arise, like the nature of the block that crystallizes first, as well as the crystallization conditions and the crystallization kinetics of each block. In this case, additional variables contribute to the possibility of crystallization of the others blocks present in the copolymer. For instance, in some diblock copolymers, employing a slow cooling rate to crystallize the first block provides enough time to form nuclei and crystallites of this block enhancing the microphase separation due to crystallization. As a consequence, the crystallization of the second block is accelerated [22]. In addition, not only the crystallization rate but also the isothermal crystallization temperature of the first block may also have an influence. At higher T_c the segregation of MD due to first-block crystallization is more favored, and the domains of the second block become larger, enhancing its subsequent crystallization, and increasing its crystallization rate [23]. Moreover, crystallization kinetics experiments conducted on block copolymers with two or three crystalline blocks under different crystallization protocols, have demonstrated that the crystallization rate of the blocks is affected by crystallization protocols employed and different effects can be observed such as plasticizing, nucleating effect, antiplasticizing and confinement. For instance, if the crystallization of the first block creates a rigid confinement and the segregation of the MD is favored, the crystallization kinetics of the second block can become faster. However, under a soft confinement, the crystallization kinetics of the second block can be slowed down [24,25].

When more than one block crystallizes, the crystals can form separately and independently from one another, and their crystalline unit cells will be similar to the ones obtained in bulk. In that case, the crystallization could be sequential, with two clearly different processes, or coincidental, where the crystallization occurs at a similar temperature. However, depending on the crystallization temperatures, chemical nature, and architecture, among others, blocks could also crystallize in a single crystalline phase that is isomorphic or isodimorphic.

Block copolymer crystallization has been recently reviewed, with special emphasis on the morphology and crystalline properties of strongly segregated (or confined) linear systems with at least one or two crystalline phases [13,16,26–28]. However, the differences in molecular architecture, melt miscibility, and the presence of potential multi-crystalline phases increases the complexity of the crystallization behaviour of these materials. The aim of this work is to review the recent literature (from 2017) on the morphology, crystalline properties, and crystallization kinetics of block copolymers with multiple crystallizable phases, focusing on the interplay of the different blocks, their miscibility and architecture as linear, stars and brushes, and the influence of others significant factors, such as additives, nucleating agents, end groups or templates. The intent is to summarize the typical trends in the crystallization process of multi-crystalline block copolymers.

2. Linear double crystalline ab and aba diblock and triblock copolymers

2.1. Linear double crystalline diblock and triblock copolymers of poly (thiophene)s

The poly(thiophene) family and its copolymers [29–38] represent the group of all-conjugated polymers more researched over the past decades. Semiconductor/dielectric conjugated polymers are mainly destinated to optoelectronic devices such as light-emitting diodes, photovoltaic cells, and organic field-effect transistors [30]. The optoelectronic properties are closely related to molecular packing, self-assembly, and nanoscale morphology. Thus, controlling the molecular stacking, crystallization behaviour, and substrate orientation is of major importance. These systems are microphase separated, and their properties are tuned as a function of the type of blocks. Fig. 1 describes some diblock copolymers based on poly(3-hexylthiophene) (P3HT). The P3HT copolymers have been widely investigated because of their high charge carrier mobility and excellent solution processability [29–35].

Different crystalline assemblies are observed in poly(3-hexylthiophene) (P3HT)-*b*-PEG (P3HT-*b*-PEG) and P3HT-*b*-PEG-*b*-P3HT diblock and triblock copolymers when crystalized in a poor solvent, such as *p*-xylene or a good solvent, such as *o*-dichlorobenzene [29]. A vertical and stratified networked microstructure is formed by highly-crystalline nanofibrils in the presence of p-xylene. The PEG and the P3HT blocks are liquid-liquid phase separated in solution. A marginal solvent like *p*-xylene is able to induce solution crystallization of P3HT chains. The P3HT block is able to phase separate and crystallize after aging in the solvent. After P3HT crystallization, a casting step induced the crystallization of the PEG block. However, in order to crystallize, the PEG block must be at a free end, as in a diblock copolymer. The fibrillar structures are a result of the solution crystallization of the P3HT chains. Then, when the PEG chains start to crystallize, a second phase separation takes place and expels the P3HT nanofibrils to the thin film surface forming the stratified fibrillar morphology (see Fig. 2a). XPS testing demonstrated that the surface layer of the film is enriched with sulfur from the P3HT block.

At the same time, GIXRD measurements confirmed the high crystallinity and ordering of the P3HT nanofibrils and the edge-on lamellar

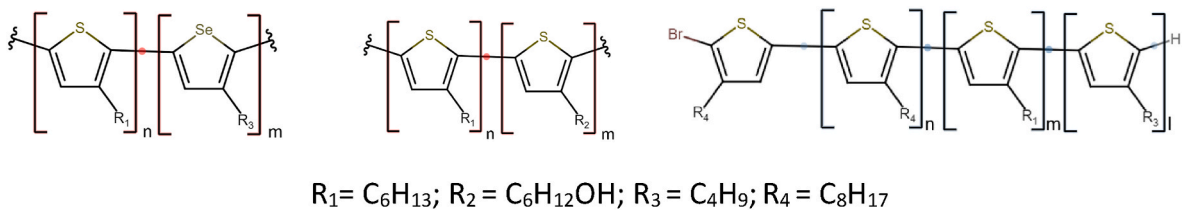

Fig. 1. Chemical structure of several P3HT diblock and triblock copolymers. Taken and modified from [30,32,33,39].

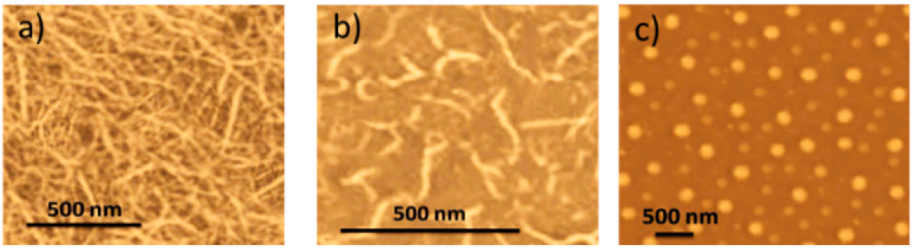

Fig. 2. Different morphological assemblies of P3HT-b-PEG and P3HT-b-PEG-b-P3HT diblock and triblock copolymers. a) PEG5000-b-P3HT50000 b) P3HT50000-b-PEG6000-b-P3HT50000, c) PEG5000-b-P3HT8000. Taken and modified from [29].

growth of the PEG block (i.e., the c-axis of the PEG crystals is parallel to the surface). However, if the PEG block cannot crystallize, the P3HT nanofibril crystals do not form a networked microstructure and do not remain at the surface but are dispersed in the PEG amorphous phase (see Fig. 2b). The ability of the PEG block to crystallize is constrained when the PEG M_w is too low or when PEG constitutes the middle block in a triblock copolymer. Attached to two neighboring rigid P3HT blocks prevents the PEG chains from arranging into crystalline lamellar structures. When *o*-dichlorobenzene is employed, a non-fibrillar morphology is formed by the P3HT block as very low crystallinity granules (see Fig. 2c). The PEG block crystallization during the spin coating step induces this discrete granular morphology for the P3HT block. However, if the PEG block is too short or in the middle of a triblock copolymer, neither the P3HT nor the PEG phases are able to crystallize, and a featureless phase-separated morphology is observed.

Cui et al. [30] reported the crystallization of all-conjugated rod–rod poly(3-hexylthiophene)-*b*-poly[3-(6-hydroxy)hexylthiophene] (P3HT-*b*-P3HHT) [30]. The assembly behaviour and rod-rod interactions were tuned by employing different pure solvents and their blends (i.e., methanol/pyridine or chloroform/pyridine). In pure pyridine, a double crystalline morphology was found by GIXRD after solvent casting the sample if the P3HT-*b*-P3HHT diblock copolymer ratio is 1:1 or higher. A schematic representation is described in Fig. 3 (left). The solvent is selective for the P3HHT block, which means it is a good solvent for P3HHT and a nonsolvent for P3HT. A fibrillar morphology is created first by the P3HT block, then, the P3HHT block crystallizes during casting. As the length of the P3HT block increases, the rod-rod interactions become stronger, and the crystallization of the P3HT block is promoted, further driven by the evaporation step. On the contrary, methanol is a poor solvent for both blocks but poorer for P3HT. In a mixed solvent solution with 40:60 methanol/pyridine ratio, both blocks crystallized. Finally, chloroform is a solvent selective for the P3HT block. In a solvent mixture of chloroform and pyridine, a double crystalline morphology is also promoted in 30:70 and 60:40 solutions. Evidences of the double crystalline nature are given by the 1D GIXRD profiles shown in Fig. 3 (right).

The Poly(3-hexylthiophene)-*b*-(polyperylene bisimide) (P3HT-*b*-PPBI) diblock copolymers [31] are phase separated in the molten state,

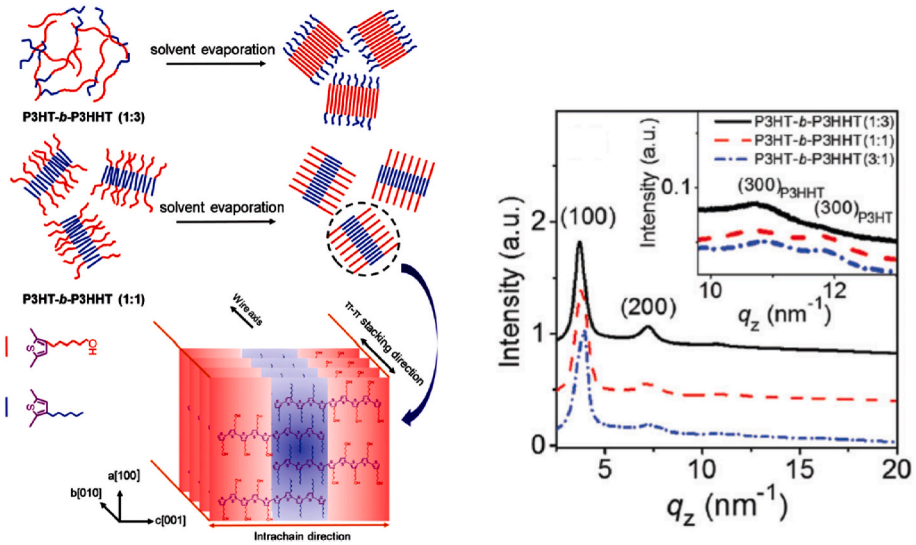

Fig. 3. (left) schematic representation of P3HT-b-P3HHT copolymers in the pyridine solution and solid state. (right) 1D GIXRD profiles. Taken and modified from [30].

exhibiting an ordered cylindrical morphology, as confirmed by SAXS. The high-order peaks are located at a ratio of 1:√3:2, which is in agreement with a hexagonal lattice of cylindrical microdomains (see Fig. 4, left). AFM and TEM analysis further confirmed the cylindrical arrangement. Since the PPBI content is higher (i.e., 73%), the morphology observed corresponded to dark P3HT cylinders inside a bright PPBI matrix (see Fig. 4, centre). This morphology prevails after the subsequent crystallization of each block on the outside and inside of the cylindrical morphology. A confined crystallization of the P3HT cylinders took place without disrupting the morphology created in the melt. DSC traces exhibited only one crystallization and one melting peak at 140 and 222 °C, respectively, corresponding to the P3HT block. However, WAXS measurements confirmed the subsequent crystallization of both blocks upon cooling from the melt (see Fig. 4b)., first the PPBI block at 180 °C and then the P3HT block at 150 °C in a confined fashion [31].

In casted thin films of poly(3-hexylthiophene)-*block*-poly(3-butylselenophene) (P3HT-*b*-P3BS) diblock copolymers [32], a more complex behaviour takes place as these blocks can co-crystallize as a function of composition and thermal treatment (i.e., annealing). P3HT and P3BS have similar structures (see Fig. 1) that provide enhanced optoelectronic properties. At higher P3HT content (63%), only the P3HT block could crystallize in the casted films. However, at intermediate compositions (P3HT:P3BS = 55:45 and 42:58), both blocks are able to crystallize individually. More interestingly, a co-crystallization phenomenon is induced in these intermediate diblock copolymers after annealing at 200 °C. Only one diffraction peak of the (010) planes was observed. The co-crystals grew with an edge-on orientation. If the annealing temperature is further increased up to 230 °C, the co-crystallization disappears, and independent crystals of both blocks remain. These observations were detected by 2D-GIXRD (see Fig. 5). Taking as reference the crystalline structures of the homopolymers, the 2D-GIXRD analysis exhibited the diffraction peaks of the P3HT form I crystal and P3BS form II crystals. In the 55:45 and 42:58 P3HT-*b*-P3BS diblock copolymers with higher P3BS content, both blocks exhibited the diffraction peaks corresponding to the individual P3HT crystals and P3BS form II crystals with the edge-on orientation [32]. Sequential crystallization takes place after phase separation induced by solvent evaporation. The P3BS block crystallizes or precipitates first from the toluene solution, as P3BS is less soluble in this solvent than P3HT, later, the P3HT block crystallizes. After annealing at 200 °C, both blocks co-crystalize, and it is possible to observe a transition from P3BS form II crystals to form I crystals. Interestingly, despite co-crystallization confirmed by 2D-GIXRD, the DSC heating scan of the annealed 55:45 and 42:58 P3HT-*b*-P3BS diblock copolymers at 200 °C exhibited two melting peaks [32], which is unexpected since co-crystals usually melt in a single peak.

The P3HT block has also been copolymerized with poly{(*N*,*N*′-bis(2-octyldecyl)-1,4,5,8-naphthalene-dicarboximide-2,6-diyl]-alt5,5′-(2,2′-bithiophene)} [33], referred to as PNDIT2. Both blocks are able to crystallize in highly oriented thin film structures by modifying the crystallization, orientation, and annealing conditions. Epitaxial crystallization induced the formation of crystalline structures with different chain orientations. Under this condition, only the P3HT block could crystallize, and it did it in a mixture of face-on and edge-on crystals, as revealed in electron diffraction patterns. In order to create a preferential orientation, a mechanical rubbing is imposed on the samples, and then, they are further annealed (See Ref. [33] for further details).

Interestingly, the mechanically oriented samples were double crystalline (see Fig. 6), as proven by the electron diffraction patterns that show the corresponding reflections of (100) PNDIT2 and (100) P3HT planes for each block. The dominant orientation of the crystals was face-on the substrate. The crystal orientation can be modified by changing the conditions. Increasing the temperature of the mechanical rubbing promotes an edge-on orientation of the P3HT crystals while the PNDIT2 remains face-on. A posterior annealing of the sample induced an edge-on configuration of both blocks [33].

The orientation and crystallization conditions also induce the polymorphism of the PNDIT2 block. Increasing the annealing temperature (from 100 to 250 °C) of epitaxially crystallized samples induces a transition from the form I face-on crystals to form II edge-on crystals. Similar observations were obtained with an increment of the mechanical rubbing temperature. A mix of edge-on and face-on form II PNDIT2

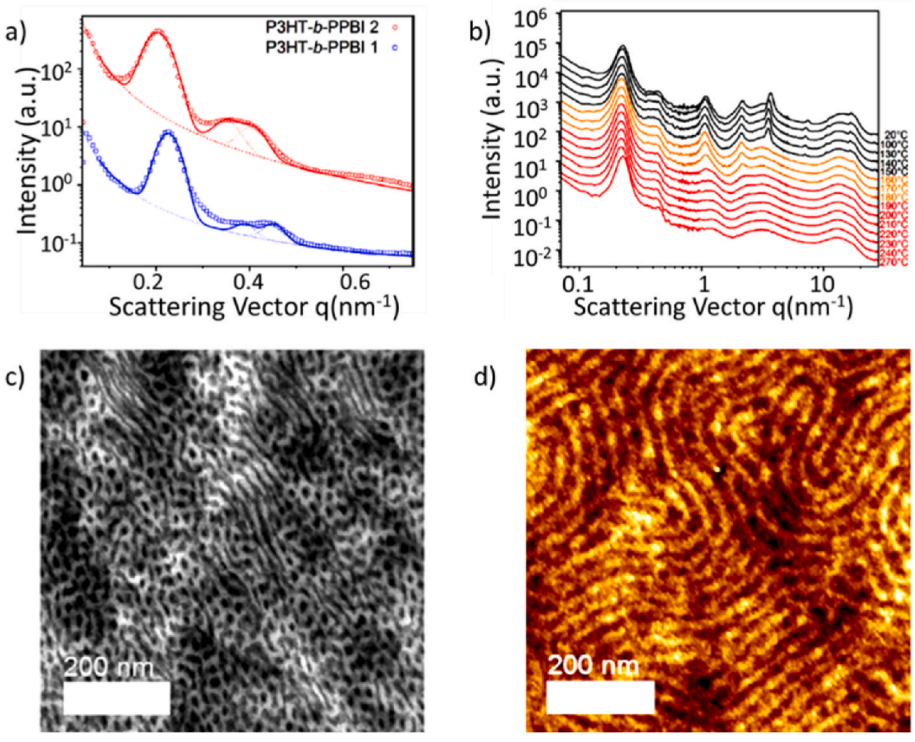

Fig. 4. SAXS, TEM, AFM, and WAXS measurements of P3HT-b-PPBI diblock copolymer with 72% of PPBI block (P3HT-b-PPBI 1). Taken and modified from [31].

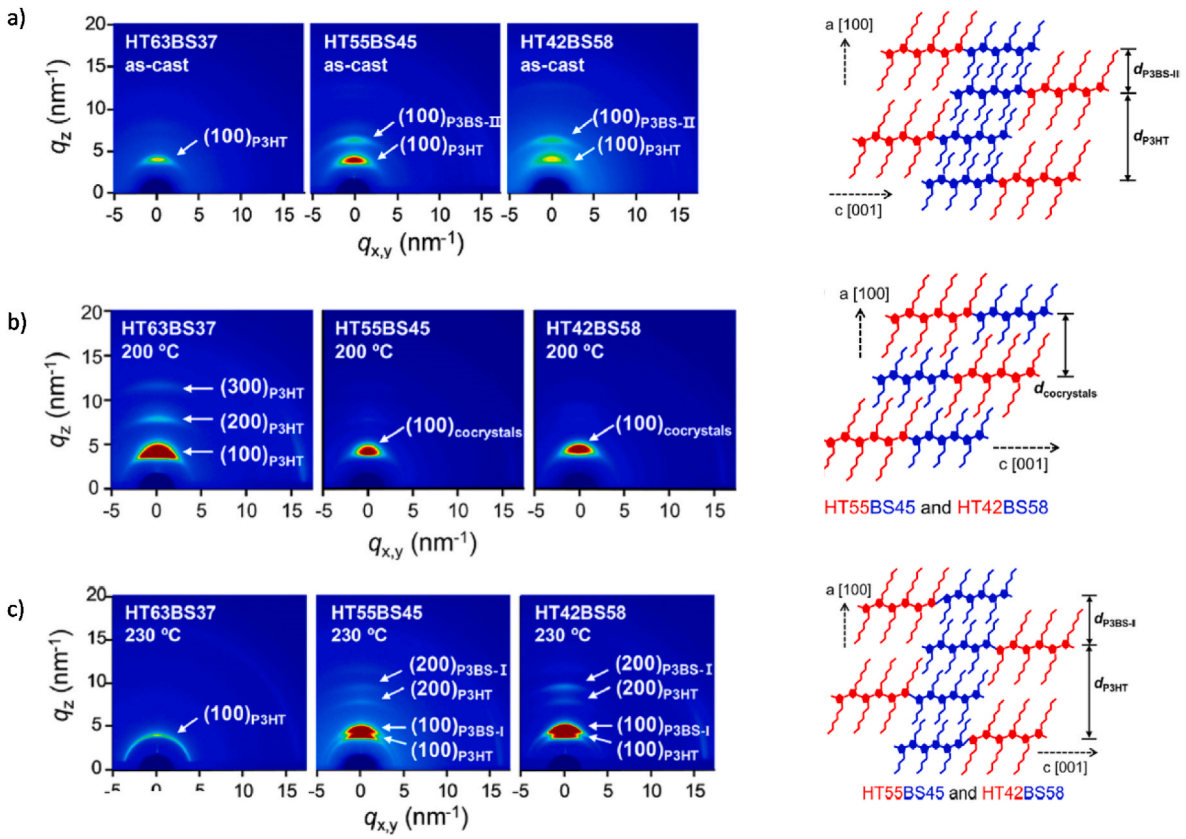

Fig. 5. 2D-GIXRD images of the P3HT-b-P3BS diblock copolymers with different HT:BS ratios: a) as cast, b) after annealing at 200 °C, and c) after annealing at 230 °C. On the left, schematic representation of the chain packing. Taken and modified from [32].

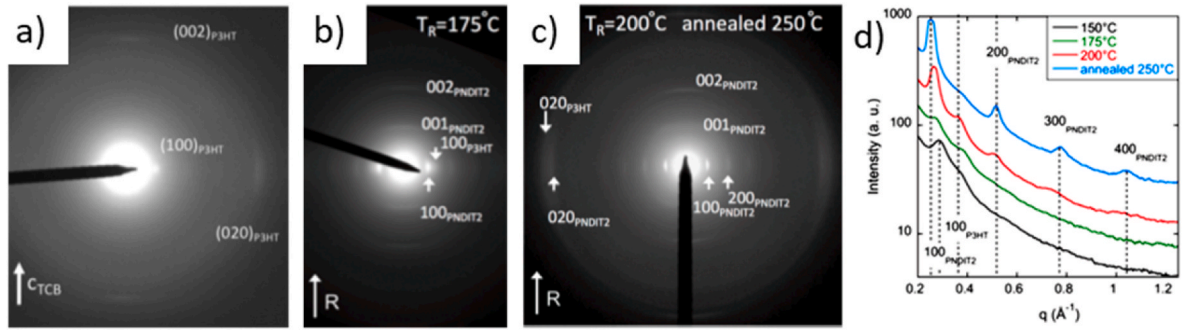

Fig. 6. Electron diffraction patterns of P3HT-b-PNDIT2 diblock copolymer films: a) Epitaxial crystallization, b) mechanical rubbing orientation and c) mechanical rubbing orientation with subsequent annealing treatment. d) Plot profiles of the ED patterns. Taken and modified from [33].

crystals was observed when the rubbing temperature employed was 200 °C, and the annealing temperature was 250 °C. Furthermore, the crystallization of the PNDIT2 block constrained the crystallization of the P3HT block, as the lattice of the P3HT crystals substantially expanded. The final lamellar morphology is of major importance in tuning the charge transport properties [33].

The P3HT has also been copolymerized in triblock architectures with several other blocks, such as poly(3-butylthiophene) (P3BT), poly(3-octylthiophene) (P3OT), or poly(3-dodecylthiophene) (P3DDT) [39]. By combining several blocks in an ABC-type triblock copolymer with different sequences, the microphase separation, crystallinity, co-crystallization, and charge transport properties can be modulated. Fig. 7 displays a schematic representation of block arrangement in these triblock copolymers [39].

These samples were cast from chloroform solutions and annealed at 150 °C. In this way, crystals grew with an edge-on orientation. The 2D-

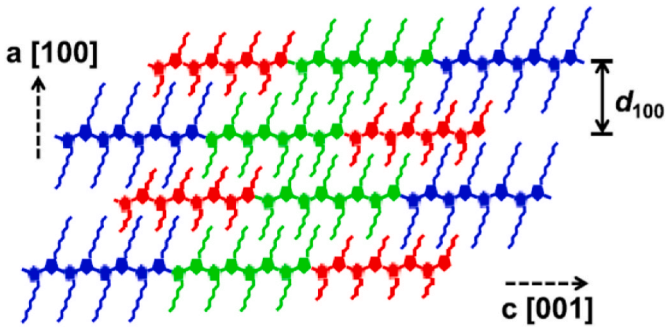

Fig. 7. Schematic representation of chain arrangement in cocrystals in P3HT triblock copolymers. Taken and modified from [39].

GIXRD experiments demonstrated that in these triblock copolymers, the blocks were co-crystallized, particularly when chloroform was used. For instance, blocks such as P3HT and P3BT are prone to co-crystallize. However, if the solvent for casting is changed to trichlorobenzene, microphase separation takes place in some copolymers, and the blocks cannot co-crystallize due to differences in the solvent affinity of the blocks.

Moreover, the DSC thermal properties of these copolymers, such as T_m, T_c, and crystallinity, reduced as the length of the alkyl side chains increased, which is a consequence of the increased chain mobility. This effect is even more critical if the block with the highest alkyl side chain length is located in the centre of the triblock, as it provides more mobility to the shortest end blocks. On the contrary, a short alkyl chain in the middle block improved the crystallinity, ultimately improving the charge carrier mobilities. The annealing conditions may destroy the co-crystallized morphology, and phase separation might take place to form separated crystals. The ability of co-crystallization or phase separation is highly influenced by the architecture of the copolymers and the types of blocks. When the two blocks susceptible to co-crystallize are neighbours, and the block with the longest alkyl side chain is at the end of the triblock copolymer, the chain mobility is not sufficiently restricted, and therefore, phase separation takes place, and blocks crystallize independently. On the contrary, if the two blocks that are able to co-crystallize are in the end and the middle block has a side chain length that is not much longer than the other two end blocks, then the co-crystallized structure remains even under strong annealing conditions.

2.2. Linear double crystalline diblock and triblock copolymers of polyethylene (PE)

Block copolymers containing polyethylene (PE) and other olefins have been of great interest over the last decades [40–45]. Being one of the most useful polymers, copolymerizing PE with other comonomers allows expanding the properties of PE and enlarges its already enormous range of applications in different sectors such as packaging, textile, aircraft, and automotive. Therefore, the crystallization behaviour of block copolymers, including PE and other comonomers such as PS, PLLA, PDLA, PEP, PCL, PEO, and PPL [46–59], has been extensively investigated over the past decades. More recently, Da Rosa et al. have been investigating the crystallization of melt-segregated block copolymers of PE, particularly in epitaxial crystallization. More recently, they have reported new studies on the crystallization of polyethylene-*b*-polypropylene (PE-*b*-PP) diblock copolymers [40,41,60], in which the PP block can be syndiotactic (sPP) or isotactic (iPP). The premise is to follow the epitaxial crystallization onto different substrates, such as crystals of *p*-terphenyl (3Ph) and benzoic acid (BA). The aim of epitaxial crystallization is to induce a preferential orientation of the crystals on a substrate or to promote the crystallization of certain polymorphic forms. The double crystalline nature of these block copolymers has been confirmed by DSC and XRD. A melt-separated structure was observed depending on composition. For instance, cylindrical PE microdomains are observed in an iPP matrix. However, the melt structure is weak as it is destroyed by the crystallization of the blocks as long as the cooling rate is slow. Both PP and PE can crystallize in the same range of temperatures, and the epitaxial crystallization drives the phase separation into an alternated lamellar arrangement of PE and iPP lamellae in the solid state. But, if the cooling rate is fast, the melt structure prevails, and the PE block is forced to crystallize inside microdomains. The iPP matrix only developed a mesomorphic form due to the quenching [40]. In the BA substrate, a double orientation of iPP lamellae and an alignment of PE lamellae were observed. On the other hand, in the 3Ph substrate, the crystalline lamellae are highly oriented along one direction [41]. Structural nanopatterns can be designed at the nanoscale by controlling the crystallization process and the alignment of the microdomains.

Other interesting PE-like block copolymers have been reported by Zapsas et al. [61], such as polymethylene-*b*-poly(vinylidene fluoride) (PM-*b*-PVDF), and Ozawa et al. [62], who studied the crystallization behaviour of polyethylene-*block*-poly(β-propiolactone) (PE-*b*-PPL). These PE-*b*-PPL diblock copolymers are strongly segregated in the melt state, as demonstrated by a lamellar microdomain structure in the molten detected by SAXS. The PE and PPL blocks in this block copolymer can crystallize sequentially or coincidentally, but in neither case, the microdomain lamellar morphology is destroyed. If the crystallization takes place simultaneously, this lamellar morphology is highly distorted, as revealed by SAXS analysis. However, if the crystallization takes place sequentially, that is, first the PE block and then the PPL block, the lamellar morphology obtained in the melt was only slightly distorted after both blocks crystallized. Which behaviour prevails will depend on the crystalline form of the PPL block, that is δ-or β-form, induced during the thermal treatment [62].

2.3. Linear double crystalline diblock and triblock copolymers of poly (lactide), poly (ε-caprolactone) and poly(ethylene oxide) (PEG or PEO)

PLA, PCL, and PEO are the three most researched biopolymers in polymer physics. Because of their outstanding biodegradability and biocompatibility properties, these materials are of great interest in several sectors, such as biomedical and packaging. However, they are usually blended or copolymerized between them and with other polymers to enhance their physical, mechanical, and biodegradation behaviour and processability. Over the last decades, extensive research has been dedicated to the morphology and crystallization behaviour of block copolymers composed of PLA [63], PCL [20], and PEO [64] and their combinations. Thus, they will be discussed profoundly in the following sections.

It is worth mentioning that because of the enantiomeric characteristics of PLA, their block copolymers englobe the three forms of PLA: PLLA, PDLA, and PDLLA. This way, linear block and stereocomplex block copolymers can be obtained by combining different monomers. This review is mainly focused on block copolymers based on PLLA enantiomeric form. However, important research has also been conducted on the crystallization behaviour of block copolymers that also include PDLA in the structure [65–68]. To give an example, PDLA-PCL diblock copolymers have been investigated by Mulchandani et al. [65] to assess the effect of the enantiomeric forms of PLA. A cold crystallization event for the PDLA block is also observed in these copolymers. As the length of the PDLA block increases, the T_{cc} becomes higher, and its melting enthalpy rises, but the melting enthalpy of the PCL block reduces. A triblock terpolymer combining PLLA, PDLA, and PCL has also been evaluated [65]. The cold crystallization event for the PLLA block is less evident. A melting peak at 210 °C revealed a sterecomplexation phenomenon between the PDLA and the PLLA block, while no melting of PLA homocrystals was detected at lower temperatures. The stereocomplex crystallites were confirmed by X-Ray diffraction [65]. Another phenomenon, such as fractionated crystallization, has also been reported in stereocomplex PEG-*b*-PLLA-*b*-PDLA triblock block copolymers for the PEG block as a result of the first crystallization of the PLA blocks [66]. During a subsequent heating scan, multiple melting peaks for the PEG block are observed when the PLA is first crystallized at lower temperatures. If the PLA blocks are crystallized at higher temperatures, then the multiple melting peaks of the PEG block tend to disappear, and only one endotherm is observed. Also, at lower T_c for the PLA blocks, the nucleation density of the PLA is higher, smaller spherulites are formed that rapidly impinge on one another, and the PEG block is forced to crystallize inside the interlamellar regions of PLA spherulites. At higher T_c PLA, the subsequent PEG crystallization might also take place inside the inter-spherulitic regions of PLA crystals [66].

2.3.1. Crystallization behaviour and crystalline structure of double crystalline AB and ABA diblock and triblock copolymers of poly (ε-caprolactone) and poly(lactide)s (PLA-b-PCL)

The PLA-*b*-PCL diblock copolymers are double crystalline systems miscible in the molten state [69,70]. Therefore, the phase separation is driven by the crystallization of the PLA block, which crystallizes at a higher temperature than the PCL block and templates the morphology of the solid state. As melt-miscible systems, the subsequent crystallization of the PCL block occurs within the interlamellar regions of the previously formed PLA crystals. Extensive research has been published over the last decades regarding PLA-*b*-PCL diblock copolymers crystallization (see Refs. [68–79]). In the present review, the relevant literature published since 2017 to the present is discussed and resumed.

For instance, and more recently, the effect of molecular weight of the PLLA block in linear PLLA-*b*-PCL diblock copolymers has been studied by Han et al. [68]. In this diblock copolymers, the length of the PCL block was kept constant. In PLLA-*b*-PCL diblock copolymers, as the PLLA crystallizes first, its crystallization affects and restricts the subsequent crystallization of the PCL block, and the final crystalline structure and crystallizability will depend on the block length ratio between the blocks. For instance, as the PLLA content increases, the T_c and T_m of the PCL block reduce, and the values are lower than in the PCL homopolymer. For the PLLA block, the T_m values are higher than in the PLLA homopolymer and tend to increase as the PLLA content is higher. Interestingly, the PCL crystals formed during cooling can affect the subsequent cold crystallization phenomena in the PLLA block. The cold crystallization event is only observed when the content of the PLLA block is majority (between 57 and 75%). In addition, in the copolymers that cold crystallize, that is, with more than 50% of PLLA, the T_{cc} of the PLLA block is lower when the content of PCL is higher. In other words, when the PCL content increases from 37 to 43%, the PCL crystallization degree also increases, and the T_{cc} of the PLLA block reduces to 2.5 °C. Thus, even though the PCL crystals are molten before the cold crystallization of the PLLA block, this richer PCL phase might enhance the crystallization ability of the PLLA block. In addition, the T_m of the PLLA block tends to reduce as the PCL content increases. The molten and richer PCL phase might induce a diluting effect over the PLLA crystals, increasing the mobility of the molecules and depressing T_m. At very high PLLA content (75%), the PCL block is no longer able to crystallize, and only the crystallization and melting of the PLLA block are observed. On the contrary, if the PLLA content is lower (14%), the PLLA block is the one that cannot crystallize and remains amorphous, only the PCL crystallization and melting transitions are observed.

A double melting peak of the PCL block was observed at intermediate compositions, while a melt-recrystallization event prior to PLLA melting was observed in the richer PLLA copolymers. Regarding the crystallinity, the crystallization degree of the PCL block decreases continuously with increasing the PLLA content since the previously formed PLLA crystals restrict and confine the crystallization of the PCL phase. In the case of the PLLA block, the behaviour observed is more complex. As the PLLA content rises, the crystallinity degree of the PLLA increases. However, if the PLLA content is further increased beyond 63%, the crystallinity degree starts to decline. As the length of the PLLA block becomes longer, its crystallization ability might be reduced [68].

During melt crystallization, the copolymers could form regular and banded spherulites depending on the crystallization temperature and the block length ratio between the blocks. A morphological transition from banding to non-banding was observed at intermediate compositions. For instance, at 117 °C, which is a temperature at which only the PLLA block can crystallize while the PCL block is molten, all the copolymers form spherulites except that one in which the PLLA content is only 14%. In this last case, a non-crystalline structure was observed. In rich PCL phase copolymers (60%), the spherulite texture is coarse and irregular without a clear Maltese cross. Interestingly, three different crystalline morphologies arise when the PLLA content increases beyond 50%. A regular twisted banded spherulite is observed when PLLA content is 75%. It is considered that the minor and molten PCL phase induces the PLLA lamellar twisting along the growth direction of the lamella. As the PLLA content reduces, the banded structure becomes more irregular until no longer banding is observed in diblock polymers with 57% of PLLA content (see Fig. 8). In the copolymer with 57% of PLLA, continuous lamellar growth along the radius direction is observed, and non-ring bands are obtained. The lamellar growth extends outward from the centre in a parallel configuration of lamellae and branches. If the PLLA content increases up to 75%, a discontinued growth of the lamellae along the radius is observed. The repetitive ring pattern represents the edge-on and flat-on lamellar twisting in banded spherulites. This alternated morphology causes extinction bands observed in POM images for banded spherulites.

The AFM images also revealed morphological differences as the PLLA content increased. In the banded spherulites of the block copolymer with 75% of PLLA, the lamellae are spread out along and deviate from the growth direction. The deflection in the growing direction can be ascribed to crystalline lamellar twisting. These crystalline aggregates are lamellar bundles and not single-layer lamella. It has been reported that the origin of the lamellar twisting is an unbalanced surface stress that disturbs the regular orientation of the crystalline lamellae. The disturbing effect might be caused by a small population of molten PCL segments in the amorphous region surrounding the PLLA crystalline lamella. As the molten PCL content increases (PLLA block length reduces), the twist of the PLLA lamellae is avoided [68].

The twisting of the PLLA lamellae can be modulated as a function of the temperature. For instance, as we have seen, the diblock copolymer with 75% of PLLA exhibited banded spherulites when it crystallized at 117 °C. The same morphological behaviour is observed when the crystallization temperature is 110 and 100 °C. However, if the crystallization

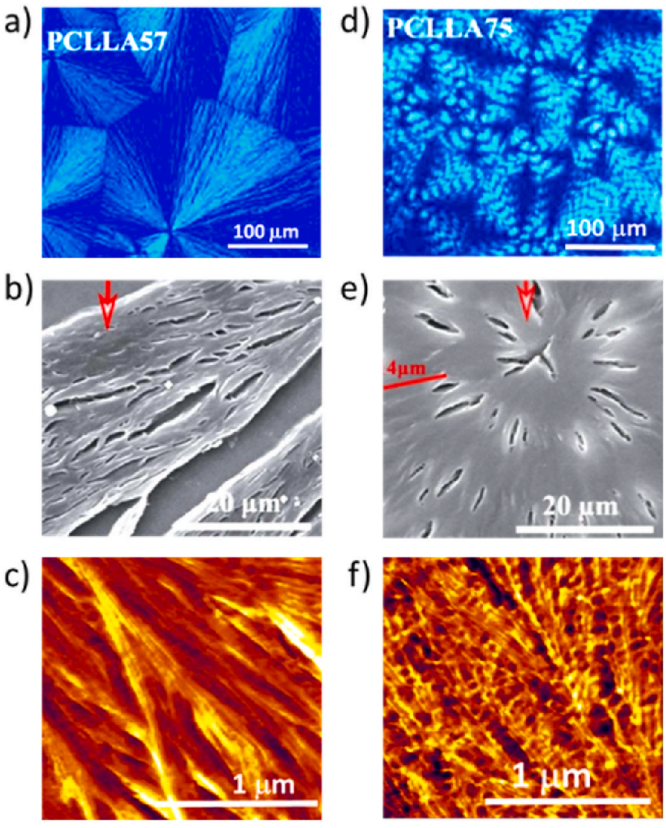

Fig. 8. Photomicrographs of PLLA–PCL copolymers with 57 and 75% of PLLA using a,d) Polarized Light Optical Microscopy (PLOM), b,e) Scanning Electron Microscopy (SEM), c,f) Atomic Force Microscopy (AFM). Isothermally crystallized at 117 °C. Taken and modified from [68].

temperature is increased up to 125 °C, no ringed extinction patterns are observed. The band spacing and spherulitic growth rate increase monotonically with the crystallization temperature until it reaches 120 °C. At temperatures higher than this, banded spherulites are no longer observed, and the crystallization rate starts to decline. An in-situ band-to-non-band morphological transition can be observed as the material is crystallized sequentially in two steps: at 120 °C, a temperature at which banded spherulites are formed, and then at 130 °C, a temperature in which regular spherulites can grow. In this way, the spherulite has a banded nucleus and regular spherulitic morphology on the edge. The reason behind the disappearance of the banded texture at high T_c might be the increased lamellar thickness obtained at higher temperatures. A thicker lamella can find more difficult to twist, and a larger band spacing is generated. At lower T_c, a thin lamella might twist easily, increasing the twisting frequency and reducing the band spacing due to the unbalanced stress caused by the faster diffusion rate of the PCL segments [68].

Regarding the spherulitic growth rate of the PLLA block in the copolymers, this value decreases as the length of the PLLA block increases since the entanglement effect is more significant as the molecular weight is higher, hindering the movement of the PLLA segments. On the contrary, increasing the PCL content improves the crystallization rate of the PLLA block because the molten PCL chains act as a diluent, enhancing the molecular mobility of the PLLA chain segments [68].

Other authors have reported similar block systems with increased PLLA block length. However, the focus is put on the crystallization of the PCL block after changing the crystalline history of the PLLA block [79]. Han et al. followed the PCL crystallization after thermal annealing at high (above PLLA melting, 180 °C) and low temperatures (with PLLA block crystallized, at 80 °C) and studied the crystalline morphology. In these block copolymers, the length of the PCL blocks is bigger than in the PLLA blocks, and in one composition, they are equal. Thus, most copolymers have a richer PCL phase. Firstly, the copolymers annealed at 180 °C exhibited a cold crystallization process for the PLLA block that was not observed when the sample was annealed at 80 °C. As expected, at 80 °C, the PLLA block can crystallize extensively, and therefore, no further crystallization takes place during the second heating. As expected, the crystallinity of the PLLA block after annealing at 80 °C is higher than the one obtained after annealing at 180 °C since the PLLA crystals are formed during the cooling scan and mostly during the cold crystallization event taking place in the heating scan. Since that at 180 °C, both PCL and PLLA blocks are molten; it is expected that the annealing process at this temperature causes a rejection of the PCL and PLLA molten blocks in the amorphous region. The sample is rapidly cooled down from 180 °C to a temperature where only the PCL block can crystallize (30, 35, and 40 °C). In this case, the PCL block establishes the crystalline structure since no significant crystallization is observed during cooling for the PLLA block.

At very high PCL content (PCL6K-PLLA1K), irregular ordinary PCL spherulites are formed. Interestingly, the copolymer with 75% of PCL (PCL6K-PLLA2K) exhibited banded spherulites at all T_c. The other copolymers exhibited a less defined spherulitic structure that became more complex and less clear as the PLLA content increased. The crystalline morphology according to the block length ratio in PLLA-PCL block copolymers can be controversial among researchers. However, it might be a regular observation that the twisting of the lamellae takes place when the block ratio between PCL and PLLA is too large. In this PCL6K-PLLA2K, the PCL spherulites exhibited banding due to unequal stresses at opposite fold surfaces of PCL lamellae caused by the dangling amorphous PLLA block in the PCL lamellae and the very few PLLA crystalline stems formed during the rapid cooling. An alternating edge-on and flat-on lamellar arrangement occur in ring-banded spherulites (see Fig. 9) [79].

Measuring the peak-to-valley difference of the banded PCL spherulites in the AFM images demonstrated that the lamellar thickness increased as the isothermal T_c increased. In addition, a higher degree of space filling in the surroundings of the twisted lamellae was observed. Similarly to the richer PLLA diblock copolymer discussed earlier, in these richer PCL diblock copolymers, the band spacing of the banded PCL spherulites tends to increase with T_c. As expected, higher T_c provides more mobility to the PCL segments and the diffusion of the molecules to the crystalline front, increasing the lamellar thickness. A thicker lamella restricts the twisting arrangements; consequently, the twisting frequency is lower, and band spacing is higher [79].

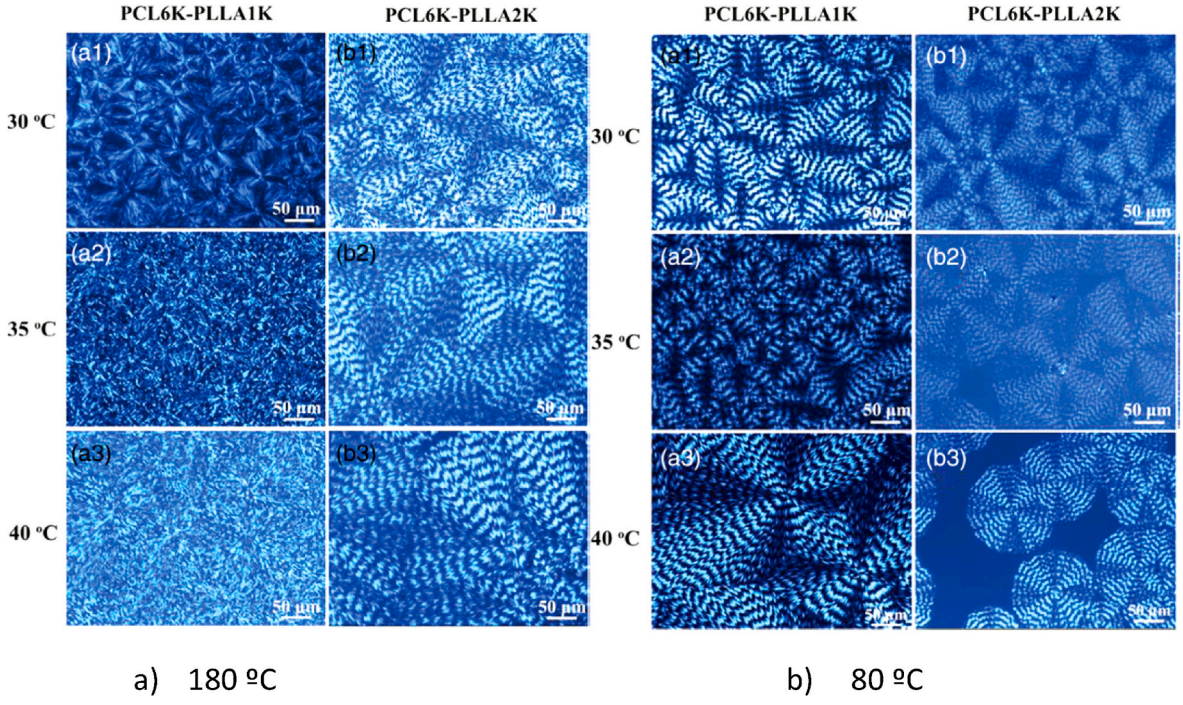

Fig. 9. POM images of PCL-PLLA copolymer spherulites isothermally crystallized at 30, 35, and 40 ◦C after annealing at 180 and 80 °C ◦C. Taken and modified from [79].

The spherulitic growth rate of these richer PCL diblock copolymers also decreases as the content of the PLLA block increases. Unlike the richer PLLA diblock copolymers, in this case, the reason behind the reduction in the growth rate is the restrictions imposed by the mostly amorphous PLLA segments attached to the PCL blocks. In addition, the lamellar twisting taking place during the spherulitic growing delays the forward growth rate of the lamellae [79].

The thermal annealing at 80 °C introduces significant morphological changes since the PLLA crystals are already formed before the crystallization of the PCL block. Again, the PCL block is subsequently crystallized at 30, 35, and 40 °C. In this case, PCL6K-PLLA1K and PCL6K-PLLA2K block copolymers with a richer PCL phase exhibited banded spherulites at all T_c (see Fig. 9b). In block copolymers with less PCL content (PCL6K-PLLA4K and PCL6K-PLLA6K), only a crystalline textured morphology is observed with less birefringence intensity. The pre-existing PLLA crystals template the subsequent crystallization of the PCL block but also affect the crystalline morphology generated since the PLLA amorphous chains and the small-size crystals disturb the growth of the PCL lamellae resulting in twisting and banded spherulites. At higher PLLA content, the restrictions over PCL crystallization are higher since the PCL chains have to crystallize inside the intra-crystalline regions of the PLLA crystals formed at 80 °C [79]. Under these annealing conditions, the band spacing also increases with T_c, and it is smaller than the one observed after annealing at 180 °C. Since the crystallinity of the PLLA block is higher after annealing at 80 °C, the greater amount of PLLA lamellar templates causes a greater unbalance stress on PCL crystallization, and as a result, the twisting frequency is reduced (shorter band spacing). The spherulitic growth rate after annealing at 80 °C also reduced in comparison with the thermal treatment a 180 °C. That is a consequence of a more frequent twisting process (reduced band spacing) that delays the crystallization of the PCL crystalline front [79].

2.3.2. *Crystallization behaviour and crystalline structure of double crystalline AB and ABA diblock and triblock copolymers of poly(lactide) and poly(ethylene glycol) (PLA-b-PEG)*

PLA block copolymers with poly(ethylene oxide) (PEO) or poly (ethylene glycol) (PEG) are also melt-miscible systems. In PLLA-*b*-PEG diblock and PLLA-*b*-PEG-*b*-PLLA triblock copolymers, both blocks are potentially crystallizable depending on the cooling conditions and thermal treatments but also on the molecular weight of the segments. Thus, by adjusting these parameters, the crystalline morphology can be intentionally tuned to obtain different properties. For this reason, the PLLA-*b*-PEG system has been extensively researched over the past decades [23,80–92]. Under standard dynamic cooling conditions, PEG homopolymer crystallizes at around 40 °C and melts at temperatures around 60 °C. When this softer polymer is copolymerized with a more rigid one, such as PLLA, the crystallization behaviour of the PEG block is modified. Moreover, the crystallization of the PLLA segment is also perturbed by the presence of the PEG block. The T_m of the PLLA block is far above that of the PEG block. Thus, upon cooling from the melt, the PLLA block always crystallizes first, and then the PEG block. As a result, the previously formed PLLA crystals might enhance, limit, or restrict the crystallization behaviour of the second block.

Recently, Bao et al. [80] reported the influence of the M_w of the PLLA and PEG segments on the crystallization behaviour. As the length of the PLLA block increases, the PLLA T_c and T_m become higher, but the PEG T_c and T_m are reduced when the copolymer is crystallized under standard non-isothermal conditions. These observations indicate that the PLLA segment restricts and limits PEG crystallization. By increasing the cooling rate, the crystallization of both blocks is delayed, and the crystallization peaks appear at lower temperatures. As the crystallization of both blocks is interrelated, the effect of the thermal annealing of the PLLA block over the PEG crystallization was evaluated. Increasing the PLLA annealing temperature from 70 to 110 °C enhanced the PEG crystallization by shifting its T_c to higher temperatures; also, the effect is more notorious as the PLLA segment is larger.

The PLLA crystals will provide good nucleation sites for the PEG block to start to crystallize. However, the overall PEG crystallinity degree was reduced with the increment in PLLA M_w. In fact, the melting behaviour of the PEG block changed significantly if the PLLA block length and the PLLA annealing temperature increased. The heating scans reflected the crystallization processes and how the different crystalline environments generated in the PLLA phase affected them. A multiple melting behaviour was observed for the PEG block, suggesting a possible fractionated crystallization. In the case of the PLLA block, the low melting peak/shoulder obeyed the melt-recrystallization mechanism previously reported for the PLLA [80].

On the other hand, WAXS measurements demonstrated that the α-form of PLLA crystals was favored after the thermal annealing [80]. According to the authors, SAXS measurements indicated a homogeneous melt, and the crystalline morphology depended on the PLLA block length. However, they reported that at shorter PLLA segments, copolymers exhibited a lamellar structure, but at higher PLLA content, scattering peaks were observed at $\sqrt{3}$ and $\sqrt{7}q^*$, which were ascribed to a hexagonally packed cylindrical structure (see Fig. 10a). This is peculiar because it contrasts with the supposedly homogeneous one-phase melt.

The structures were confirmed by TEM. The annealing of the PLLA block promoted a lamellar arrangement of alternated lamellae, as was confirmed by SAXS. Increasing the annealing temperature induced a better-packed lamellar structure. In almost all copolymers, the subsequent crystallization of the PEG block did not introduce alteration in the crystalline packing previously formed by the PLLA crystals. However, in one intermediate composition, a new lamellar arrangement emerged. Two separated scattering peaks with comparable intensity appeared (see Fig. 10b), indicating two lamellar stacks family coexisting, and the long period values demonstrated larger PEG domain size. Clearly, the M_w of the blocks and the surrounding environment composed of the PLLA block crystals greatly affect the crystallization behaviour of the PEG block.

The crystallization rate in block copolymers is also determined by the interrelation between the blocks. The isothermal crystallization kinetics of the PEG block was monitored after the prior annealing of the PLLA block (with differences in M_w) at different temperatures. In this way, the influence of different crystalline environments of the PLLA phase over the subsequent PEG crystallization was observed [80]. The PEG block was isothermally crystallized at 38 °C, while the PLLA block was previously annealed at temperatures higher than PEG T_m, between 70 and 140 °C [80]. Interestingly, if the PLLA segment is short, the PEG block crystallization rate is the fastest but almost constant with the annealing temperatures. However, if the PLLA block is the larger one, the effects become more significant, and the crystallization rate of the PEG block rapidly decelerates, with more emphasis at low PLLA annealing temperatures. The reason is probably the soft confinement effects caused by the larger PLLA crystals, forcing the PEG block to crystallize inside the interlamellar nanodomains making it more difficult for PEG to crystallize. The overall PEG crystallization kinetics is more favored at higher PLLA annealing temperatures [80] (see Fig. 11).

In double crystalline triblock PLLA-*b*-PEG-*b*-PLLA copolymers, the high melting peak corresponds to the PLLA crystalline phase, while the low melting peak (around 60 °C) belongs to the melting of PCL crystals. However, the crystallization ability of both blocks will depend on the molecular weight of each block since the PLLA blocks located in the extremes of the copolymer chain might restrict the crystallization of the middle PEG block. Several authors have reported this effect of block content on the crystallization behaviour of AB and ABA block copolymers [81–85]. For instance, in triblock copolymers reported by Li et al. [81], if the length of the PLLA block is fixed, the PEG segment only can crystallize when its M_w is three times the M_w of the PLLA block. Otherwise, the PEG block cannot crystallize upon cooling from the melt [81]. As the PLLA block crystalizes first, the PLLA crystals limit the crystallization of the middle PEG block inside the interlamellar regions of the previously formed PLLA crystals, and phase separation cannot

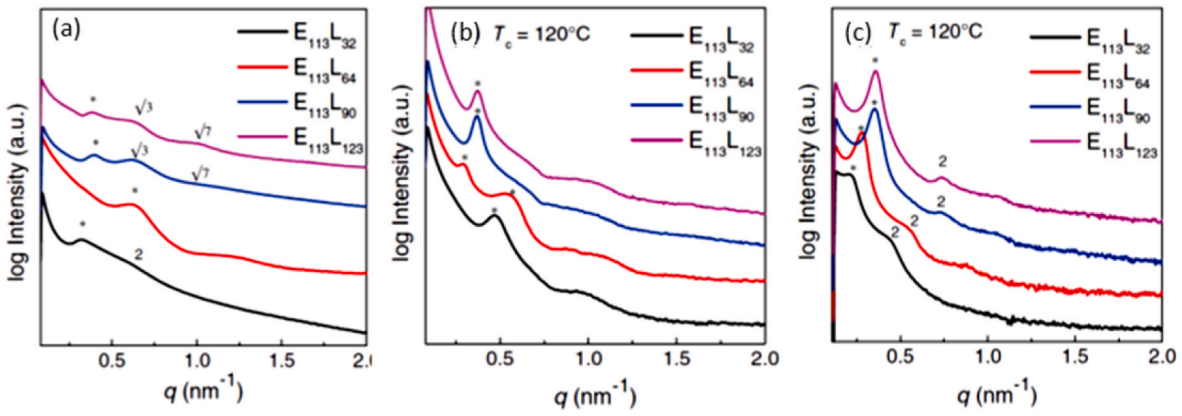

Fig. 10. SAXS patterns obtained at (a,b) room temperature and at (c) 70 °C of PEG-b-PLLA diblock copolymers. Thermal history: (a) the samples were cooled from 190 °C to room temperature directly, (b,c) the samples were cooled to room temperature after the PLLA block crystallized at T_c = 120 °C during the two-step crystallization process. Taken and modified from [80].

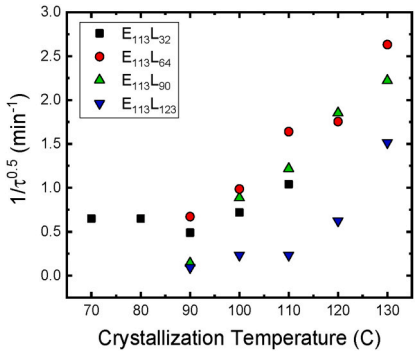

Fig. 11. Inverse of Avrami calculated $\tau^{0.5}$ of PEG block in PEG-b-PLLA after PLLA block crystallized at various Tc, PLA's Data extracted from [80].

occur. When the PEG content is relatively high, crystallization-driven phase separation occurs, and both blocks can crystallize. In these triblock copolymers, the T_c and T_m of the PLLA block increased as the PLLA content (or PLLA block length) was increased [81,83]. Similar results on PLLA T_m behaviour have been reported by Wang et al. [82] in ABA triblock copolymers based on poly(L-Lactic acid) and methoxy polyethylene glycols (MPEG), PLLA-*b*-MPEG-*b*-PLLA. In addition, the common cold crystallization process of PLLA is also modified by PEG composition in these triblock terpolymers. Particularly, when PEG content increases, the T_{cc} first decreases and then starts to increase [83]. The flexible PEG block might increase the mobility of the PLLA first, enhancing its crystallization. But longer PEG chains might induce a diluent effect over PLLA chains, shifting the T_{cc} to higher temperatures [83]. Also, the double melting peak phenomenon typical of PLLA block in copolymers and homopolymers was observed [81]. This behaviour has been attributed to polymorphism in PLLA and/or to a melt-recrystallization process of the PLLA crystals during heating.

The crystallization degree achieved is also influenced by the length of the blocks [82]. As the content of the PLLA block increases, the crystallinity of the middle PEG phase decreases. When the M_w of the PLLA segments is very high, the PEG phase remains amorphous, and only the PLLA block can crystallize. Similar results have been reported by Baimark et al. [86]. The flexible PEG chains are attached to both ends of the rigid crystalline PLLA lamellae inside the interlamellar stacks, hampering the mobility required in order to crystallize. In analogous AB diblock copolymers, the mobility of the PCL chains after PLLA crystallization is less hindered since the MPEG segments are free in one end, and therefore, the restrictions are less significant, and the crystallization ability of the MPEG block is less compromised. For this reason, the crystallization degree of the PEG block in the triblock copolymers is lower than in the analogous diblock copolymers. If the proportion of the PEG phase becomes larger, the PEG segments suffer less restriction from the PLLA crystals, and its crystallization is favored [82,83]. Thus, the T_m and χ_c of the PEG block increased. Moreover, the PLLA block length must be four times larger in order to inhibit the PEG crystallization [82].

Different observations have been reported regarding the PLLA block crystallinity in PLLA-*b*-PEG-*b*-PLLA triblock copolymers. For instance, Yun et al. [83] reported an increase in PLLA χ_c with higher PEG content (shorter PLLA block length). As the PLLA block segments are shorter, they gain mobility, and the crystallization is enhanced. On the contrary, Wang et al. [82] reported that PLLA crystallinity increases with PLLA M_w until some point and after, starts to decrease. As the length of the PLLA block rises, PLLA crystallization is also favored by the extra mobility provided by the PEG soft segments. However, beyond a critical PLLA M_w value, the chain entanglements become important, and the viscosity increases, hindering the crystallization process of the PLLA block [82]. It is interesting that beyond a critical PLLA M_w value, the PLLA crystallinity values were slightly larger in the triblock copolymer than in the analogous diblock copolymer. The reason behind this behaviour is that the PLLA chain entanglements and viscosity are higher in the diblock copolymer compared to the triblock copolymer of similar PLLA content, in which the PLLA chain length is split in two as they are located at both ends. Thus, PLLA segments in the triblock copolymer are more prone to crystallize, and the PLLA crystallization degree increases. If the PLLA blocks are too short, the highly flexible and larger PEG block in the triblock copolymer makes more difficult the ordering of the PLLA chains into crystalline structures due to the extra mobility induced, and therefore, the PLLA crystallization degree in the triblock is slightly lower than in the diblock copolymer [82]. The PLLA T_m value is also reduced if the PEG content becomes larger, which is probably caused by a diluent effect from the molten PEG segments, reducing the PLLA lamellar thickness that can be achieved. If the PEG proportion is too large (i.e., five times larger than the PLLA composition), the PLLA block cannot crystallize and remains amorphous. On the contrary, if the PLLA block length is larger, the PLLA T_m value increases. To sum up, the length of the PEG block modifies the crystallization ability of the PLLA block. A suitable M_w of the PEG block might improve the crystallization of the PLLA block due to the diluent effect that enhances the mobility of PLLA chains to some extent. However, if the PEG M_w is too large, the mobility of the PLLA block might become so high that the nucleation would be difficult, obstructing the crystallization process of the PLLA block [82]. The length of the PEG block influenced the equilibrium melting temperature of the PLLA block.

The T_g of the PLLA block also modified and shifted to lower temperatures as the PEG content in the ABA triblock copolymer increases

since longer, and molten PCL segments provide extra mobility to the PLLA chains, reducing the temperature at which the glass transition takes place.

The crystallization kinetics of PLLA-*b*-PEG-*b*-PLLA triblock copolymers have been studied by Yun et al. [83]. The slow crystallization kinetics of PLLA homopolymers is a well-known fact. However, copolymerizing PLLA with a soft block such as PEG contributes to enhancing its crystallization kinetics by accelerating it. All the PLLA-*b*-PEG-*b*-PLLA triblock copolymers exhibited faster crystallization kinetics of the PLLA block, and this improvement was more significant as the PEG block content increased. However, if the PEG proportion is too high (26.2%), a negative effect takes place over PLLA kinetics, and the crystallization rate is reduced (see Fig. 12). The reduction of the PLLA crystallization time as the PEG content increases obeys the longer middle PEG segment that provides extra mobility to the adjacent PLLA chains, favoring its crystallization. In addition, shorter PLLA segments (PEG content increases) led to more rapid crystallization. However, if the PEG block is too large, the PLLA crystallization kinetics become slower due to a diluent effect over the PLLA chains [83]. Spherulitic growth rate behaviour agreed well with DSC results. PLOM microscopy revealed that nucleus density reduced and the spherulite size increased after introducing the PEG block [83].

The crystallization kinetics of PLLA-*b*-PEG diblock copolymers under non-isothermal conditions have also been monitored through the Fast Scanning Calorimetry (FSC) technique. This novel technique emerged in order to analyze processing relevant cooling rates properly and to study the kinetics of fast transformations and reorganization of metastable materials during heating. In polymers, FSC is allowed to investigate crystallization kinetics in a wide range of cooling rates and temperatures upon fast cooling from the melt or fast heating from the glassy state, employing a high degree of supercooling [93,94].

Chen et al. [87] evaluated the non-isothermal crystallization behaviour of PLLA-*b*-PEG diblock copolymers and the analogous PEG homopolymer employing two cooling methods. In the first method, the sample was fast-cooled from the melt at different cooling rates down to −80 °C to follow the sequential crystallization of both blocks. In the second method, the sample was first fast cooled down to 60 °C at a fixed cooling rate (2000 K/s) that suppressed PLLA crystallization and then was cooled again until −80 °C at different cooling rates to observe the crystallization of the PEG block surrounded by a vitreous PLLA phase.

By employing methodology 1, both blocks were able to crystallize sequentially, the PLLA block at 75 °C and the PEG block at −25 °C. Nevertheless, at very high cooling rates (2000 K/s), the crystallization of both blocks was suppressed. In addition, as the cooling rate increases, the PEG crystallization peak slightly shifts to lower temperatures because the time to crystallize is less (see Fig. 13). In addition, the crystallinity of the PEG block after cooling with method 1 is higher than the one obtained after employing method 2 [87]. It seems that the previously formed PLLA crystals contributed to enhancing the

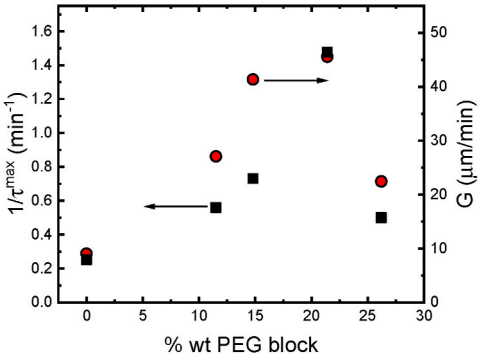

Fig. 12. Top: Inverse of maximum tao and spherulitic growth rate at 100 °C versus the weight percent of PEG. Graph plotted from data taken of ref [83].

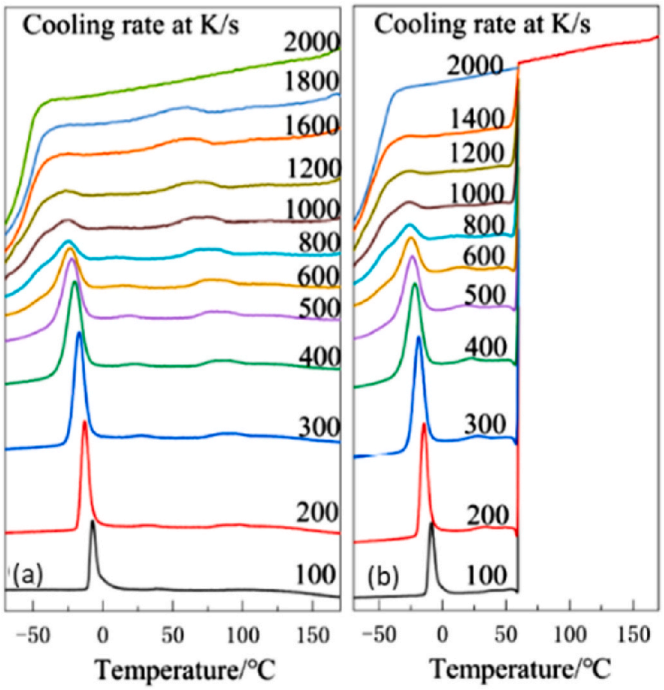

Fig. 13. FSC Non-isothermal crystallization curves (a,b) at different cooling rates of PEG-b-PLLA in method 1 (a) and method 2 (b). Taken and modified from [87].

subsequent crystallization of the PEG block. It is more difficult for the PEG chains to rearrange into ordered crystalline structures, coming from the mixed phase that includes an almost vitreous (and rigid) PLLA amorphous phase and molten PEG chains.

2.3.3. Crystallization behaviour and crystalline structure of double crystalline AB and ABA diblock and triblock copolymers of poly (ε-caprolactone) and poly(ethylene oxide) or poly(ethylene glycol) (PCL-b-PEO, PCL-b-PEG)

The PCL-*b*-PEO and PCL-*b*-PEG diblock and triblock copolymers have been widely investigated over the past decades [95–112]. As their thermal transitions appear at similar temperatures and their solubility parameters are comparable, evaluating their crystallization behaviour represents a challenge, and different crystallization phenomena can be observed, such as sequential and coincident crystallization as a function of the M_w of the segments and the crystallization conditions. In general, the crystallization of both blocks is conditioned by the following:

1. The length of the PCL block. As the PCL block length becomes larger, the PEO block might not crystallize [96–98].
2. Symmetry. Double crystalline copolymers are observed in symmetric or almost symmetric blocks [97,99].
3. Crystallization conditions. Quenching from the melt induced the crystallization of the PEO block as the crystallization kinetics of the PEO block is faster. However, if the sample is slowly cooled at 2 °C/min until 50 °C and isothermally crystallized at that temperature for 15 min, the crystallization of the PCL block was promoted, and its crystallinity degree increased while the crystallinity of the PEO block reduced [97].
4. Other blocks. Another approach to modifying the crystallinity of the PCL block is to include a small amount of L-lactide comonomer to reduce the high crystallinity of the PCL block. Le Kim et al. [100] synthesized poly(ε-caprolactone-*co*-lactide)-*b*-polyethylene glycol-*b*-poly(ε-caprolactone-*co*-lactide) (PCLL-*b*-PEG-*b*-PCLL) for nanoemulsions applications. The authors demonstrated that T_m and ΔH_m

reduced as the content of L-lactide increased. The presence of the L-lactide chains disrupts the chain packaging of the PCL segments.

As PCL and PEO crystallize and melt in the same temperature range, one of the strategies to manipulate the crystallization order in diblock copolymers with similar M_w, T_c, and T_m of the blocks is inducing the crystallization from a solution through a solvent-casting technique. By employing solvents with different solubility parameters, one of the blocks crystallizes first, then the other. Brigham et al. [99] employed toluene, acetone, and chloroform as solvents to tune the crystallization of symmetric PCL-*b*-PEO diblock copolymers into films. The experimental technique used to follow the crystallization during drying was FTIR-ATR, and specific bands for the appearance of each block were identified. In this way, the crystallization order was determined.

FTIR-ATR spectra demonstrated that chloroform and acetone provided similar nucleation and crystallization order as the PCL block crystallized first in these two solvents. This result is similar to melt-crystallized symmetric PCL-*b*-PEO diblock copolymers. On the contrary, toluene induced the opposite crystallization order since the PEO block crystallized before the PCL block. In fact, the PCL block state was mainly amorphous, as the crystalline PCL band did not appear. Different solvents allow tuning the nucleation and crystallization sequence due to the solubility parameters (δ) differences. The δ value of toluene is closer to the δ value of PCL than that of the PEO block. Therefore, PEO becomes more insoluble and crystallizes [99].

Other slightly soluble solutions in which the copolymer can precipitate at temperatures slightly below room temperature were used to tune the crystallization order of the blocks. ATR-FTIR analysis demonstrated that the PCL block crystalizes first in methyl ethyl ketone and ethyl formate. On the contrary, the PEO block is the one that crystallizes first when ethyl acetate is used, and it does it at a faster rate. Square single crystals of PEO and truncated-lozenge, or hexagonal, PCL single crystals, were produced accordingly. The crystalline morphology of the double crystalline blocks obtained due to crystallization in each solvent is observed in Fig. 14. The middle and left images correspond to the solvents in which the PCL crystallizes first, and the right ones are those in which the PEO crystallizes first.

The morphological observations demonstrated that the large-scale assembly is influenced by several factors, such as the crystallization order, preassembly in solution, and competition between solvent−polymer and substrate−polymer interactions. Except for acetone and toluene, all the other samples exhibited a polycrystalline morphology with birefringent patterns. Ethyl acetate and chloroform were the solvents with more capacities for the growing of PCL and PEO crystals, respectively. FTIR-ATR demonstrated that both blocks were crystalline. In addition, the copolymers grew under an edge-on arrangement, although the absence of birefringence in toluene might be related to a flat-on growth. In order to remove the solvent effects, the samples were melt crystallized, and the PCL blocks always preferred to crystallize first [99].

The length of the PCL block indeed affects the crystallization order in solution-crystallized samples regardless of the solvent employed. In PCL-*b*-PEO diblock copolymers with increased PCL content, Tower et al. [96] demonstrated that PCL block crystalizes first, and the minor PEO chains provided a diluent effect that is more significant than the ones resulting from the solvent employed (e.g., chloroform, toluene, or THF). At larger PCL content, the PCL block dominates the crystallization process and is more extensive than the PEO block. It took a large undercooling to induce the crystallization of the PEO block. Besides chloroform and acetone [99], PCL also crystallizes first in THF. However, the interaction of the PEO block with the solvent delayed its crystallization and crystallinity degree. Additionally, the crystallization temperature had a minimal effect on the crystallization ratio since both blocks are able to crystallize at the temperatures employed [96].

2.3.4. Other linear diblock copolymers containing PLA, PCL, or PEO

Many other comonomers have been copolymerized with PLA, PCL, and PEO, such as poly(butylene adipate) (PBA) [113], poly(γ-butyrolactone) [114,115], poly(δ-valerolactone) [116], poly(*p*-dioxanone) [117,118], poly(2-isopropyl-2-oxazoline) [119], poly(ethylene brassylate) [120], poly[oligo(3S-iso-butylmorpholine-2,5-dione)]-diol [121] (PIBMD), thioether containing ω-hydroxyacid (TEHA) [122], poly(perfluorooctylethyl acrylate) (PFA) [123], poly(*N*-octylglycine) [124], poly(hexamethylene 2,5-furandicarboxylate) [125], poly(*N*-(2-phenylethyl) glycine) [126], polymethylene [127], polyethylene [47,48,58,59,128,129], poly(1,4-butadiene) [130] polyamide [131] (Pebax) [132],

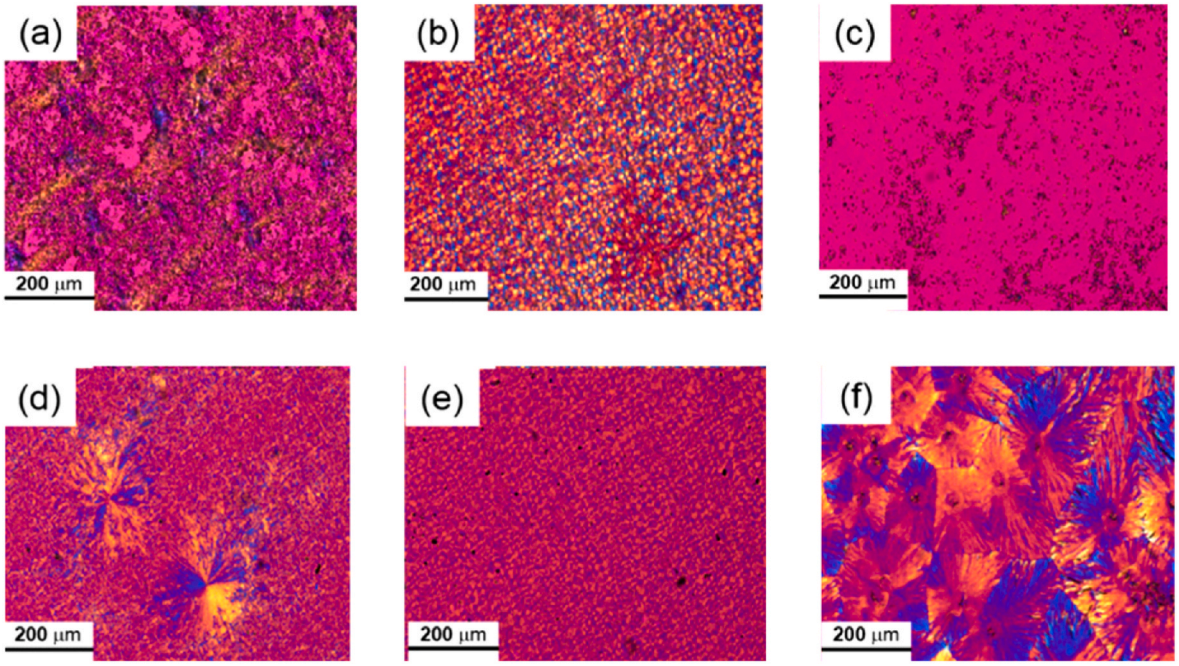

Fig. 14. POM images of 10K−10.3K PEO-b-PCL films prepared from various solvents: (a) acetone, (b) chloroform, (c) toluene, (d) ethyl formate, (e) methyl ethyl ketone, and (f) ethyl acetate. Taken from [99].

among others. Most of these systems are miscible in the molten state, but some are in the medium or strong melt segregation regimes. However, in all cases, the diblock copolymers formed double crystalline structures.

For instance, in PLLA block copolymers with PBA [113], this block crystallized and melted at lower temperatures than the PLLA block. Similar to the PLLA-*b*-PCL and PLLA-*b*-PEO copolymers. The addition of the PBA enhanced the crystallizability of the PLLA block as its cold crystallization peak shifted to lower temperatures. Nucleation and diffusion processes are improved. Upon cooling from the melt, an annealing step was necessary to induce the crystallization of the PLLA block due to its slow crystallization kinetics. On the other hand, the PLLA phase nucleates the subsequent crystallization of the PBA block, shifting its T_c to higher temperatures as PLLA content increases. The α-and β-crystal forms of the PBA block were detected. Interestingly, these block copolymers exhibited hints of segregation when block composition was PLLA-*b*-PBA 75/25, as distinct domains were observed in the amorphous state through PLOM. However, it is not clear if phase segregation remained after the crystallization of both blocks [113].

The PCL-*b*-PIBMD diblock copolymers are also partially phase-segregated. In the molten state, a bicontinuous spinodal pattern was observed by AFM in thin films of the samples (30 nm) [121]. Upon crystallization, the PIBMD crystals formed at higher temperatures restricted the crystallization of the PCL blocks. If the sample is annealed at a temperature where only the PIBMD can crystallize, the extent of PIBMD crystallization is so enhanced that the subsequent crystallization of the PCL block can be highly suppressed. On the other hand, if the sample is quenched to PCL crystallization, the nucleation and growth of PIBMD crystals are hindered, allowing the PCL crystals to develop. The PIBMD crystals could be formed in a later cold crystallization event. Thus, the double crystalline nature can be tuned by modifying the crystallization conditions and thermal treatments [121]. In thin films of PCL-*b*-PIBMD diblock copolymers, the solid-state morphology was modified from edge-on (or flat-on) lamellae to spinodal-like and fibrillar patterns as a function of the thin film thickness and thermal treatment [121].

Unlike the previous examples, Nojima et al. [123] reported strongly segregated block copolymers composed of poly(ethylene glycol)-*block*-poly(perfluorooctylethyl acrylate) (PEG-*b*-PFA-C8). At the molten state, these copolymers exhibited a microphase-separated lamellar morphology that was not destroyed upon crystallization of the blocks. Therefore, each block is forced to crystallize inside its own lamellar phase. However, the extent of the crystallization can be modified by changing the crystallization conditions in one step or two steps. In one-step crystallization, the sample was rapidly cooled to the PEG T_c, and upon cooling, the PFA phase also crystallized. But the PFA crystalline phase generated was loosely packed (less ordered), causing a weak restriction on PEG crystallization, and as a result, a higher PEG crystallinity degree was obtained. However, the crystallization kinetics was slower because of the low PEG chain density at the interface. On the contrary, in a two-step crystallization, the PFA phase was first crystallized until saturation and after the PEG block was crystallized. Under this condition, a highly ordered crystalline PFA phase is developed, and the phase separation is even more enhanced. Thus, the subsequent PEG crystallization is highly restricted inside the long-range lamellar morphology, and the PEG crystallinity degree and crystallite size are reduced. However, the improvement in the phase segregation contributed to the increase in the crystallization kinetics of the PEG block as the density of the PEG chains became higher [123].

2.4. Crystallization behaviour and crystalline structure of double crystalline AB and ABA diblock and triblock copolymers of poly (hydroxybutyrate) family

P3HBV-*b*-P3HB-*b*-P3HBV triblock copolymer, which is a triblock copolymer of poly (hydroxybutyrate) (PHB) and a random copolymer of poly (hydroxybutyrate-*co*-valerate) (P3HBV-*b*-P3HB) has been biosynthesized by Nakaoki et al. [133] As synthesized and cast from chloroform, this triblock copolymer is double crystalline since two endothermic peaks are observed in the DSC 1st heating scan at 60 and 170 °C that corresponded to the melting of the valerate and the butyrate crystals. After cooling, no crystallization was detected, but in the subsequent heating scan, a cold crystallization event took place at 98 °C, and then, those crystals melted at 162 °C, which is an indication that only the butyrate moieties were able to crystallize on heating. The analogous diblock copolymer was analyzed for comparison purposes. In this case, only the PHB block is crystalized from casting. Moreover, in this copolymer, the PHV block did not crystallize either upon cooling or heating. Only the PHB block crystallized upon cooling, and it did it entirely, as no cold-crystallization phenomenon was observed on subsequent heating. Thus, it is possible that the end molten PHVB block chains limited the crystallization capacity of the middle PHB block in the triblock copolymer during cooling. Therefore, this block can only crystallize after heating from the glassy state. In the diblock copolymer, as the PHB block is a free end, it is possible to rearrange it in an ordered structure [133]. Interestingly, when crystallizing from casting in chloroform, a double crystalline triblock copolymer is obtained as the content of the PHBV blocks, in the end, is increased. Thus, the ability of the PHV segments to crystallize is influenced by their molecular weight. Since these crystals could not be developed upon cooling or heating, the authors [133] varied the cooling rate, but not even reducing it down to 1 °C/min these segments could crystallize upon cooling. Only slight changes in the subsequent cold-crystallization peak of the PHB block were observed due to changes in the cooling rate. These observations were confirmed by X-ray diffraction examinations [133]. A double crystalline nature has also been detected by Shi et al. [134] using X-ray diffraction in PHBV triblock copolymers in which this block is in the middle, surrounded by a PEG block at both ends. Again, the length of each block will impact the ability to grow crystals. Other authors have reported the crystallization behaviour of other PHA block copolymers [135].

3. Linear multi-crystalline ABC and ABCD multiblock terpolymers and quaterpolymers

Since the last decade, the group of Müller et al. has been deeply exploring the nature of multi-crystalline block copolymers with three and four different potentially crystallizable blocks [24,25,136–142], with special emphasis on the block interplay over crystallization kinetics and the superstructural morphology. It represents a new area of knowledge that seeks more specialized systems with complex properties modulated at the nanoscale. Fig. 15 describes the chemical structures of these novel linear ABC and ABCD multiblock copolymers synthesized at KAUST by the group of Prof. Nikos Hadjichristidis [143–147]. As the number of crystallizing blocks increases, the analysis of the crystallization behaviour becomes more challenging. Particularly when some blocks crystallize and melt in the same range of temperatures or share crystallographic diffraction peaks. Thus, identifying the crystallization sequence and phases is intricate.

The tricrystalline nature of complex block copolymers has been extensively studied in PEO-*b*-PCL-*b*-PLLA triblock terpolymers, with a special interest in the superstructural morphology and the crystallization kinetics of the different blocks [24,25,136,140–142,148]. Each of them will affect the crystallization behaviour of the other two and the final properties of the system. These terpolymers are melt-miscible, and therefore phase segregation is only driven by the subsequent crystallization of each block. In this system, the PLLA block crystallized first and formed a spherulitic template at the microscale; then, the PCL block crystallized inside this template, and finally, the PEO block, also inside the template, as demonstrated by WAXS and DSC experiments. As a miscible system, the PCL and PEO blocks had no option but to crystallize inside the interlamellar regions of the PLLA crystals. SAXS experiments and theoretical simulations, as well as AFM microscopy, clearly

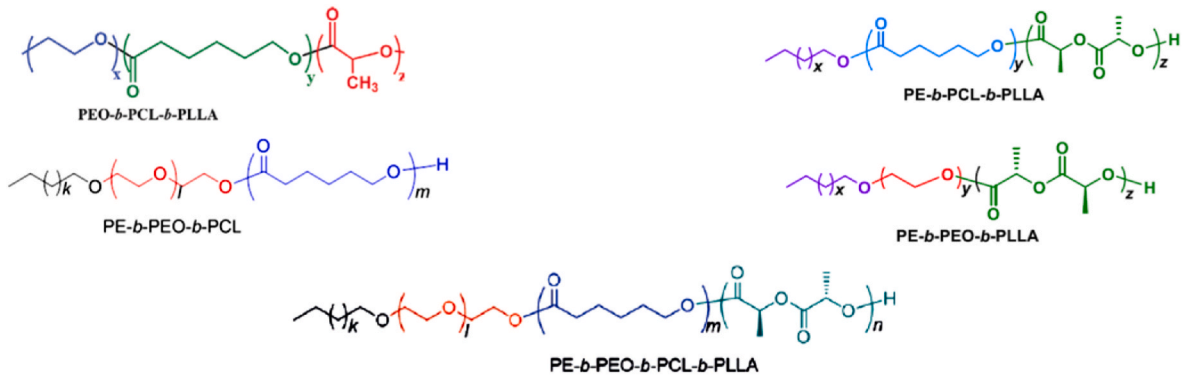

Fig. 15. Chemical structure of triblock terpolymers and tetrablock quaterpolymers.

demonstrated an alternated/interdigitated lamellar structure in which both PCL and PEO lamellae (see Fig. 16) or only one lamella of either PCL or PEO had grown randomly in between two lamellae of PLLA [136]. Therefore, three different lamellae with different lamellar thicknesses coexist and arrange inside the spherulitic morphology. Therefore, triple crystalline spherulites of these PEO-*b*-PCL-*b*-PLLA triblock terpolymers can be obtained at the appropriate compositions.

Moreover, a comprehensive analysis of the crystallization kinetics of these tricrystalline systems revealed several complex phenomena. Depending on the crystallization conditions and the physical properties of the blocks, such as molecular weight, composition, and structure, different effects such as plasticization, nucleation, anti-plasticization,

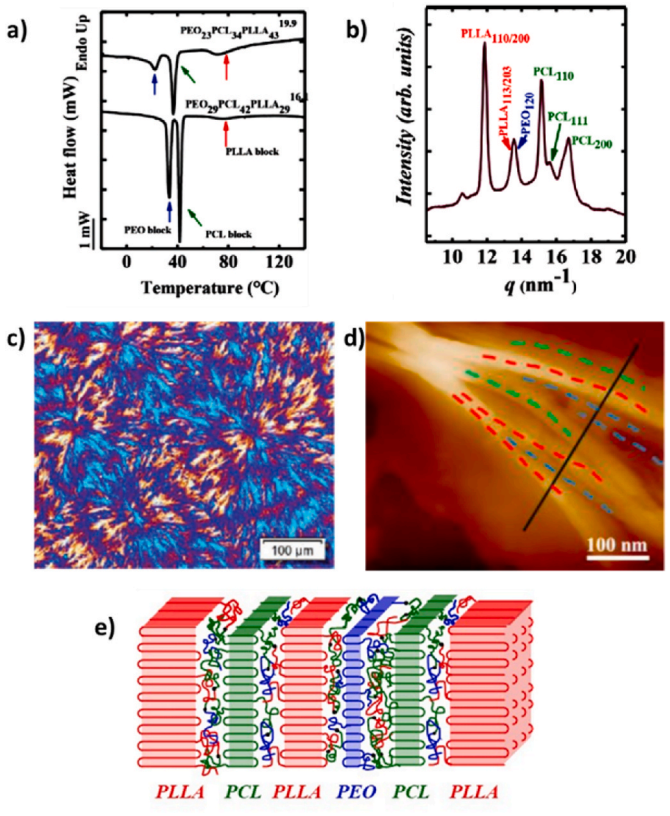

Fig. 16. Description of triple crystalline PEO-b-PCL-b-PLLA triblock terpolymer by a) DSC, b) WAXS, c) PLOM micrograph showing spherulitic morphology, d) AFM microscopy, dotted lines indicated the PLLA (red), PCL (green) and PEO (blue) interdigitated lamellae, and e) Schematic representation of the interlamellar assembly. Taken and modified from [24,136].[24,136]. (For interpretation of the references to colour in this figure legend, the reader is referred to the Web version of this article.)

and confinement might take place that can also determine whether one of the blocks can remain fully amorphous or semicrystalline. If the PLLA phase is semicrystalline, it might nucleate the crystallization of the PEO and PCL blocks, increasing their crystallization kinetics, but if the PLLA phase is amorphous, an anti-plasticizing effect prevails that reduces the crystallization kinetics of the PCL block. On the other hand, the molten PEO and PCL phases during PLLA crystallization constituted a plasticizer for the PLLA phase, shifting the supercooling needed for crystallization to lower temperatures but increasing the overall crystallization rate. Finally, the PEO block, being the last block in crystallizing after the other two, suffered a hard confinement that reduced its crystallization kinetics. These PEO-*b*-PCL-*b*-PLLA triblock terpolymers were thermally fractionated successfully by the Successive Self-Nucleation and Annealing (SSA) technique, which demonstrated being a useful tool to thermally separate the three crystalline phases in the triblock terpolymer [24].

Unlike the PEO-*b*-PCL-*b*-PLLA triblock terpolymers, which are completely miscible in the melt, other ABC triblock terpolymers might exhibit phase segregation due to the immiscibility of one of the blocks. It is the case of the PE-*b*-PEO-*b*-PCL [137], PE-*b*-PEO-*b*-PLLA [138], and PE-*b*-PCL-*b*-PLLA [138,143] triblock terpolymers synthesized by Ladelta et al. [143] and studied by Matxinandiarena et al. [137,138] (see Figs. 15 and 16). Including a PE block modified the ordering of the molten phase, and a lamellar arrangement was observed by SAXS analysis in the four copolymers at 160–170 °C, a temperature at which all blocks are melted (see Fig. 17). The reason is that PE is not miscible with either PEO, PCL, or PLLA because the solubility parameter (δ) of PE is very far from that of PEO, PCL, and PLLA (i.e., $\delta_{PE} = 7.9$ *vs.* $\delta_{PEO} = 9.9$, $\delta_{PCL} = 9.39$, $\delta_{PLLA} = 9.79$ $(cal/cm^3)^{1/2}$) [91,149].

The extent of the phase segregation is not only a reflection of the solubility parameters but the block type, molecular weight, and composition. In the PE-*b*-PEO-*b*-PCL [137] sample, a broad scattering peak in the melt is observed in the triblock terpolymer with lower PE molecular weight (see Fig. 17a). However, increasing the PE block M_w in the terpolymer promotes clear phase segregation in the melt as two strong diffraction peaks were detected in the SAXS pattern that denoted lamellar and interpenetrated morphologies (see Fig. 17b). On the other hand, if the block that increases length and content is the PLLA block, which is more miscible with the PEO and PCL middle blocks, then the molten phase becomes less segregated (see Fig. 17c vs. Fig. 17d) [138]. That is probably due to a diluent effect caused by the PLLA phase.

However, these systems are only weakly segregated since the phase structure in the melt undergoes a break-out process by the subsequent crystallization of the blocks and is substituted by a new crystalline lamellar arrangement in the solid phase, as detected by SAXS (see Fig. 17 at 30 °C). The scattering peaks disappeared or shifted to lower q values. Moreover, the triple crystalline structure of these terpolymers was confirmed by DSC and WAXS. In the PE-*b*-PEO-*b*-PCL [137] samples, both experiments demonstrated that the PE block crystallized first, and

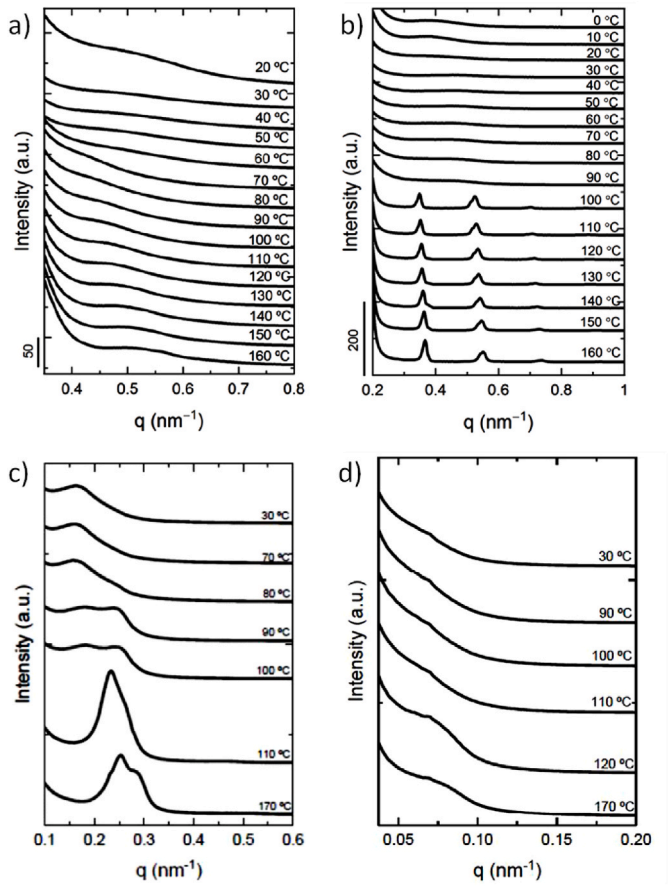

Fig. 17. SAXS patterns of a) $PE_{22}^{7.1}$-b-$PEO_{46}^{15.1}$-b-$PCL_{32}^{10.4}$, b) $PE_{37}^{9.5}$-b-$PEO_{34}^{8.8}$-b-$PCL_{29}^{7.6}$, c) $PE_{21}^{2.6}$-b-$PEO_{32}^{4.0}$-b-$PLLA_{47}^{5.9}$ d) $PE_{21}^{7.1}$-b-$PCL_{12}^{4.2}$-b-$PLLA_{67}^{23}$ triblock terpolymers taken during cooling from the melt at different temperatures. Taken and modified from [137,138].

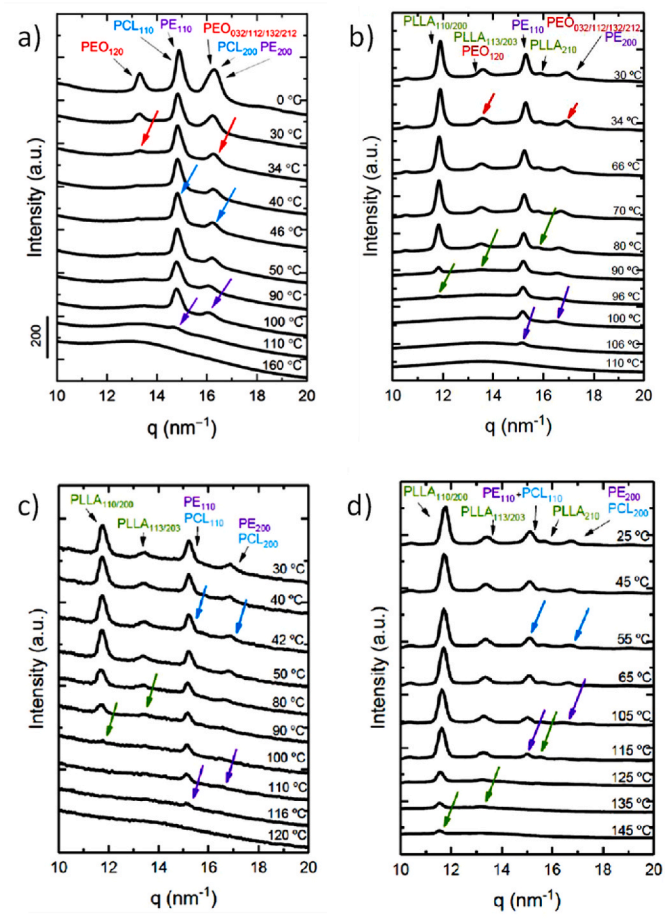

Fig. 18. WAXS patterns of triple crystalline a) $PE_{37}^{9.5}$-b-$PEO_{34}^{8.8}$-b-$PCL_{29}^{7.6}$ (Cooling rate: 20 °C.min^{-1}) b) $PE_{21}^{2.6}$-b-$PEO_{32}^{4.0}$-b-$PLLA_{47}^{5.9}$ (Cooling rate: 20 °C.min^{-1}) c) $PE_{21}^{7.1}$-b-$PCL_{12}^{4.2}$-b- $PLLA_{67}^{23}$ (Cooling rate: 20 °C.min^{-1}) d) $PE_{21}^{7.1}$-b-$PCL_{12}^{4.2}$-b-$PLLA_{67}^{23}$ (Cooling rate: 1 °C.min^{-1}) triblock terpolymers taken during cooling from the melt at different temperatures. Taken and modified from [137,138].

then the PCL and PEO block crystallized very close to each other since both blocks crystallized and melted at similar temperatures. On the other hand, if a PLLA block is incorporated into the terpolymer, as in PE-*b*-PCL-*b*-PLLA and PE-*b*-PEO-*b*-PLLA samples [138], the blocks that crystallize in the same range of temperatures are the PE and the PLLA.

WAXS analysis is a useful technique to elucidate the crystallization and melting order of the blocks when these transitions overlap or take place very closely. For instance, WAXS measurements taken on cooling demonstrated for the copolymer with PE, PEO, PLLA, and PCL blocks the following trends:

- PE-*b*-PEO-*b*-PCL triblock terpolymers [137], the PE block crystallized first, and then, the PCL block crystalized some degrees before the PEO block (see Fig. 18a)
- In the case of the PE-*b*-PEO-*b*-PLLA sample, the PE block also crystallized first and before the PLLA block, and finally, the PEO block (see Fig. 18b).
- In the PE-*b*-PCL-*b*-PLLA terpolymer, the PE block also crystallized before the PLLA block. But, if the cooling rate is reduced as low as 1 °C/min, the crystallization sequence is modified, and the PLLA block had the ability to crystallize first and before the PE block. Thus, the crystallization order can be reversed by modifying the cooling conditions (see Fig. 18c vs. d) [138]. Because its slow crystallization kinetics, a very low cooling rate allowed the PLLA block to start developing its crystallization at a higher temperature. It can be seen in Fig. 18d that both PLLA and PE blocks crystallized simultaneously over a range of temperatures [138].

The WAXS analysis allows correctly assigning the crystallization peaks observed during the DSC scans upon cooling from melt (see Fig. 18). Particularly, Fig. 19 shows the crystallization sequence of the blocks and how reducing the cooling rate can induce a reversion in the crystallization order. Special mention has the analogous PE-*b*-PEO diblock copolymer. In this double crystalline copolymer, the PE block is crystallized in several steps in a fractionated manner when the PE content is the lowest [137]. If the length and content of the PE block are increased, this block is crystalized in a unique sharp peak at a higher temperature. In addition, in the terpolymer, the PE block started to crystallize from a segregated melt, which enhanced this block's crystallization ability. As a result, the crystallization degree of the PE block also improved.

The order of the crystallization will define the superstructural morphology of the terpolymers; for example, in the PEO-*b*-PCL-*b*-PLLA triblock terpolymers, the PLLA block crystallizes first and templates the subsequent crystallization of the other two blocks with clear changes in birefringence. However, such changes are not well-defined in the terpolymers with a PE block (i.e., PE-*b*-PEO-b-PCL [137], PE-*b*-PCL-*b*-PLLA, and PE-*b*-PEO-*b*-PLLA). In PE-*b*-PEO-*b*-PCL [137] terpolymer, the block that crystallized first, the PE block, developed very small and barely observed spherulites (see Fig. 20a). The subsequent crystallization of the other PCL and PEO blocks was also hardly noticeable. However, following the changes in the light intensity during the cooling scan gave evidence of the crystallization events taking place. When each block started crystallizing, a significant increment in the light intensity was observed at specific temperatures. Those temperatures agreed well with

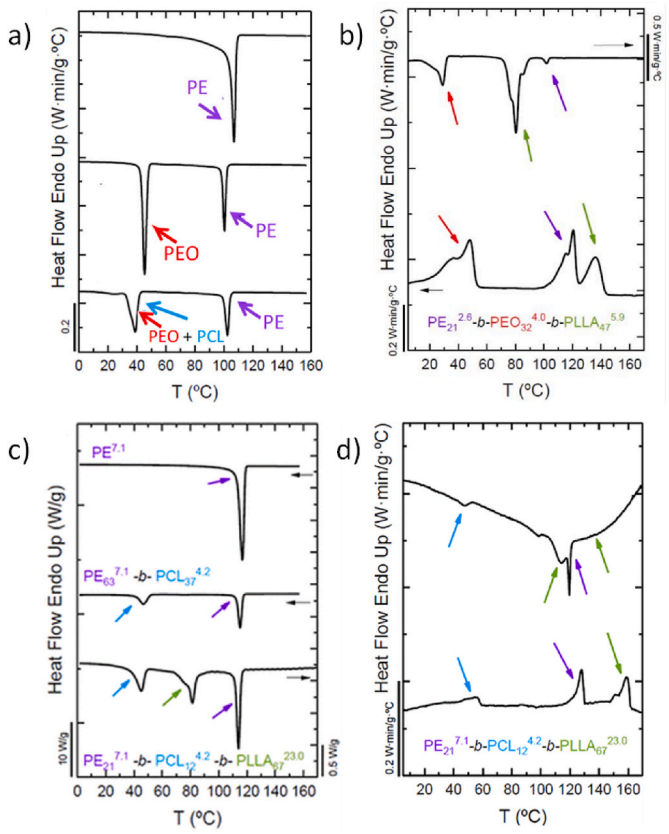

Fig. 19. DSC cooling and heating scans of triple crystalline PE-b-PEO-b PCL, PE-b-PEO-b-PLLA, and PE-b-PCL-b-PLLA triblock terpolymers and analogous double crystalline diblock copolymers. A) $PE_{37}^{9.5}$-b-$PEO_{34}^{8.8}$-b-$PCL_{29}^{7.6}$ (Cooling rate: 20 °C.min^{-1}), b) $PE_{21}^{2.6}$-b-$PEO_{32}^{4.0}$-b-$PLLA_{47}^{5.9}$ (Cooling and heating rate: 1 °C.min^{-1}), c) $PE_{21}^{7.1}$-b-$PCL_{12}^{4.2}$-b-$PLLA_{67}^{23}$ (Cooling rate: 20 °C.min^{-1}), d) $PE_{21}^{7.1}$-b-$PCL_{12}^{4.2}$-b-$PLLA_{67}^{23}$ (Cooling and heating rate:1 °C.min^{-1}). Taken and modified from [137,138].

the crystallization ranges observed by DSC and WAXS analysis.

In the PE-*b*-PCL-*b*-PLLA terpolymer, the first crystallized block is the one that determines the entire morphology. For instance, at high cooling rates (i.e., 20 °C/min), the PE block crystallized and formed very small spherulites (see Fig. 20b), as expected. However, if the cooling rate is reduced to 1 °C/min, the PLLA block is the one that templates the morphology, and very large negative spherulites, with lamellae radially growing, are developed (see Fig. 20c). However, because of the low content of the PE and PCL blocks, it is very difficult to detect morphological changes by optical microscopy as the subsequent crystallization of the other blocks takes place. Nevertheless, in all these terpolymers, as being only weakly segregated, the first block creates the superstructural morphology inside which the other two blocks are forced to crystallize.

Adding a fourth block raises the intricacy of block copolymer crystallization to a higher level. The complexity of having four blocks with the potential ability to crystallize independently lies on the interplay of different thermodynamic factors since each block's miscibility and crystallization kinetics will influence the crystallizability of the other three blocks. Ladelta et al. [144] synthesized for the first time an ABCD tetrablock quaterpolymer with four crystalline phases composed of PE, PEO, PCL, and PLA (PE-*b*-PEO-*b*-PCL-*b*-PLLA) (see Fig. 15). DSC analysis performed at 10 °C/min revealed the crystallization phenomena of all phases. The PEO and PCL blocks melted very close to each other, near 60 °C, as expected. Then, two small endothermic peaks attributed to the melting of the PE and the PLLA block crystals were observed in the high temperature melting range. To favor PLA crystallization, an annealing treatment and a slow cooling rate (1 °C/min) were required. The existence of the four crystalline phases was observed by XRD at room temperature, although it was not simple to identify them since many crystallographic planes of the blocks overlap with each other [144].

These particular tetrablock quaterpolymers exhibit a fascinating melt structure due to the differences in melt miscibility between the different blocks [139]. It is well reported that PLLA, PEO, and PCL blocks are miscible in the melt (see refs. in Ref. [24]). However, when PE is included in these block copolymers, phase segregation could take place due to the intrinsic immiscibility of PE with polar blocks. SAXS experiments in the molten state confirmed a lamellar arrangement of the different phases in these ABCD quaterpolymers. However, the phase segregation was only observed when the length of the PE block was long enough (i.e., 9.500 g/mol) (see Fig. 21a, Q2 quaterpolymer sample). A sharp diffraction peak at low q values and a weaker second-order reflection at 2q were observed at 180 °C, a temperature at which all blocks are molten. These tetrablock quaterpolymers are only weakly segregated, as the molten lamellar structure is destroyed as the crystallization of the blocks takes place. At 25 °C, the crystalline lamellar arrangement scattered X-rays at lower q values. As each block contributes to the segregation strength, phase segregation depends on the composition and molecular weight of each block.

These complex and novel block copolymers are tetracrystalline (see Fig. 21b and c). The four blocks have the potential to crystallize, given that composition, molecular weight, and cooling conditions are correctly tuned. Despite that many diffraction peaks of the blocks overlap, WAXS experiments confirmed the crystallization sequence upon cooling from the melt: first the PLLA block, then the PE, later the PCL, and finally the PEO block [139]. Moreover, each block crystallized independently (see Fig. 21b and c). Interestingly, in one of the quaterpolymers, the PLLA was unable to crystallize, while the other three blocks did. Although the PLLA content and molecular weight in both quaterpolymers were similar, evidence of PLLA crystallization was not observed by both DSC and WAXS analysis in one of them. The reason behind this behaviour lies in the tacticity differences between the PLLA blocks in both quaterpolymers.

A low isotacticity of the PLLA block hinders the crystallization ability of the PLLA chains. Thus, not only content and molecular weight influence the crystallization behaviour, but also other factors such as the

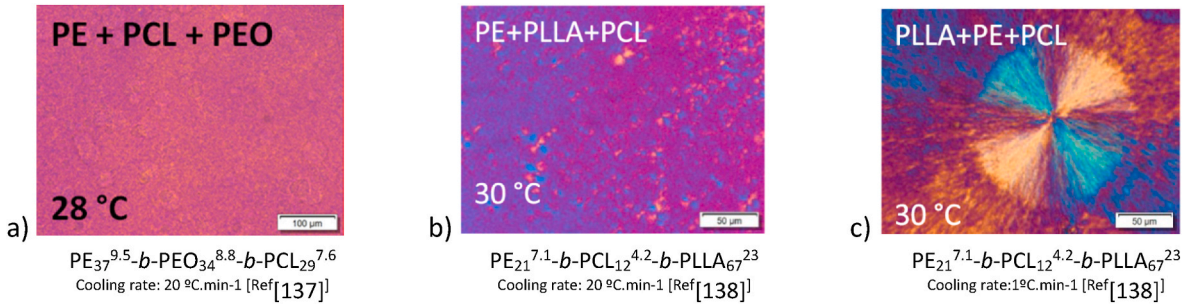

Fig. 20. PLOM micrographs of PE-b-PEO-b PCL and PE-b-PCL-b-PLLA triple crystalline triblock terpolymers. Taken and modified from [137,138].

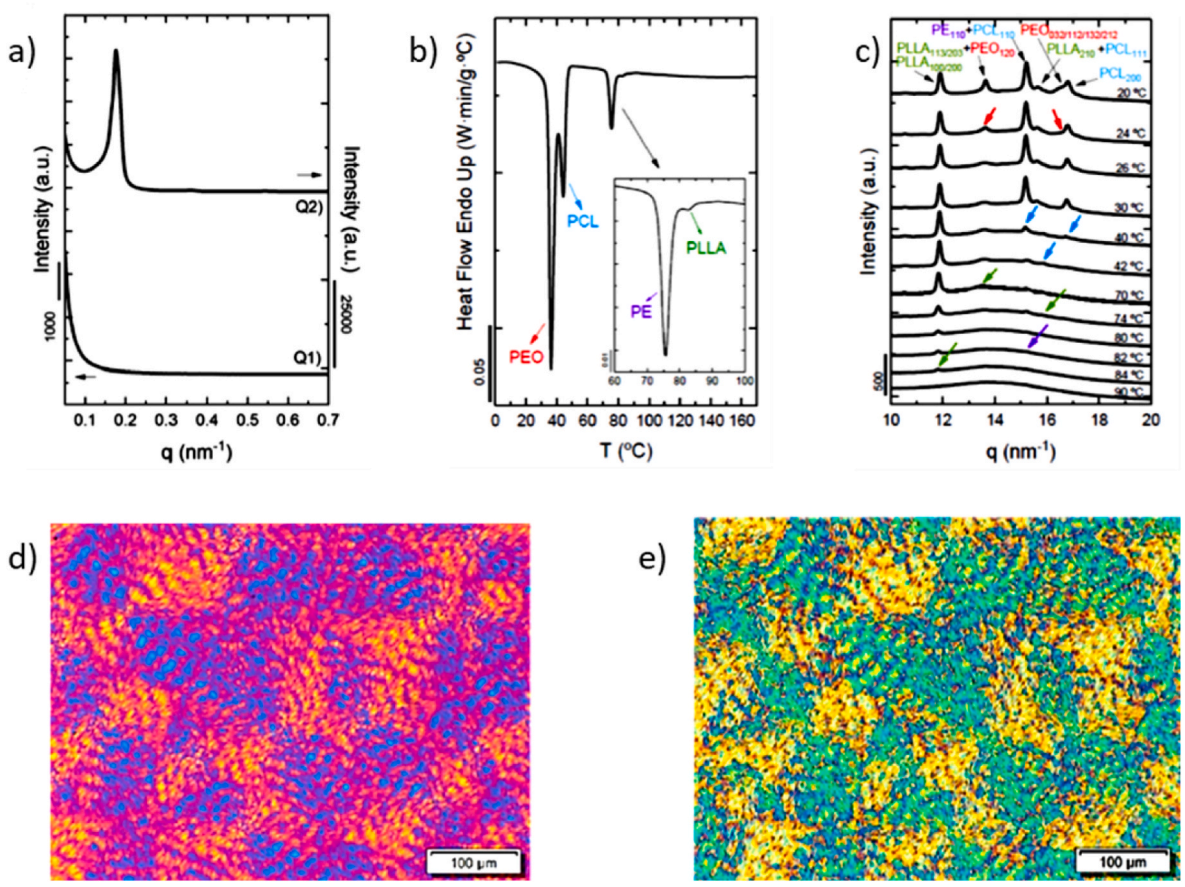

Fig. 21. Description of tetra crystalline PE-b-PEO-b-PCL-b-PLLA tetrablock quaterpolymers by a) SAXS, b) DSC, c) WAXS, and d) and e) PLOM microscopy. PLOM micrographs showing the spherulitic morphology and the change in birefringence. Taken and modified from [139].

block nature. The morphology of these quaterpolymers is defined by small spherulitic structures observed by PLOM, in which sequential changes in light, brightness, and birefringence patterns take place and give evidence of the sequential crystallization events of each block. In Fig. 21d, PLLA has been isothermally crystallized to promote larger spherulites. The subsequent crystallization of the other three blocks is clearly observed through the change in the intensity of the transmitted light and birefringence (see Fig. 21e). Fig. 21e shows the unique morphology of tetracrystalline spherulites composed of four different crystal types, which still keeps a high level of superstructural order as indicated by the clear Maltese Crosses in the impinged negative spherulites and the presence of banding. However, following the crystallization behaviour is quite complicated since the crystallization events of the PLLA and PE overlap, as well as those of the PCL and PEO, since the crystallization range temperatures are similar. Additional nanoindentation experiments revealed that inferior mechanical properties (storage modulus and hardness values) were observed in the quaterpolymer with a smaller fraction of PE and PLLA crystals, as expected [139].

4. Other architectures: stars, combs, multiblock, and segmented block copolymers

4.1. Star, comb, and miktoarm double crystalline diblock copolymers

Highly branched star, comb, and star-comb scPCL-*b*-PLLA diblock copolymers have been investigated by Leng et al. [150] Analogous linear PCL-*b*-PLLA diblock copolymers were also synthesized for comparison purposes. The copolymers were synthesized by sequential copolymerization of CL and L-LA monomers, and the content of the PCL block in scPCL-*b*-PLLA diblock copolymers were 28, 40, 50, and 73%. Fig. 22 describes the architecture of these diblock copolymers.

The crystallization behaviour is highly affected by the composition of the blocks in the star comb copolymer. As the length of the PCL block became longer than PLLA, the T_m and ΔH_m values of the PCL block also increased. On the contrary, the thermal properties of the PLLA block did not follow a clear tendency with PLLA composition. The PLLA block tends to crystallize to a larger extent when the composition is near 50:50; the molten PCL phase in the diblock causes a diluent effect on the PLLA crystallization, providing extra mobility and flexibility to the PLLA chains, enhancing their capacity to crystallize. However, if the length of the PLLA block is too large, this block did not crystallize, possibly due to the slow crystallization kinetics of the PLLA, particularly at large M_w.

Similar to linear diblock copolymers, in these *sc*PCL-*b*-PLLA, a rapid cooling from melt hinders the crystallization of the PLLA block due to its slow crystallization kinetics, as confirmed by WAXS analysis. However, if the sample is previously isothermally crystallized at 110 °C for 2 h, at this temperature, the PCL block is molten, but the PLLA block can crystallize extensively. Since these are melt-miscible diblock copolymers, the PCL block has no other option than to crystallize inside the interlamellar regions of the PLLA crystals during the subsequent cooling from the isothermal step. Therefore, the previously formed PLLA crystals template the crystallization for the second block. If the PCL content is too small (28%) (PCL block length too short), WAXS analysis confirmed that this block could not crystallize. Increasing the PCL content enhanced the crystallization of the PCL block [150].

To establish the influence of the molecular architecture, linear, star, linear comb, and star comb PLLA-*b*-PCL diblock copolymers with similar compositions were analyzed. From DSC analysis, it is clear that the PCL phase highly improves the crystallization ability of the PLLA block in the

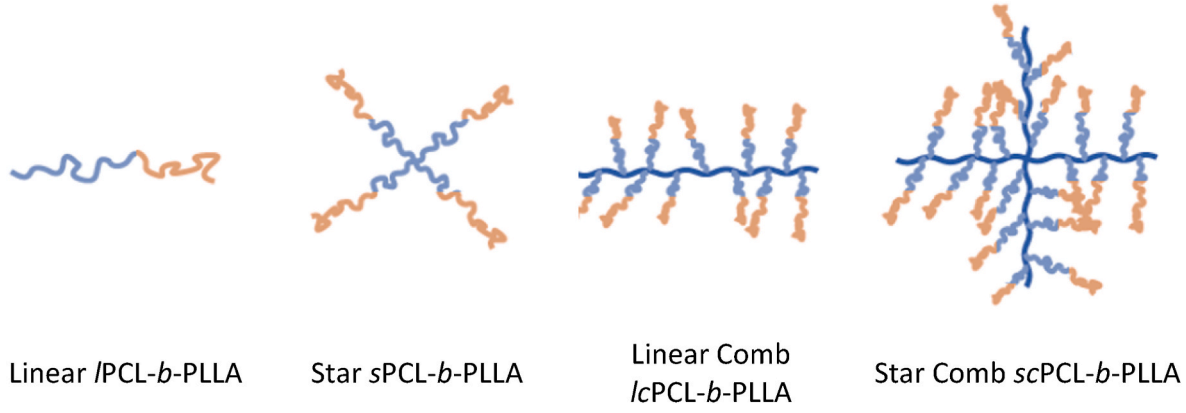

Fig. 22. Schematic representation of the architecture of the PCL-b-PLLA diblock copolymers. The branches in all copolymers are formed by a PCL-b-PLLA diblock structure (PCL block is light blue and PLLA block is light orange). Taken and modified from [150]. (For interpretation of the references to colour in this figure legend, the reader is referred to the Web version of this article.)

star and linear comb configurations. The crystallinity of the PCL block is also improved. In these copolymers, the PLLA block is at the extreme of the branches. Compared to linear, the star and linear comb shape configurations have more end groups and provide larger free volume that increases the flexibility and mobility of the polymer chains. In the scPLLA-*b*-PCL diblock copolymer, the more complex topological architecture of the star comb configuration restricted the crystallization of both blocks to some extent. WAXS analysis of melt crystallized samples confirmed the DSC results. Both blocks crystallized in the star and linear comb configurations, while in the linear and star comb architectures, the PLLA block remained amorphous due to topological constraints. A spherulitic morphology templated by the PLLA block is observed in most copolymers, with a characteristic birefringence change due to subsequent PCL crystallization along the previously formed PLLA crystals [150].

Four-armed star PLLA-*b*-PCL diblock copolymers with increasing PLLA content were double crystalline [151]. However, WAXS analysis demonstrated that the crystallization form of the PLLA block differs with PLLA content. For instance, in block copolymers with a lower PLLA content, this block forms α-or δ-form crystallites, while at higher PLLA content, the dominant crystalline form is the α-form. As the PLLA content increases, the PLLA crystallinity determined by WAXS increases while that of the PCL block reduces. However, for low PLLA contents, this block cannot crystallize, and only the PCL crystallites are observed. The thermal properties (T_m, ΔH_m) of PLLA and PCL blocks in the star copolymers decreased with decreasing the content (molecular weights) of PLLA and PCL blocks, respectively. Thus, the molecular weight of each block determines the crystalline lamellar thickness. Compared to star-shaped PLLA homopolymer that cannot crystallize, the improvement of the PCL chains over the PLLA crystallization is again demonstrated [151].

Isothermal crystallization kinetics experiments demonstrated that the content of the PLLA block (block length) in those star copolymers in which the PLLA block can crystallize does not significantly influence the crystallization rate. The Avrami index n was close to 3 for all the samples [151]. Crosslinking of the star block copolymers by diisocyanate was conducted to create a network to improve the toughness of the material. However, the crosslinking reactions disturb the crystallization ability of the star diblock copolymers, and the crystallinity reduces. Only the PCL block remained crystalline after crosslinking. That is a result of the higher segmental mobility of PCL. This behaviour was confirmed by WAXS and DSC analysis [151]. The ΔH_m values for PCL and PLLA blocks were higher before crosslinking than after. Crosslinking also alters the crystallization kinetics as the Avrami index values are reduced, and only poor crystalline superstructures are obtained [151].

Star and miktoarm block-shaped diblock copolymers were also evaluated by Yan et al. [152] (see Fig. 23). In star block copolymers, the crystallization of the PCL block is highly reduced. However, in the miktoarm architecture, the crystallization behaviour of PCL is enhanced, as measured by DSC. In the star configuration, the PCL block is in the middle, and the PLLA block is in the extreme, with enough flexibility and molecular mobility to rearrange crystalline structures. This configuration might cause restrictions over the middle PCL block and limit its crystallization.

However, in the miktoarm configuration, the PCL and PLLA blocks are linked to the macroinitiator directly and independently. As a consequence, the PCL block crystallization became easier, and both crystallization peaks for the PCL and PLLA segment were observed in the DSC cooling scan. The melting peak of the PLLA block also became wider. The WAXS analysis confirmed the DSC results. Very weak peaks for PCL crystals were observed in the star-shaped copolymers. Nevertheless, the intensity of the PCL peaks in the miktoarm copolymer increased. When the crystalline polymer chains are connected at the same point (miktoarm copolymers), each segment can crystallize freely and maintain the original crystal conformation. On the contrary, in the star copolymer, the outer PLLA block segment will restrict the mobility and crystallizability of the inner PCL block [152].

Xiang et al. [153] also evaluated the crystallization of the PLLA block in 4 star block copolymers of PLLA and PEG, with two PLLA ends confined and high PLLA content. Upon cooling from the melt at different cooling rates, the PLLA T_c and ΔH_c increased as the cooling rate decreased since slower rates provide more time for the polymer chains to arrange into crystalline structures. This behaviour is similar to the one observed in linear architectures. However, the values are lower than the ones obtained in the analogous linear copolymers. Unlike the PLLA-*b*-PCL star copolymers reported by Leng et al. [150], in this case, the branch structures in the PLLA-*b*-PEG star copolymers increased the steric hindrance and viscosity, disturbing the PLLA crystallization. This effect became even more significant when the PLLA block was joined to the macroinitiator at one end and the PEG block at the other, restricting the PLLA mobility. This indicates that the crystallization behaviour is not only a reflection of the molecular architecture, and other factors such as cooling conditions and M_w should be considered. On the contrary, PLLA T_m and ΔH_m remained similar in all star copolymers, and the values diminished as the cooling rate increases.

Star block copolymers based on both PEO and PCL are reported by Wei et al. [154] In these copolymers, the PEO block is joined on one end to the macroinitiator and on the other end to the PCL block. Both blocks crystallized coincidentally due to their symmetrical composition. These star copolymers exhibited lower T_m, Tc, and crystallinity compared to the linear versions. Very interesting morphologies were developed in solution-cast films by a slow evaporative crystallization procedure. The

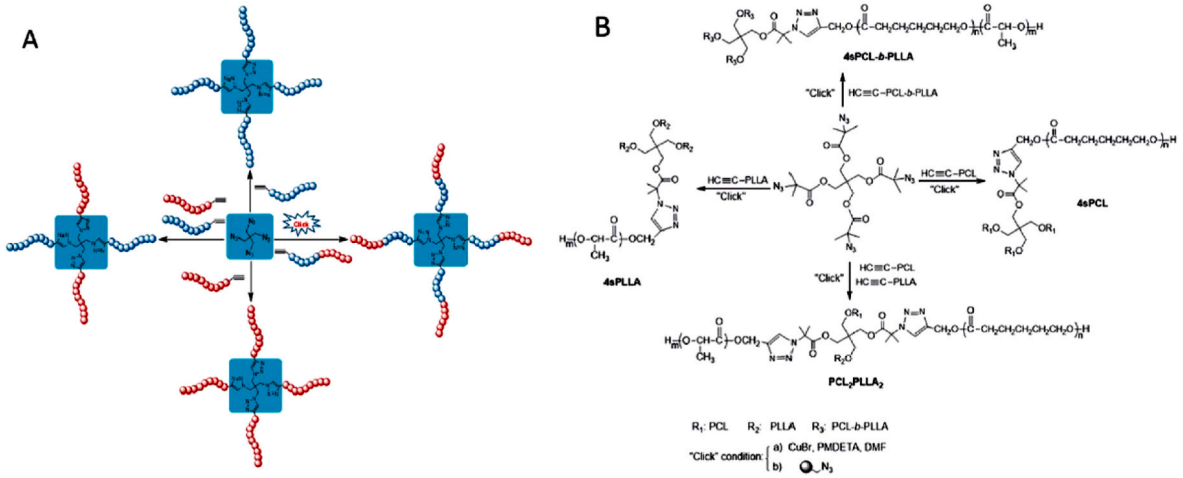

Fig. 23. Synthetic strategy (A) and route (B) of star, star-block, and miktoarm star diblock copolymers. Taken and modified from [152].

micro-scale structure was composed of well-defined ring-banded concentric spherulites with a characteristic Maltese cross extinction pattern, as previously reported in linear counterparts with symmetrical compositions. The PCL block dominated the morphology as it started crystallizing first and controlled the periodic growth [154].

These star copolymers had also been synthesized in a miktoarm architecture, and the crystallization behaviour has been analyzed by Zhang et al. [155] Moreover, comparisons with analogous linear copolymers have been established. Similar to star copolymers reported by Wei et al. [154], these PCL-*b*-PEG miktoarm copolymers also exhibited lower T_m and T_c. In this case, the core of the miktoarm star polymer might hinder their crystallization. Increasing the length of blocks favored the crystallization and produced an increment T_m values.

By comparing these works, we can acknowledge the effect of the molecular architecture: star block [154] vs. miktoarm star block [155] on the thermal properties of copolymers containing PCL and PEO/PEG blocks. Having a similar molecular weight of both blocks (around 2.0–2.7K) in both star copolymers, it is clear that the miktoarm configuration enhances the crystallization as the T_m of PCL and PEG blocks were 50.9–55.7 °C and 46.7 °C, respectively [155]. While in the star block architecture, these values were lower, the T_m of PCL and PEO blocks were 42.7 and 39.8 °C [154], respectively. In this last one, the PEO block is joined at one end to the macroinitiator core and the other to the PCL block. Thus, its crystallization is, to some extent, more limited than in the miktoarm configuration, in which the PEG block is freely jointed in one of its ends. In addition, other miktoarm star block copolymers are composed of PCL and PDMS, and the crystallization behaviour is similar to the aforementioned copolymers. As the PCL content increases, the crystallization of the PDMS block (which crystallizes after) is reduced [156]. Similar results are recently reported by María et al. [157] in miktoarm copolymers containing PEO and PVDF. The star arms crystallized faster than the analogous precursors. In addition, the PVDF phase exhibited polymorphism in the precursors but an exclusive β crystalline phase in the miktoarm copolymer [157].

Besides stars, brush or comb constitute another interesting architecture in block copolymers. Nikovia et al. [158] reported statistic/block brush copolymers consisting of a polynorbornene (PNBE) backbone with PLLA and PCL side chains. The arrangement of these side chains can be a brush or statistic (see Fig. 24e and f). Both PLLA and PCL formed independent crystalline lamellar phases in the symmetrical composition. However, if the PCL content is reduced to 20%, its crystallization is suppressed regardless of the molecular architecture. That is a similar tendency to linear and star PLLA-*b*-PCL copolymers with low PCL content (e.g., 25% [68], 28% [150]), in which, in neither case, the PCL was able to crystallize. Likewise, the statistic and brush copolymers

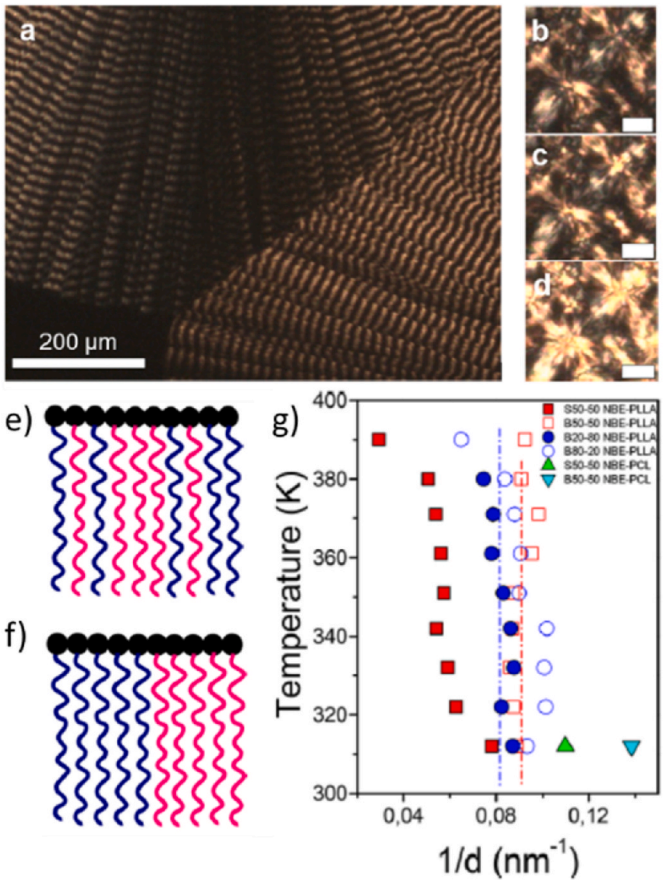

Fig. 24. a) PLOM image of banded spherulites of the symmetrical brush copolymer taken under isothermal conditions at 393 K. Only PLLA can crystallize, b) subsequent crystallization of the PCL phase in the symmetrical statistical copolymer. Birefringence change. Schematic representation of molecular architecture e) statistics, f) brush, g) Temperature dependence of the inverse long period from SAXS analysis. (Right) Taken and modified from [158].

exhibited lower T_m and T_c than the analogous macromonomers.

The macromolecular architecture affected the crystallization behaviour. For instance, the PLLA block, usually characterized by a slow crystallization, could only cold-crystallize in the statistical copolymer. However, in the brush copolymer, this block crystallized upon cooling

from the melt. Interestingly, the PLLA isothermal crystallization rate was faster and the PLLA lamellar thickness was larger, particularly in the symmetrical 50-50 PLLA-*b*-PCL statistic copolymers (see Fig. 24g (closed red squares)), in comparison to the analogous PLLA-*b*-PCL brush copolymer of the same composition (open red squares). On the contrary, the PLLA lamellar dimension in the brush copolymer was similar regardless of composition. Being melt-miscible copolymers, the PLLA phase templates the morphology, and a significant change in the brightness accounted for the subsequent crystallization of the PCL phase inside the previously formed PLLA crystals. Clear PLLA banded spherulites were formed in the symmetrical brush copolymer (see Fig. 24 a-d).

4.2. Multiblock and segmented block copolymers

Unlike strictly linear double crystalline AB diblock copolymers, the crystallization behaviour in multiblock copolymers might be hampered in one of the phases [159,160]. For instance, PLLA-*b*-PCL diblock copolymers have been extensively reported as a double crystalline system, in which the initial crystallization of PLLA templates the subsequent crystallization of the PCL block, and the morphology remained unaltered. However, Jeon et al. [160] have reported PLLA-*mb*-PCL multiblock or segmented copolymers in which only PLLA block achieved some crystallization. Even at very high PCL content, this block could not crystallize, which means that composition is only one of the factors to be tuned in order to obtain a double crystalline nature. This section will focus only on multiblock copolymers with a double crystalline nature.

4.2.1. PBS based multiblock copolymers

PBS is one of the most promising biodegradable aliphatic polyesters due to its advantageous thermal and mechanical properties, similar to a commodity polymer like polyethylene. However, it lacks good impact resistance, and its high crystallinity limits its crystallization rate. For that reason, PBS has been copolymerized with other monomers to reduce its crystallinity and improve processability, chemical resistance, and mechanical performance. Several blocks such as PCL [161,162], PLA [163], poly(tetramethylene oxide) (PTMO) [164], poly(butylene sebacate) (PBSe) [165], and poly(butylene fumarate) (PBF) [166] have been incorporated to PBS copolymers following a multiblock structure with hard and soft segments. Some of these multiblock copolymers are phase segregated in the melt, and in many of them, the PBS block crystallizes first.

A double crystalline system involves PBSe as a comonomer. The PBSe phase improves the tensile mechanical properties of the PBS-*mb*-PBSe, increasing the elongation at break. The mechanical behaviour reflects the crystallinity and morphology of these segmented copolymers, in which both phases can crystallize, provided the cooling conditions are suitable and adjusted. In these multiblock PBS-*mb*-PBSe copolymers [165], both phases can crystallize. Upon cooling from the melt at 5 °C. min^{-1}, two well-separated crystallization exotherms are observed. The PBS block crystallizes at high temperatures and then crystallizes the PBSe block at lower temperatures. Increasing the content of the PBSe blocks reduces the T_c and the crystallinity of both phases compared to the homopolymer, as expected. The molten PBSe chains might induce a plasticizing effect over the PBS crystallization.

On the other hand, as a melt-miscible system, the crystallization of both phases takes place sequentially, and PBS crystallization that happens first templates the morphology of the system, forcing the PBSe crystallization to occur inside the PBS interlamellar regions and restricting its crystallization ability. No important changes were observed in the T_m of both phases, except for a rather small decrease in the melting peak. In the case of copolymers with PBS, a small crystallization exotherm just before the melting is commonly observed for the PBS phase. It obeys a melt-recrystallization (reorganization) event similar to the one observed in other polyesters, such as PLLA. WAXS analysis confirmed the double crystalline nature of these multiblock copolymers with no influence on the crystal structure of each block. Both phases crystallized separately and sequentially upon cooling. As PBS templates the crystalline morphology into spherulites, only a distinctive, although slight, change in birefringence accounted for PBSe crystallization [165].

When copolymerized with PCL, the impact strength of PBS greatly enhances. Because of that, it is interesting to understand the crystallization behaviour. Double crystalline PBS-mb-PCL diblock copolymers have been reported by Huang et al. [161] and Ponjavic et al. [162] Huang et al. [161] demonstrated the reversibility of the alternated lamellar structure in these copolymers induced by sequential crystallization/melting thermal protocol. Despite being a melt-segregated system, the PBS phase that crystallizes first can disrupt this segregation and is ordered in 3D spherulitic structures inside which the subsequent PCL phase crystallizes. Each block crystallizes separately in its own crystalline structure, and the crystallization of the PCL block did not modify the crystalline morphology previously templated by the crystallization of the PBS block. Similar to linear PLLA-*b*-PCL diblock copolymers, only the magnitude of the birefringence changes. SAXS evaluations showed that the periodic lamellar structure is recovered prior to the PCL phase crystallization if the sample is again heated and the PCL crystals are melted.

In segmented polyurethane copolymers based on PBS and PEG, the non-isothermal crystallization kinetics of the PBS segment was enhanced after the inclusion of a high content of PEG [167]. Unlike the PBS-*mb*-PCL copolymers, in these copolymers, both segments are miscible. The PBS chains crystallize first, and then the PEG chains. Thus, the mobility of the molten PEG chains improved the crystallizability of the PBS segment. Intermediate compositions exhibited a double crystalline nature. The 3D superstructural morphology revealed banded spherulites in all compositions. As the PEG content increased, the periodicity of the lamellar twisting became larger. The Avrami indexes obtained were between 2 and 4 for both segments [167].

The analysis of the crystallization behaviour becomes more complex when the thermal properties of both segments are nearby. Huang et al. [164] reported PBS-*mb*-PTMO block copolymers with high content of PTMO phase, in which the crystallization temperatures of both blocks were close to each other. The PBS was isothermally crystallized at different times to isolate the crystallization effect of this block. As the crystallization time of the PBS block increases, the PTMO block crystallizes in a fractionated manner upon subsequent dynamic cooling. Longer crystallization times enriched the crystalline phase of the PBS block and partially confined the PTMO chains in the PBS interlamellar regions, reducing the PTMO T_c.

Unlike the PBS multiblock copolymers mentioned above, in the PBS-*mb*-PLLA [163] system, the PLLA blocks crystallize and melt at higher temperatures than the PBS blocks. Therefore, the first crystallization of the PLLA block conditions the crystallization of the PBS blocks. As a melt-miscible system, the PLLA forms superstructures inside which the PBS block crystallizes after cooling from the melt. The expected change in birefringence was observed. The observation of a single T_g confirmed the melt miscibility through DSC measurements [163]. Only a double crystalline system is obtained when the PBS composition is 80%. Two clear endothermic peaks were observed in the heating scan and corresponded to the sequential melting of the PBS and PLLA crystals. But, if the composition is reduced to 30%, the PBS block cannot crystallize. Moreover, compared to the PLLA homopolymer, the PLLA T_m in the copolymer was reduced due to a diluent effect caused by the molten chains coming from the previously melted PBS crystals. The effect of the composition is clear in the microstructural morphology. At high PLLA content (70%), the superstructures formed were 3D spherulitic-like with some distortion and ill-defined banding. However, this morphology changed radically when PLLA content was very low (20%), and a dendritic structure was observed (see Fig. 25b). Consider that both samples were crystallized at a temperature at which only the PLLA block can crystallize. The subsequent crystallization of the PBS block at lower temperatures is nucleated by the previously formed PLLA crystals. Since

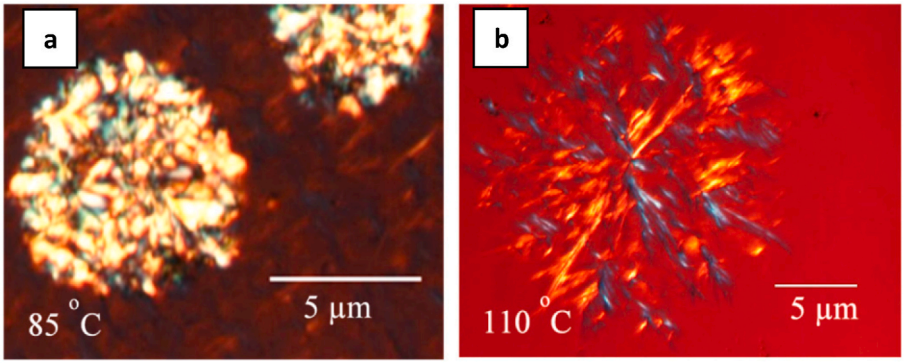

Fig. 25. *PLOM micrographs of multiblock copolymers (a) $LL^{5.4}_{70}$-mb-$BS^{7.4}_{30}$ and (b) $LL^{5.4}_{20}$-mb-$BS^{7.4}_{80}$ during isothermal crystallization at the indicated T_c. Taken from* Ref. [163].

double crystallization is only observed when PBS is in majority, confinement of the PBS block during crystallization is not expected [163].

The crystallization features of both blocks are affected by the crystallizability of the other block [163]. The overall crystallization rate of each block in the copolymer was reduced compared to the analogous homopolymer. The previously crystallized PLLA block affected the crystallization of the PBS block. The PLLA crystals retarded the crystallization of the PBS block, even though it is not a confined environment. In the other case, the crystallization kinetics of the PLLA blocks was also retarded, probably due to the presence of the molten PBS chains, enhancing the mobility of the PLLA chains excessively (see Fig. 26) [163]. The Avrami index agreed well with the morphology observed by PLOM, as values around 3 were obtained in PBS-*mb*-PLLA multiblock copolymer with high PLLA content. An index value of 3 indicates an instantaneously nucleated three-dimensional superstructure [163] (see Fig. 25).

The abovementioned observations are comparable with the crystallization behaviour of PDLA-*b*-PBS-*b*-PDLA triblock copolymer [168]. In this system, the PDLA block also melts at a higher temperature than the PBS block. Despite being a linear block copolymer, the crystallization kinetics are analogous as the block crystallized slower than the homopolymers. However, the triblock copolymer with shorter PDLA blocks exhibited a faster crystallization rate. Depending on the T_c, the crystallization rate might be reduced if the length of the PDLA block is too large. The subsequent crystallization of the PBS block (after crystallizing the PDLA block until saturation) revealed that medium PDLA block lengths enhanced the crystallizability of the PBS block as a result of the nucleating effect caused by the PDLA crystals. However, if the content of PDLA is too high, the crystallization rate of the PBS block is reduced due to space restrictions. The Avrami fitting to the crystallization kinetics data revealed similar behaviour to the PBS-*mb*-PLLA [163] since *n* values mainly close to 3 were obtained for the PDLA and PBS block. A three-dimensional and heterogeneous nucleation mechanism dominated the crystallization behaviour [169]. The *n* value reduced as the restrictions to PBS crystallization became more significant (increased PDLA content) [168–170].

Another system in which the second comonomer melts at a higher temperature than PBS is the PBS-*mb*-PBF multiblock copolymer. The fumarate units are copolymerized with succinate units to introduce double bonds in the main chain that can act as site units for further crosslinking reactions. In this way, polyesters with enhanced and elastomeric properties can be obtained. However, analyzing the crystallization behaviour is more complex because the melting temperatures of both blocks are close to each other (111 and 129 °C, for PBS and PBF, respectively [166]), and the similarity between chemical structures of the blocks can induce an isomorphic or isodimorphic co-crystallization behaviour [171]. Also, crosslinking can modify the crystallinity.

Sheikholeslami et al. [166] evaluated the crystallization behaviour of uncrosslinked and crosslinked PBS-*mb*-PBF multiblock copolymers. From DSC analysis, only one melting peak was observed during the second heating scan, and the T_m value shifted from 115 to 118 °C as the content of PBF increased from 10 to 30% (see Fig. 27). The authors claim that the increased T_m with composition revealed an isomorphic co-crystallization behaviour. That means that both comonomers of similar configurations crystallize together in a single crystal lattice. In isodimorphic crystallization, the T_m values first decrease and then increase; both comonomers crystallize in their own structures with some inclusions of the other comonomer as a function of composition or even coexisting together. In these multiblock copolymers, the T_m value is between both homopolymers and increases with PBF composition [166], which means that PBS and PBF are probably co-crystallizing in a

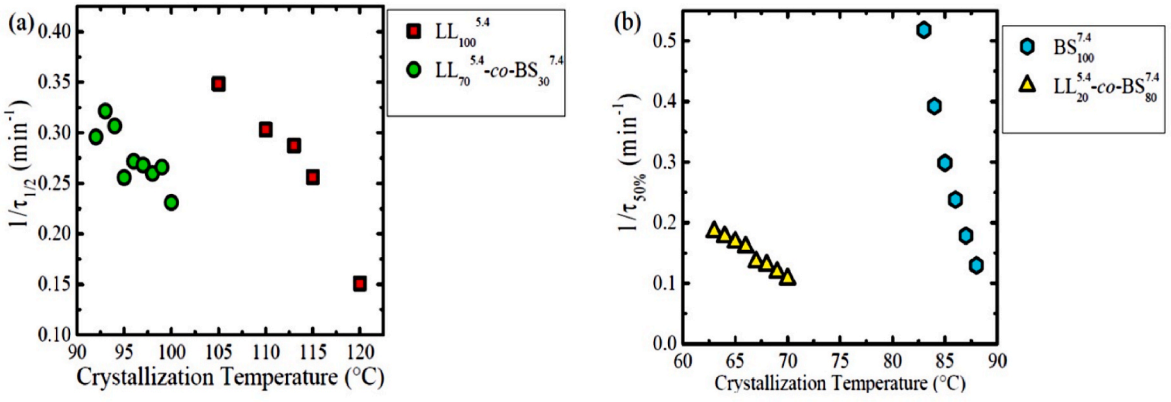

Fig. 26. *Overall crystallization rate ($1/\tau_{50\%}$ exp) versus crystallization temperature (T_c) for (a) PLLA homopolymer and PLLA blocks within the $LL^{5.4}_{70}$-mb-$BS^{7.4}_{30}$ copolymer; and (b) PBS homopolymer and PBS blocks within $LL^{5.4}_{20}$-mb-$BS^{7.4}_{80}$ multiblock copolymers. Taken from* Ref. [163].

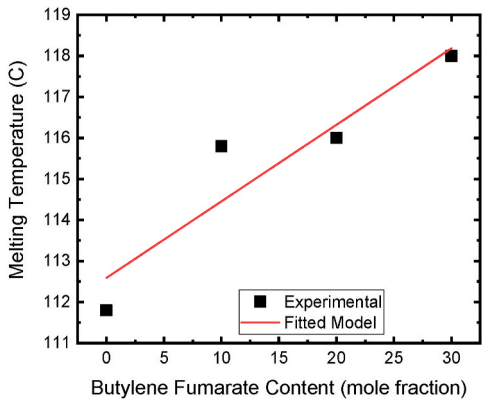

Fig. 27. Composition dependence of the melting temperature of PBS-BF short-segmented block copolymers. Taken from Ref. [166].

single crystal unit with the majority of PBS segment chains. However, the authors should have provided further evidence by WAXS analysis to confirm modifications of the crystalline lattice due to the isomorphism.

In addition, increasing the PBF content in the copolymer reduced the supercooling, which indicated that the PBF segments enhanced the crystallization ability of the PBS-*mb*-PBF multiblock copolymers. The analysis of the non-isothermal crystallization kinetics also revealed a faster crystallization rate in the multiblock copolymers with 30% PBF. The fitting to the Avrami equation suggested the formation of spherulitic superstructures as n values were 3 [166]. The reason behind the enhanced crystallization might be the slightly rigid double bond in the PBF that could reduce to some extent the very high mobility of the highly flexible PBS chains, inducing the chain folding at shorter times or higher crystallization temperatures. If the sample is crosslinked, the crystallization kinetics become slower as the molecular mobility and the diffusion ability are reduced (see Fig. 28).

Finally, another interesting copolymer from the PBS family is poly (butylene succinate-*co*-adipate) (PBSA). The PBSA is a random copolymer with increased flexibility and lower crystallinity than the PBS. This random copolymer has been copolymerized with PLLA to obtain soft-hard segment block copolymers. Wu et al. [172] have reported the crystallization behaviour of these PBSA-*mb*-PLLA multiblock copolymers and the effect of different nucleating agents: talc, nanosized zinc citrate (ZnCC), and 1,10-(ethane-1,2-diyl)bis(3-henylurea) (BUr1). The three nucleating agents increased the melt crystallization temperature and crystallinity of the PLLA segment. However, no influence was observed in the PBSA phase, as it seems that this phase remained amorphous in the copolymer. Although the PBSA prepolymer can crystallize pure and with nucleating agents, its crystallization was

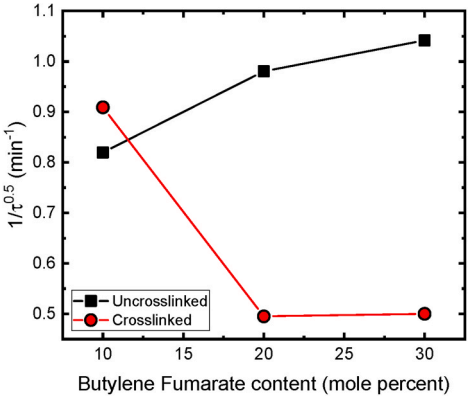

Fig. 28. Inverse of tao 50% with the butylene fumarate content uncrosslinked and crosslinked copolyesters. Taken from Ref. [166].

suppressed when copolymerized with PLLA, particularly at lower concentrations.

4.2.2. Other multiblock copolymers

Other multiblock copolymers, different from the PBS family, include poly(ether-*mb*-amide) [173], poly(ethylene terephthalate)-*mb*-poly (oxyhexane) [174], poly(butylene terephthalate)-*b*-poly(ethylene oxide)-*b*-poly(propylene oxide)-*b*-poly(ethylene oxide) [159] and poly (hexamethylene carbonate)-*co*-poly(hexamethylene urethane) [175], poly(amide-*b*-ether) [176], to mention a few. These segmented copolymers include soft and hard segments as characteristic features. They are also double crystalline and exhibit some phase segregation. Poly (ether-*mb*-amide) multiblock copolymer (PEAc) [173] are built with long-chain carbon polyamide 1012 (PA1012) as hard segments and poly (tetramethylene oxide) (PTMO) as soft segments. These multiblock copolymers are partially segregated in the melt, although the crystallization of the PA1012 hard segments disrupts the phase segregation. The weak melt-segregation was demonstrated not by standard SAXS experiments but by rheological measurements. A nonlinear relationship between log G′ and log G″ is exhibited by the copolymer in the melt state, demonstrating microphase separation to some extent since the storage modulus (*G*') and the loss modulus (G") are sensitive to phase separation. In addition, two clear glass transitions corresponding to each segment were detected by DMA experiments. That is also a sign of melt segregation, although phase segregation is weak. Upon cooling from the melt, the PA1012 hard segments started to crystallize first (between 120 and 160 °C), destroyed the microphase separation, and templated the morphology for the subsequent crystallization of the other segment (see Fig. 29). Then, the PTMO segment also crystallized at approximately 0 °C, and a double crystalline copolymer was obtained. Increasing the PTMO content caused a diluent effect over PA1012 crystallization, as its crystallization temperature is shifted to lower values due to partial miscibility between the segments. Moreover, as the PTMO phase became larger, the spherulitic structure became more diffuse, and the border of the spherulites was less clear. The morphology resembled more 2D axialitic structures(see Fig. 29) [173].

The authors [173] performed an exhaustive analysis of the interlamellar assembly of these PA1012-mb-PTMO multiblock copolymers employing SAXS technique. Despite the rheological and DMA analysis showing some weak segregation, these multiblock copolymers are apparently melt-miscible since no scattering signal in the molten state (i.e., 220 °C) was observed. The absence of scattering might obey the negligible electron density difference between the amorphous phases of PA1012 and PTMO. Then, as the copolymers are cooled down, the long-period values are reduced as temperature decreases due to the crystallization of PA1012 phase and the contraction of the mixed PA1012/PTMO amorphous phase. The lamellar arrangement of the PA1012 crystals is detected, developing from 165 to 40 °C. Interestingly, at around 0 °C, the long period was further and largely reduced (see Fig. 30b). This point agrees with the crystallization onset of the PTMO segments at lower temperatures. The variation of the lamellar thickness can be further analyzed through the K(z) functions (see Fig. 30c). This way, the lamellar thickness of the crystalline (l_c) and amorphous (l_a) phases can be calculated. The increase of l_a value at 40 °C with PTMO content obeyed the contribution of the amorphous and molten PTMO-rich phase. That gave evidence of the localization of the amorphous PTMO-rich phase inside the interlamellar amorphous regions of the PA1012 spherulites. The excluded PA1012/PTMO amorphous phase to the region between the PA1012 lamellae enlarged the periodic interlamellar distance. After PTMO crystallization at −40 °C, the crystalline lamellar thickness l_c is further decreased because the PTMO lamellae are partially intercalated between the PA1012 lamellae [173].

Similar to PA1012-mb-PTMO samples, the multiblock copolymers based on poly(ethylene terephthalate)-*mb*-poly(oxyhexane) (PET-*mb*-poly(1,6 HD)) reported by Flores et al. [174] exhibited a weakly segregated amorphous phase as DMTA, and Flash DSC also detected two

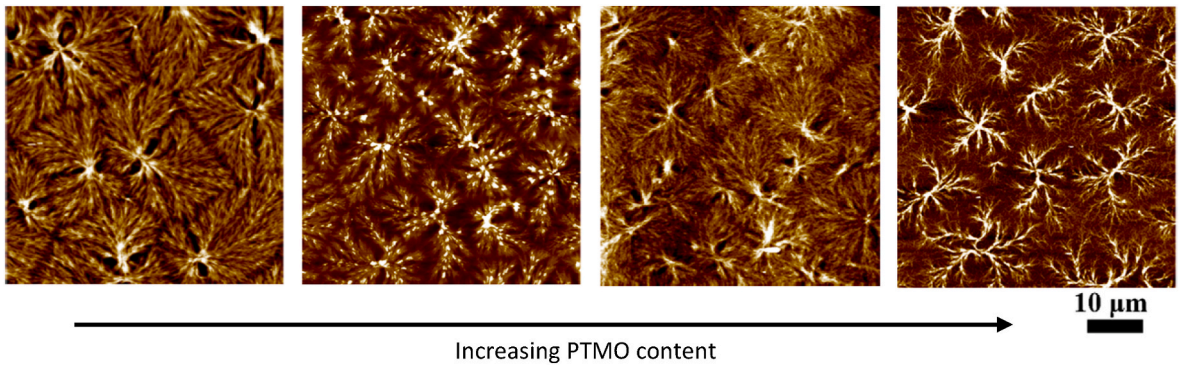

Fig. 29. AFM height images of PA1012-mb-PTMO copolymers thin films with a thickness of 200 nm cooled from melt at 10 °C.min^{-1} and observed at room temperature. Taken from [173].

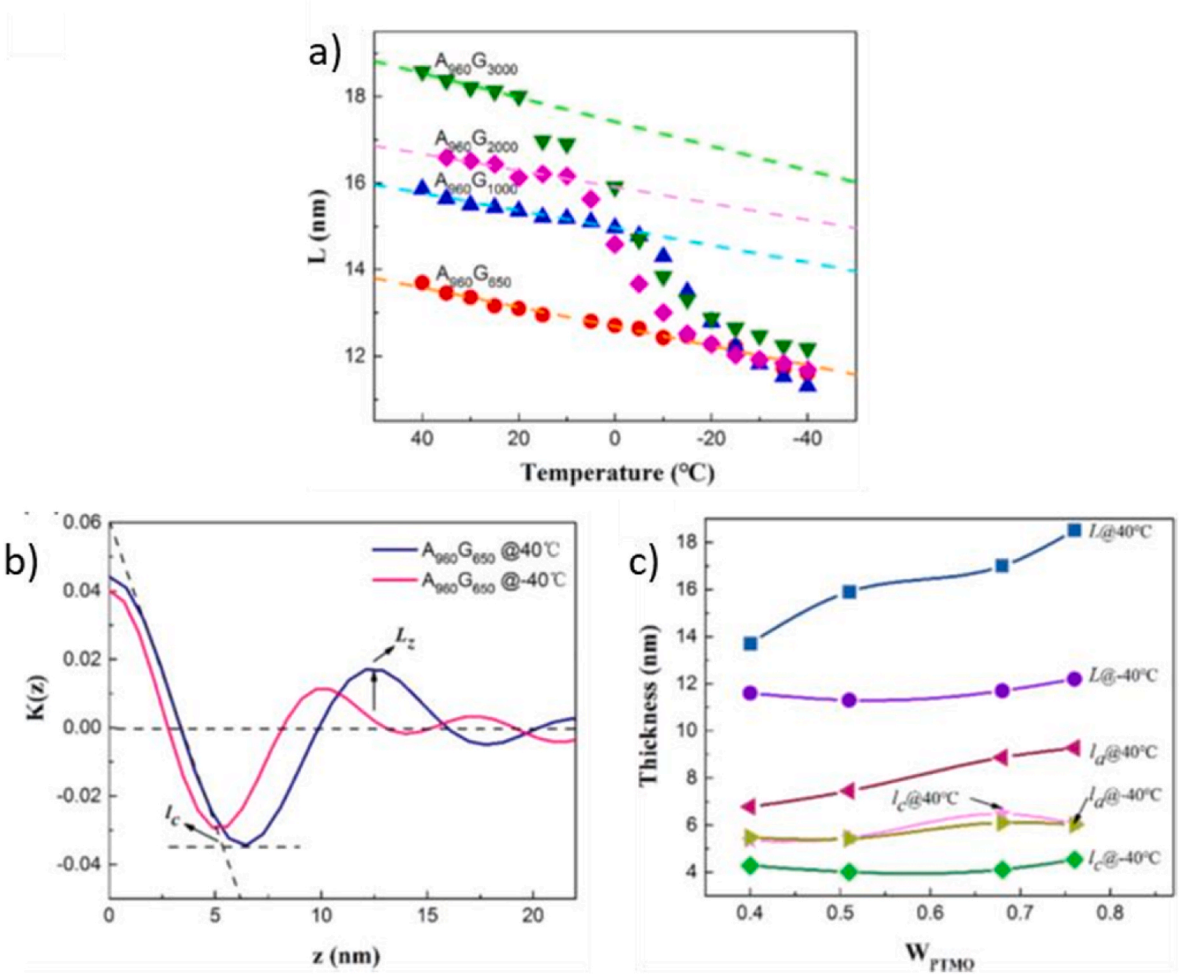

Fig. 30. *a)* a) Lorentz corrected 1D integrated SAXS curves of PA1012-mb-PTMO copolymers during cooling, b) calculated long period (L) value of PA1012-mb-PTMO samples, c) K(z) curves derived from SAXS data, and d) calculated long period from SAXS curve (L), calculated long period from K(z) curves (Lz), lamellar thickness (l_c) and thickness of amorphous regions (l_a). Taken and modified from Ref. [173].

glass transitions. Each T_g corresponds to each segment (see Fig. 31a). These PET-*mb*-poly(1,6 HD) multiblock copolymers are double crystalline, with melting temperatures around 50 and 240 °C. SAXS also showed no segregation in the melt, denoting only partial immiscibility. The glass transitions observed in Fig. 31a could demonstrate that in the PET-rich phase, a small amount of poly(1,6 HD) chains is dissolved, which is responsible for the depression of the PET T_g. If the poly(1,6 HD) content increases, this reduction is more important due to a plasticizing effect (see Fig. 31a).

Correspondingly, the poly(1,6 HD)-rich phase might include some polymeric chains from the PET phase. Flores et al. [174] conducted a comprehensive analysis of the crystallization kinetics. Due to their differences in their crystallization temperatures (poly(1,6 HD) crystallizes at much lower temperatures than PET), while the PET segment is isothermally crystallized, the poly(1,6 HD) segment is molten. Compared to PET homopolymer, a reduction in the overall

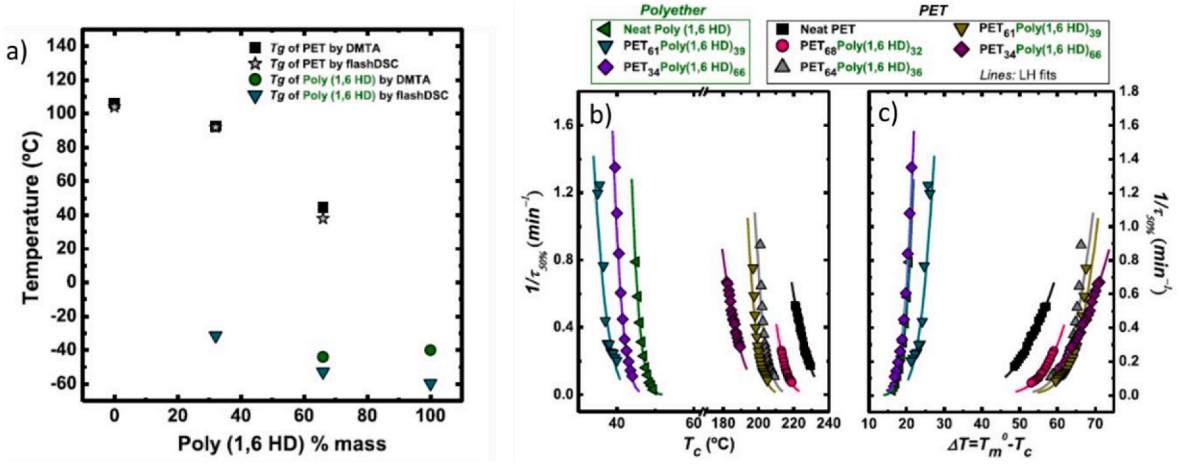

Fig. 31. a)T_g values of some copolymers PET_xpoly(1,6 HD)$_y$ as a function of poly(1,6 HD) content in the copolymer b) Overall crystallization rate ($1/\tau_{50\%}$) as a function of isothermal T_c and supercooling ($T_m^o - T_c$) for PET-mb-poly(1,6 HD) copolymers. Taken and modified from Ref. [174].

crystallization rate of the PET phase within the copolymers was observed (see Fig. 31b). Since these are segmented copolymers, the molten poly(1,6 HD) chains tethered to both ends of the PET segments provided excessive mobility that ultimately can difficult the crystallization of the PET segments close to them. Therefore, the crystallization kinetics of the PET is reduced. Similar behaviour is exhibited by the poly (1,6 HD) segments. However, in this case, the restrictions imposed for the previously formed PET crystals are the ones responsible for the decrease in the poly(1,6 HD) crystallization kinetics. These observations are similar to the crystallization behaviour observed in PCL, PEG and PLLA linear block copolymers. The poly(1,6 HD) segments are obligated to crystallize inside the interlamellar zones of the PET spherulites.

Fitting the crystallization data to the Avrami equation provided morphology information through the Avrami index. Avrami values near 2 for poly(1,6 HD) segments indicated that 2D instantaneously growing crystals (axialites) are formed due to the restrictions caused by the PET segments crystallized first. If the content of PET is increased, this index is further reduced to 1. It is very difficult for the poly(1,6 HD) segments to be nucleated as they are confined inside the interlamellar regions of the PET crystals. From the Lauritzen and Hoffman fitting to the DSC data, it was also demonstrated that as the content of poly(1,6 HD) segments increased, the confinement effect of the PET segments was less severe. Moreover, more energy is required to induce the crystallization of both segments compared to the corresponding homopolymers [174].

Thermal fractional treatment is a useful technique to explore the effects of the segmental architectures in multiblock copolymers. Zhang et al. [175] applied the Successive Self-nucleation and Annealing (SSA) methodology (see Fig. 32) to poly(hexamethylene carbonate)-*co*-poly (hexamethylene urethane) (PHCU) segmental block copolymers. In these multiblock copolymers, the urethane segments (PU) and the carbonate segments (PC) undergo cocrystallization; some PC segments are included inside the PU-rich phase crystals and vice versa. Distortions in the crystalline structure detected by WAXD gave evidence of a cocrystallization phenomenon. Thus, a possible isomorphic-like behaviour was

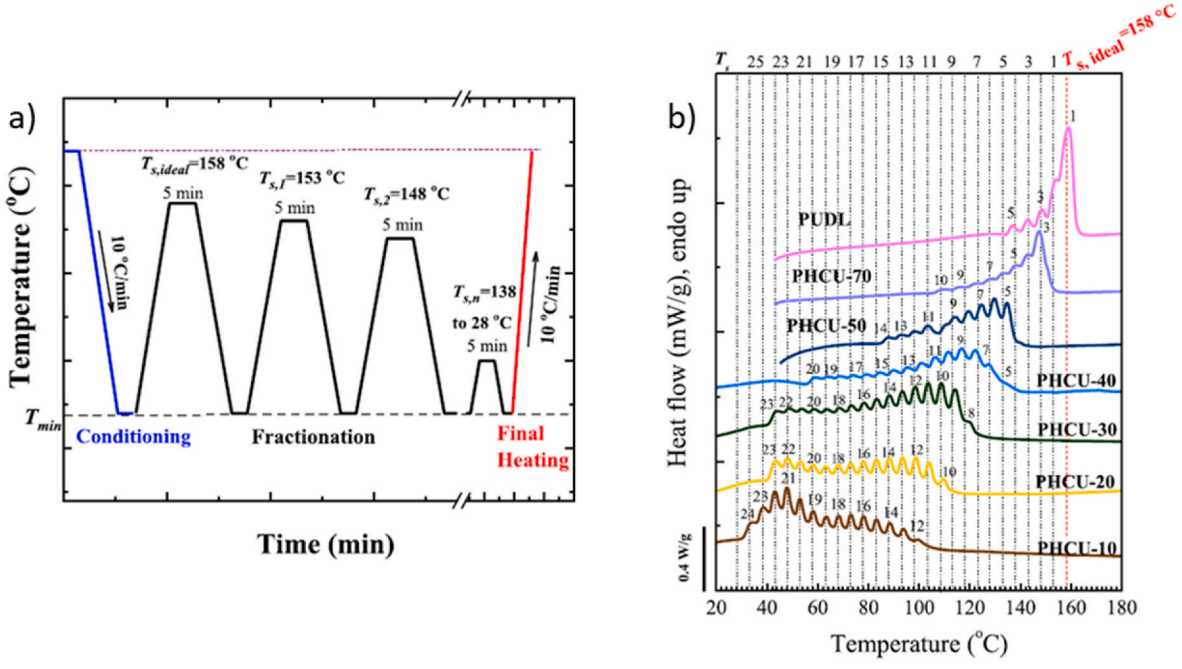

Fig. 32. a) Temperature scan procedure for SSA thermal treatment. b) DSC heating scans for SSA fractionated PHCU copolymers and PUDL oligomer at 10 °C/min. Taken and modified from Ref. [175].

observed. However, the SSA technique allowed for thermally fractionating the segmented copolymer in two clear populations when the content of the PU segments is reduced (see Fig. 32). The fractions that melt at higher temperatures correspond to the PU-rich phase, while the lower temperature fractions belong to the PC-rich phase. The generation of two distinctive crystalline phases allowed the discarding a clear isomorphism in these copolymers with low PU content. WAXD analysis demonstrated the existence of the PC crystalline phase. Sequential crystallization and melting of PC and PU rich phases occurred when the PU content was as low as 10%. The cooling conditions also affected the crystallization behaviour as the lamellar thickness increased as the PU content and cooling rate were reduced. In higher PU content copolymers, the cocrystallization phenomenon prevailed [175].

5. Other components: effect of nanofillers and other additives on the crystallization behaviour of block copolymers

5.1. Effect of processing additives

Some additives are mixed with block copolymers to improve specific properties. Triblock ABA copolymers composed of PLLA-*b*-PEG-*b*-PLLA may lack the suitable melt flow properties to be processed using traditional polymer processing techniques such as injection molding and film blowing. To improve the melt strength of PLLA copolymers, smaller chain extender molecules are added to form long-chain branched structures through end-chain reactions [86,177]. The chain extenders that are commonly used are epoxy-based molecules (ver Fig. 33), and the extent of chain extension and the final melt flow properties depend on the reaction conditions and the content of the chain extender [177].

In this triblock terpolymers, the middle PEG block was not able to crystallize after melt cooling the sample, probably due to its short content in the copolymer (17%) and a restriction effect caused by the previously formed PLLA crystals that limited the crystallization ability of this block located in the middle. However, the flexible PEG block's presence enhanced the PLLA block's cold crystallization during the second heating scan as this block is molten at the temperatures PLLA block cold crystallizes. The molten PEG segments induced a plasticizing effect over the PLLA crystallization, increasing the mobility of the PLLA chains. In fact, a longer middle PEG block enhanced the chain mobility and crystallization ability of the PLLA end blocks; consequently, the PLLA χ_c increased [86].

Adding an epoxy-based chain extender to the triblock copolymer modified crystallization behaviour [86,177]. Increasing the chain extender content from 1 to 4% led to a reduction of the PLLA block T_c during cooling and an increase of the PLLA block T_{cc} during heating, probably as a result of the limited PLLA chain rearrangement and mobility caused by the long-chain branches formed from the reactions with the chain extender. Similarly, the PLLA crystallization degree reduced as the content of the chain extender increased [86]. In fact, PLLA χ_c decreased by approximately 66% with the presence of 4% of chain extender, indicating that the chain extension reactions might

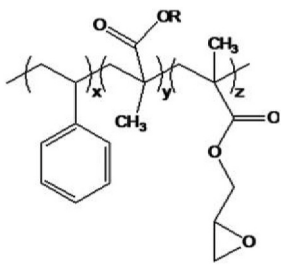

Fig. 33. Molecular structure of epoxy-based chain extender. R is an alkyl group. x and y are each between 1 and 20 as well as z is between 2 and 20. Taken from [177].

inhibit the crystallization ability of the PLLA block. Confirmation of reactions between PLLA and the chain extender was provided by NMR [177]. The chain extension reactions did not alter the T_g of the copolymers [86].

Some antioxidant additives may influence the double crystalline nature of block copolymers. Polyurethane synthesized from a tailor-made linear triblock copolymer of PLLA and PCL exhibited the crystalline fractions from the PCL and PLLA blocks, as was demonstrated by X-ray diffraction. Catechin was added to this PU copolymer as a natural antioxidant derived from flavonoids found in winery residues. The presence of this additive caused an increase in the halo amorphous, and the intensity of the reflection peaks $2\theta = 16.8^\circ$ and 19.2° corresponding to PLLA and PCL crystals, respectively. However, the catechin loaded at 5% reduced the molecular mobility of the PCL block as its T_g increased to 7 °C. In fact, part of this block could not crystallize during the cooling scan, and cold crystallization phenomena were observed during the subsequent heating. The T_{cc} increases as the catechin content is higher. Similar behaviour was observed in the PLLA block. In the neat polymer, no cold-crystallization phenomenon was observed in the second heating for the PLLA block, and only crystal melting was observed. However, after adding 1, 3, and 5% of catechin, the PLLA block cold crystallized, and the T_{cc} increased as the catechin content increased. That is an indication of molecular mobility restrictions imposed by this additive which ultimately did not contribute to enhancing the crystallinity, and the crystallization degree of both PCL and PLLA blocks reduced as catechin content increased [178].

5.2. Effect of nucleating agents

Nanoparticles usually act as nucleating agents, enhancing the heterogeneous crystallization of polymer systems. Nanocellulose fibers (NCF) and whiskers (CNW), as well as carbon nanotubes (CNT), are the most investigated nanoparticles in combination with polymer blends and composites, polymer grafting, and copolymers [179–182]. The shish-kebab structure is a well-reported characteristic morphology of polymer-fibrilar nanocomposites after crystallization. When the polymeric chains are constituted by potentially crystallizing block copolymers, the final morphology is also tuned by the block composition or block length.

For instance, Ochoa et al. [180]. and Le et al. [181]. have studied the crystallization behaviour of PE-*b*-PEG diblock copolymers with different compositions in the presence of nanoparticles such as NCF [180] and CNT [181]. The copolymer usually decorates the surface of the nanoparticle (see Fig. 34a). Particularly, symmetrical (50-50) PE-*b*-PEG diblock copolymers that were solution crystallized in the presence of CNT were double crystalline [181]. Two exothermic peaks corresponding to the PE and PEG blocks crystallization were identified in the cooling scan. Moreover, a three-degree shift towards higher temperatures was detected by the PE block in the presence of the CNT. Being the first block in crystallizing, this increase in T_c denoted the enhanced PE crystallization due to the nucleating effect caused by CNT. On the contrary, in comparison to the pure copolymer, the PEG block T_c was reduced in the CNT nanocomposite. Since the PEG block is the second on crystallizing, the authors explained this opposite behaviour due to the less favorable alignment of PEG chains to the CNT, which disrupt their crystallization [181].

However, if the block content is reduced to 20%, the PE or the PEG block cannot crystallize on cooling, not even in the presence of CNT. That is the importance of block length or composition to develop double crystalline systems. Moreover, the most interesting observation of the high M_w symmetrical PE-*b*-PEG diblock copolymers was the splendid shish-kebab structures observed by TEM (see Fig. 34b and c). This structure is double crystalline, and as the length of the blocks is increased, a more stable and regular structure is formed, and better interactions of the PE segments over the CNT surface are promoted [181] (see Fig. 34b vs Fig. 34c). The isothermal crystallization temperatures

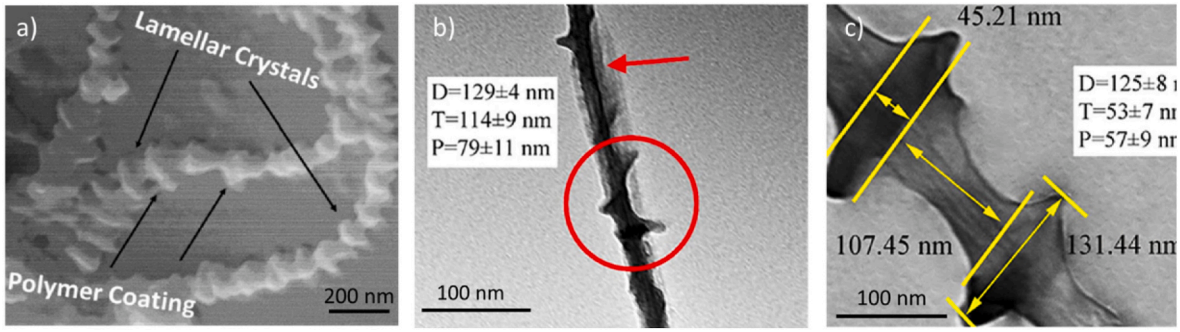

Fig. 34. a) SEM image PE-b-PEG diblock copolymers crystallized in the presence of NCF and TEM images of b) low M_w and c) high M_w, both symmetrical 50-50 PE-b-PEG diblock copolymers after 6 h crystallizing in the presence of CNT. Taken and modified from [180,181].

were 69 °C for the low M_w copolymer and 95 °C for the high M_w copolymer. At these temperatures, only the PE block can crystallize. However, upon subsequent cooling, the PEG block also crystallized.

5.3. Effect of terminal end groups

Polyhedral oligomeric silsesquioxane (POSS) macromolecules have been of great interest over the past decades. POSS is an organic-inorganic hybrid molecule with an inorganic silica-like core surrounded by a shell of eight organic-reactive or non-reactive groups. Incorporating this POSS nanocage in polymeric chains can improve the tensile properties and modify the crystallization behaviour. POSS has been polymerized with PCL and PHBV to form organic-inorganic multiblock copolymers [183]. DSC experiments demonstrated that the three phases, PCL, PHBV, and POSS are in the crystalline state, although not simultaneously. Depending on block composition, these multiblock copolymers could be double or triple crystalline. Only diffraction peaks corresponding to the POSS and PHBV crystalline phases were detected by XRD. In contrast, no diffraction signals were observed for the PCL segments, regardless of the somehow high PCL content (between 25 and 44%). The POSS units might highly restrict the PCL crystallization.

DSC experiments on heating revealed that PHBV cold crystallization overlaps with PCL crystals melting. In addition, the subsequent melting of the PHBV and POSS crystals is observed. The crystallization degree of the PHBV is reduced probably because POSS molecules interrupt the regularity of the polymeric chains in order to crystallize [183]. Similarly, in POSS terminated PCL-*b*-PLLA diblock copolymers [184], the POSS end groups restricted the crystallization of the PLLA block because this block is directly joined to the POSS units that hampered the mobility of the PLLA chains. Annealing the sample at 100 °C improved the crystallizability of the PLLA block, increasing its crystallinity degree. Unlike the aforementioned copolymers, in this PCL-*b*-PLLA diblock copolymers, the POSS units might act as nucleating sites as the PCL crystallization was enhanced, probably to the tendency of the POSS units to locate at the PCL phase [184].

Other organic-inorganic composites include segmental copolymers of PCL and PEG cross-linked by in situ-generated silsesquioxane structures [185]. Due to the presence of these structures, phase separation took place at the micro and the nanoscale. Despite being miscible polymers, PCL and PEG, when crosslinked, a globular morphology of a PEG-rich phase immersed in a PCL matrix was obtained as it was detected by optical microscopy and SAXS. In the nanoscale, the silsesquioxane nanoparticles were detected by TEM. These segmental block copolymers were double crystalline, as confirmed by WAXS. Despite having similar crystallization and melting ranges, the PCL segment crystallized before the PEG segment. The crystallinity was also affected by the crosslinking degree, and this factor usually causes a reduction in the crystallinity of the polymeric chains as the chain folding becomes more difficult. Moreover, the PCL Tc increased in the segmental copolymers, probably due to the presence of the inorganic structures that could enhance the crystallization ability. On the contrary, the PEG Tc was shifted to lower temperatures, which means that the crystallization of the PEG segments was, to some extent, hindered by the previous crystallization of the PCL. The final morphology is complex. As phase segregated, spherical domains of PEG are dispersed in PCL rich phase, both of them having a non-mixed 3D spherulitic structure. It is proposed that in the interlamellar and inter-spherulitic amorphous regions, the polysilsesquioxane (PSQ) inorganic nanoparticles acted as cross-linking nodes [185]. Interestingly, completely miscible PEG-*b*-PCL block copolymers can be segregated in the melt and in the solid state by the sole inclusion of the PSQ moieties.

Some linear block copolymers are functionalized with 2-Ureido-4-pyrimidone (UPy) units as end functional groups to enhance their physical properties [186–190]. The UPy units are included as chain extenders in order to obtain supramolecular polymers (SPM) with improved molecular weight. In addition, these units provide better mechanical performance, shape memory behaviour, and self-healing properties [186,187]. Including these UPy units will surely influence the crystallization behaviour of block copolymers. In fact, it has been reported a depression in the crystallization temperature.

Jing et al. [186] reported the crystallization behaviour of SPM based on PLA-*b*-PCL-*b*-PLA triblock copolymers synthesized from POSS initiator and functionalized with UPy units. The double crystalline nature was confirmed by DSC and WAXS experiments. POSS might enhance the crystallization ability of the copolymers by increasing the nucleation sites. As an organic-inorganic hybrid molecule, the POSS initiator improved the crystallization behaviour of the PLA-*b*-PCL-*b*-PLA triblock copolymers: larger T_c and crystallinity degree were exhibited by both PCL and PLLA blocks. On the contrary, the inclusion of the UPy units hindered the crystallization of these copolymers since reduced T_c, T_m, and crystallinity degreed were detected by DSC in both blocks. These UPy units expand the polymeric chains and destroy their structural regularity, which ultimately makes it difficult for the chain to fold into the perfect crystalline arrangement. However, the inclusion of POSS molecules into UPy functionalized PLA-*b*-PCL-*b*-PLA triblock copolymers contributed to reduce the negative effect of the UPy units by supplying extra nucleating sites for polymer crystallization. Enhanced crystallization was also observed in stereocomplex SMP of PLLA-*b*-PCL-*b*-PLLA and PDLA-*b*-PCL-*b*-PDLA copolymer blends, in which the POSS accelerated the crystallization of PLA blocks. However, the crystallizability of the PCL block was reduced [187].

5.4. Effect of rigid confinement inside anodic alumina oxide templates (AAO)

Anodic alumina oxide templates (AAO) [191] impose rigid confinement that hinders the crystallization of potentially crystallizable diblock copolymers such as PEO-*b*-PCL copolymers. Because the PCL block crystallizes first, the subsequent crystallization of the PEO block becomes severely hampered due to a confinement effect caused by both the

AAO rigid template and the previously formed PCL crystals. Thus, the nucleation process of the minor PEO block can be completely suppressed. On the other hand, the PCL block can crystallize through a homogeneous nucleation mechanism [192].

6. Conclusions

The crystallization of complex block copolymer has been reviewed, and the most relevant parameters that determine the number of chemically different crystalline structures that could be obtained in such systems could be summarized as follow:

1. *The relative amount of the crystallizable blocks*. There is a minimum amount of the block for the crystallization of a second phase. That amount is correlated with other parameters, like architecture, the crystallization temperature of the other blocks, the chemical nature of the block, and its relationship with the other blocks presented in the copolymer. If the other parameters remain the same, an increase in the amount of the crystallizable block is expected to increase the degree of crystallinity and the crystallization temperature. However, it has been reported that for PLLA, an excessive increase in the molecular weight could lead to a decrease in the crystallization degree. On the other hand, if the second crystallizable block (from the melt) remains constant in length and relative amount, and the first block is too large, the crystallization might be depressed.

2. *Crystallization temperature*. Comparing one block with the other crystallizable blocks, the crystallization temperature is critical to the possibilities of whether that block will crystallize. If the block is cooled from the melt, the block with the highest T_c will crystallize first. When one of the blocks is crystallized, then the crystallization of the second block can be either enhanced or hampered. The already crystalline block can nucleate the next one, improving the crystallization, or can induce confinement effects restricting the crystallizability of the second, third, or subsequent blocks. Other competitive effects, such as plasticizing and antiplasticizing can also be found in the crystallization of multiple blocks.

3. *Architecture*. The physical constraints that chemical architecture imposes also influence the crystallization process. Different crystallization behaviours are observed whether the block copolymers have a linear, star, or comb structure. In the case of linear triblock copolymers, the middle block has a lower possibility of crystallizing. Conversely, the ones with a free end have more probability of undergoing crystallization. A similar feature is reported for star copolymers, where the enhanced mobility favors the crystallization process.

4. *Chemical nature and morphology*. The segregation strength between the blocks will surely affect the potentiality for crystallizing all the phases present in the block copolymer and will determine the final crystalline morphology. In melt-miscible systems, phase segregation is driven by the sequential or simultaneous crystallization of different blocks, and a mixed alternated multi-lamellar morphology is developed in the end. The first block that crystallizes at higher temperatures forms spherulites (either from a mixed melt or by break-out from a weakly segregated melt) that template the morphology of the copolymer. The other blocks that can crystallize will do it in the interlamellar space of the previous block. In strongly segregated systems, the crystalline morphology is set by the phase assembly in the melt, and the crystallization phenomenon is forced to occur either inside the matrix or the MDs generated. Inside the MDs, it is possible to observe a relative depression of the crystallization due to the possible lack of availability of suitable nuclei, which also depends on the MDs volume. Either mixed or well-separated morphologies can induce enhancing or restricting effects over the potentially crystallizable phases. For instance, the crystallization ability could be reduced if the blocks are melt-segregated. However, double crystallization has been reported with the conservation of segregation. A particular case is copolymers with blocks with similar chemical structures because they can co-crystallize; however, this process is also sensitive to thermal treatments, architecture, and composition.

5. *Cooling rate conditions*. Since the crystallization kinetics of the blocks are affected just by being blocks in a copolymer, the rate of cooling will affect the crystallization degree and morphology of the blocks. By changing the cooling speed, different environments as crystalline and vitreous phases, can be induced. It has been reported that slow cooling rates increase the probability of obtaining multiple crystalline structures. At the same time, fast cooling rates can suppress the crystallization of some blocks with respect to others. Thus, multiple crystalline possibilities can be tuned by modifying the crystallization conditions.

Understanding the crystallization behaviour of block copolymers continuously becomes more challenging as more complex structures have been designed over the past years. The addition of up to four different potentially crystallizable blocks has broadened the possibilities for tunning the potential features of these systems at the nanoscale, which is highly relevant in different high-performance applications in several sectors such as optoelectronics photovoltaic, biomedical, and membranes, among others. Besides the chemical nature and molecular architecture (linear, stars, combs, multiblocks) of the block copolymers, their combination with other additives, nanofillers, and end-group modifications will also affect their crystallization behaviour. Moreover, highly novel techniques such as Flash Chip Calorimetry, and Hyphenated Rheology Techniques (Rheo-NMR, Rheo-SAXS, and Rheo-Optics/-Microscopy combinations), are starting to be used in polymer crystallization analysis over the last years, they will surely contribute to a more deep exploration and comprehension of the crystalline nature in block copolymers and their property-structure relationships. The rapid developments in more precise and profound methods to better assess the complex phenomena involved will also allow gathering important information not only on the crystallization behaviour of these very complex block copolymer systems but to provide strategies on how to suitable process these materials in order to obtain specific properties.

CRediT author statement

Jordana K. Palacios, Conceptualization, Investigation, Writing - Original Draft, Writing - Review & Editing, Visualization, Rose Mary Michell, Conceptualization, Investigation, Writing- Review & Editing, Visualization, Alejandro Muller, Conceptualization, Writing - Review & Editing.

Declaration of competing interest

The authors declare that they have no known competing financial interests or personal relationships that could have appeared to influence the work reported in this paper.

Data availability

This is a review paper. We have given the references of the data we have cited. We have also obtained permissions to reproduce Figures

Acknowledgements

This research was funded by the Spanish Ministry of Science, Innovation, and Universities (MICINN) through the grant PID2020-113045GB-C21 and by the Basque Government through grant IT1309-19.

References

[1] J.M. Schultz, Polymer Crystallization: the Development of Crystalline Order in Thermoplastic Polymers, American Chemical Society Publication, Oxford University Press., New York, 2001.
[2] L. Mandelkern, Crystallization of polymers, in: Equilibrium Concepts, vol. 1, Cambridge University Press, Cambridge, 2002.

[3] L. Mandelkern, Crystallization of polymers, in: Kinetics and Mechanisms, vol. 2, Cambridge University Press, Cambridge, 2004.
[4] E. Piorkowska, G.C. Rutledge, Handbook of Polymer Crystallization, Wiley, Hoboken, New Jersey, USA, 2013.
[5] D. Cavallo, A.J. Müller, Polymer crystallization, in: K. Matyjaszewski, Y. Gnanou, N. Hadjichristidis, M. Muthukumar (Eds.), Macromol. Eng. Synth. Macrosc. Mater. Appl., second ed., Wiley-VCH GmbH, 2022, pp. 1–57.
[6] U.W. Gedde, M.S. Hedenqvist, Fundamental Polymer Science, second ed., Springer Nature, Switzerland, 2019.
[7] I.W. Hamley, The Physics of Block Copolymers, Oxford University Press, Oxford, 1998.
[8] V. Abetz, P.F.W. Simon, Phase behaviour and morphologies of block copolymers, 2005, https://doi.org/10.1007/12_004.
[9] A.J. Müller, V. Balsamo, M.L. Arnal, T. Jakob, H. Schmalz, V. Abetz, Homogeneous nucleation and fractionated crystallization in block copolymers, Macromolecules 35 (2002) 3048–3058, https://doi.org/10.1021/ma012026w.
[10] A.J. Müller, V. Balsamo, M.L. Arnal, Nucleation and crystallization in diblock and triblock copolymers, 2005, https://doi.org/10.1007/12_001.
[11] A.J. Müller, M.L. Arnal, V. Balsamo, Crystallization in block copolymers with more than one crystallizable block, 2007, https://doi.org/10.1007/3-540-47307-6_13.
[12] S. Li, R.A. Register, Crystallization in copolymers, in: Handb. Polym. Cryst., 2013, pp. 327–346, https://doi.org/10.1002/9781118541838.ch11.
[13] R.M. Van Horn, M.R. Steffen, D. O'Connor, Recent progress in block copolymer crystallization, Polym. Cryst. 1 (2018), https://doi.org/10.1002/pcr2.10039.
[14] C.M. Bates, F.S. Bates, 50th anniversary perspective: block polymers-pure potential, Macromolecules 50 (2017) 3–22, https://doi.org/10.1021/acs.macromol.6b02355.
[15] I.W. Hamley, Block copolymers, in: Encycl. Polym. Sci. Technol., John Wiley & Sons, Inc, 2002, pp. 457–482.
[16] C. Yu, Q. Xie, Y. Bao, G. Shan, P. Pan, Crystalline and spherulitic morphology of polymers crystallized in confined systems, Crystals 7 (2017) 147, https://doi.org/10.3390/cryst7050147.
[17] R.M. Michell, A.J. Müller, Confined crystallization of polymeric materials, Prog. Polym. Sci. 54–55 (2016) 183–213, https://doi.org/10.1016/j.progpolymsci.2015.10.007.
[18] A.J. Müller, M.L. Arnal, A.T. Lorenzo, Crystallization in nano-confined polymeric systems, in: Handb. Polym. Cryst., 2013, pp. 347–378, https://doi.org/10.1002/9781118541838.ch12.
[19] Y.-L. Loo, R.A. Register, A.J. Ryan, Modes of crystallization in block copolymer microdomains: breakout, templated, and confined, Macromolecules 35 (2002) 2365–2374, https://doi.org/10.1021/ma011824j.
[20] S. Huang, S. Jiang, Structures and morphologies of biocompatible and biodegradable block copolymers, RSC Adv. 4 (2014) 24566–24583, https://doi.org/10.1039/c4ra03043e.
[21] W. Li, H. Nie, H. Shao, H. Ren, A. He, Synthesis, chain structures and phase morphologies of trans-1,4-poly(butadiene-co-isoprene) copolymers, Polymer 156 (2018) 148–161, https://doi.org/10.1016/j.polymer.2018.10.002.
[22] D. Zhou, J. Sun, J. Shao, X. Bian, S. Huang, G. Li, X. Chen, Unusual crystallization and melting behavior induced by microphase separation in MPEG-b-PLLA diblock copolymer, Polymer 80 (2015) 123–129, https://doi.org/10.1016/j.polymer.2015.10.066.
[23] J. Yang, Y. Liang, C.C. Han, Effect of crystallization temperature on the interactive crystallization behavior of poly(l-lactide)-block-poly(ethylene glycol) copolymer, Polymer 79 (2015) 56–64, https://doi.org/10.1016/j.polymer.2015.09.067.
[24] J.K. Palacios, G. Liu, D. Wang, N. Hadjichristidis, A.J. Müller, Generating triple crystalline superstructures in melt miscible PEO- *b* -PCL- *b* -PLLA triblock terpolymers by controlling thermal history and sequential crystallization, Macromol. Chem. Phys. 220 (2019), 1900292, https://doi.org/10.1002/macp.201900292.
[25] J.K. Palacios, A. Mugica, M. Zubitur, A.J. Müller, Crystallization and morphology of block copolymers and terpolymers with more than one crystallizable block, Cryst. Multiph. Polym. Syst. (2018) 123–180, https://doi.org/10.1016/B978-0-12-809453-2.00006-2.
[26] C. De Rosa, R. Di Girolamo, A. Malafronte, M. Scoti, G. Talarico, F. Auriemma, O. Ruiz de Ballesteros, Polyolefins based crystalline block copolymers: ordered nanostructures from control of crystallization, Polymer 196 (2020), 122423, https://doi.org/10.1016/j.polymer.2020.122423.
[27] C. Yang, Z. Li, J. Xu, Single crystals and two-dimensional crystalline assemblies of block copolymers, J. Polym. Sci. (2022), 20210866, https://doi.org/10.1002/pol.20210866 pol.
[28] H. Schmalz, V. Abetz, Block copolymers with crystallizable blocks: synthesis, self-assembly and applications, Polymers 14 (2022) 696, https://doi.org/10.3390/polym14040696.
[29] S. Agbolaghi, F. Abbasi, S. Abbaspoor, Double/single phase segregation and vertical stratification induced by crystallization in all-crystalline tri/diblock copolymers and homopolymer blends of poly(3-hexylthiophene) and poly (ethylene glycol): double/single phase segregation and vertical stratification, Surf. Interface Anal. 49 (2017) 630–639, https://doi.org/10.1002/sia.6202.
[30] H. Cui, X. Yang, J. Peng, F. Qiu, Controlling the morphology and crystallization of a thiophene-based all-conjugated diblock copolymer by solvent blending, Soft Matter 13 (2017) 5261–5268, https://doi.org/10.1039/C7SM01126A.
[31] C.D. Heinrich, M. Fischer, T. Thurn-Albrecht, M. Thelakkat, Modular synthesis and structure analysis of P3HT- *b* -PPBI donor–acceptor diblock copolymers, Macromolecules 51 (2018) 7044–7051, https://doi.org/10.1021/acs.macromol.8b01301.
[32] X. Shang, Y. Yin, S. Chen, M. Zhu, D. Zhai, X. Liu, J. Peng, Unravelling the correlation between microphase separation and cocrystallization in thiophene-selenophene block copolymers for organic field-effect transistors, Macromolecules 53 (2020) 10245–10255, https://doi.org/10.1021/acs.macromol.0c01395.
[33] V. Untilova, F. Nübling, L. Biniek, M. Sommer, M. Brinkmann, Impact of competing crystallization processes on the structure of all-conjugated donor–acceptor block copolymers P3HT- *b* -PNDIT2 in highly oriented thin films, ACS Appl. Polym. Mater. 1 (2019) 1660–1671, https://doi.org/10.1021/acsapm.9b00220.
[34] B. Timmermans, G. Koeckelberghs, Chiral expression of co-crystallizing poly (thiophene)- *block* -poly(selenophene) copolymers, Polym. Chem. 11 (2020) 2715–2723, https://doi.org/10.1039/C9PY01775E.
[35] E.L. Kynaston, K.J. Winchell, P.Y. Yee, J.G. Manion, A.D. Hendsbee, Y. Li, S. Huettner, S.H. Tolbert, D.S. Seferos, Poly(3-alkylthiophene)- *block* -poly(3-alkylselenophene)s: conjugated diblock Co-polymers with atypical self-assembly behavior, ACS Appl. Mater. Interfaces 11 (2019) 7174–7183, https://doi.org/10.1021/acsami.8b18795.
[36] L. Li, Q. Zhao, S. Chen, Z. Lin, J. Peng, Unfolding the cocrystallization–charge transport correlation in all-conjugated triblock copolymers via meticulous molecular engineering for organic field-effect transistors, Nano Energy 100 (2022), 107489, https://doi.org/10.1016/j.nanoen.2022.107489.
[37] L. Li, H. Zhan, S. Chen, Q. Zhao, J. Peng, Interrogating the effect of block sequence on cocrystallization, microphase separation, and charge transport in all-conjugated triblock copolymers, Macromolecules 55 (2022) 7834–7844, https://doi.org/10.1021/acs.macromol.2c00406.
[38] L. Li, L. Li, X. Liu, J. Peng, Tuning cocrystallization, microphase separation, and optical property of all-conjugated triblock copolymers by molecular engineering, ACS Appl. Polym. Mater. 4 (2022) 8461–8470, https://doi.org/10.1021/acsapm.2c01372.
[39] D. Zhai, M. Zhu, S. Chen, Y. Yin, X. Shang, L. Li, G. Zhou, J. Peng, Effect of block sequence in all-conjugated triblock copoly(3-alkylthiophene)s on control of the crystallization and field-effect mobility, Macromolecules 53 (2020) 5775–5786, https://doi.org/10.1021/acs.macromol.0c00598.
[40] C. De Rosa, A. Malafronte, R. Di Girolamo, F. Auriemma, M. Scoti, O. Ruiz de Ballesteros, G.W. Coates, Morphology of isotactic polypropylene–polyethylene block copolymers driven by controlled crystallization, Macromolecules 53 (2020) 10234–10244, https://doi.org/10.1021/acs.macromol.0c01316.
[41] C. De Rosa, R. Di Girolamo, A. Cicolella, G. Talarico, M. Scoti, Double crystallization and phase separation in polyethylene—syndiotactic polypropylene di-block copolymers, Polymers 13 (2021) 2589, https://doi.org/10.3390/polym13162589.
[42] Z. Nie, X. Liu, W. Yu, Shear-induced crystallization of olefin multiblock copolymers: role of mesophase separation and hard-block content, Polymer 198 (2020), 122535, https://doi.org/10.1016/j.polymer.2020.122535.
[43] L. Qian, Y. Wang, Y. Lu, Y. Men, Crystallization behavior of impact copolymer polypropylene revealed by fast scanning chip calorimetry analysis, Polymer 239 (2022), 124441, https://doi.org/10.1016/j.polymer.2021.124441.
[44] S. Li, S.B. Myers, R.A. Register, Solid-state structure and crystallization in double-crystalline diblock copolymers of linear polyethylene and hydrogenated polynorbornene, Macromolecules 44 (2011) 8835–8844, https://doi.org/10.1021/ma201951j.
[45] S.B. Myers, R.A. Register, Crystalline-crystalline diblock copolymers of linear polyethylene and hydrogenated polynorbornene, Macromolecules 41 (2008) 6773–6779, https://doi.org/10.1021/ma800759b.
[46] P. Rangarajan, R.A. Register, L.J. Fetters, W. Bras, S. Naylor, A.J. Ryan, Crystallization of a weakly segregated polyolefin diblock copolymer, Macromolecules 28 (1995) 4932–4938, https://doi.org/10.1021/ma00118a022.
[47] A.J. Müller, A.T. Lorenzo, R.V. Castillo, M.L. Arnal, A. Boschetti-de-Fierro, V. Abetz, Crystallization kinetics of homogeneous and melt segregated PE containing diblock copolymers, Macromol. Symp. 245–246 (2006) 154–160, https://doi.org/10.1002/masy.200651321.
[48] A.J. Müller, R.V. Castillo, M. Hillmyer, Nucleation and crystallization of PLDA-6-PE and PLLA-6-PE diblock copolymers, Macromol. Symp. 242 (2006) 174–181, https://doi.org/10.1002/masy.200651025.
[49] A. Boschetti-de-Fierro, A.T. Lorenzo, A.J. Müller, H. Schmalz, V. Abetz, Crystallization kinetics of PEO and PE in different triblock terpolymers: effect of microdomain geometry and confinement, Macromol. Chem. Phys. 209 (2008) 476–487, https://doi.org/10.1002/macp.200700434.
[50] L. Sun, Y. Liu, L. Zhu, B.S. Hsiao, C.A. Avila-Orta, Pathway-dependent melting in a low-molecular-weight polyethylene-block- poly(ethylene oxide) diblock copolymer, Macromol. Rapid Commun. 25 (2004) 853–857, https://doi.org/10.1002/marc.200300320.
[51] H. Schmalz, A. Knoll, A.J. Müller, V. Abetz, Synthesis and characterization of ABC triblock copolymers with two different crystalline end blocks: influence of confinement on crystallization behavior and morphology, Macromolecules 35 (2002) 10004–10013, https://doi.org/10.1021/ma020983f.
[52] C. Weiyu, K. Tashiro, M. Hanesaka, S. Takeda, H. Masunaga, S. Sasaki, M. Takata, Relationship between morphological change and crystalline phase transitions of polyethylene-poly(ethylene oxide) diblock copolymers, revealed by the temperature-dependent synchrotron WAXD/SAXS and infrared/Raman spectral measurements, J. Phys. Chem. B 113 (2009) 2338–2346, https://doi.org/10.1021/jp8092435.

[53] T. Sakurai, H. Nagakura, S. Gondo, S. Nojima, Crystallization of poly (ε-caprolactone) blocks confined in crystallized lamellar morphology of poly (ε-caprolactone)-block-polyethylene copolymers: effects of polyethylene crystallinity and confinement size, Polym. J. 45 (2013) 436–443, https://doi.org/10.1038/pj.2012.164.

[54] T. Sakurai, S. Nojima, Significant increase in the melting temperature of poly(ε-caprolactone) blocks confined in the crystallized lamellar morphology of poly (ε-caprolactone)-block-polyethylene copolymers, Polym. J. 43 (2011) 370–377, https://doi.org/10.1038/pj.2011.4.

[55] S. Nojima, K. Ito, H. Ikeda, Composition dependence of crystallized lamellar morphology formed in crystalline-crystalline diblock copolymers, Polymer 48 (2007) 3607–3611, https://doi.org/10.1016/j.polymer.2007.04.053.

[56] T. Sakurai, Y. Ohguma, S. Nojima, Morphological evolution during isothermal crystallization observed in a crystalline-crystalline diblock copolymer, Polym. J. 40 (2008) 971–978, https://doi.org/10.1295/polymj.PJ2008092.

[57] H. Ikeda, Y. Ohguma, S. Nojima, Composition dependence of crystallization behavior observed in crystalline-crystalline diblock copolymers, Polym. J. 40 (2008) 241–248, https://doi.org/10.1295/polymj.PJ2007150.

[58] R.V. Castillo, A.J. Müller, M.-C. Lin, H.-L. Chen, U.-S. Jeng, M.A. Hillmyer, Confined crystallization and morphology of melt segregated PLLA-b-PE and PLDA-b-PE diblock copolymers, Macromolecules 41 (2008) 6154–6164, https://doi.org/10.1021/ma800859y.

[59] V. Balsamo, Y. Paolini, G. Ronca, A.J. Müller, Crystallization of the polyethylene block in polystyrene-b-polyethylene-b-polycaprolactone triblock copolymers, 1: self-nucleation behavior, Macromol. Chem. Phys. 201 (2000) 2711–2720, https://doi.org/10.1002/1521-3935(20001201)201:18<2711::AID-MACP2711>3.0.CO;2-6.

[60] R. Di Girolamo, A. Cicolella, G. Talarico, M. Scoti, F. De Stefano, A. Giordano, A. Malafronte, C. De Rosa, Structure and morphology of crystalline syndiotactic polypropylene-polyethylene block copolymers, Polymers 14 (2022) 1534, https://doi.org/10.3390/polym14081534.

[61] G. Zapsas, Y. Patil, P. Bilalis, Y. Gnanou, N. Hadjichristidis, Poly(vinylidene fluoride)/polymethylene-based block copolymers and terpolymers, Macromolecules 52 (2019) 1976–1984, https://doi.org/10.1021/acs.macromol.8b02663.

[62] S. Osawa, R. Hijikawa, H. Marubayashi, S. Nojima, Effects of crystal structure of poly(β-propiolactone) blocks on the cooperative crystallization of a polyethylene-block-poly(β-propiolactone) diblock copolymer, Polymer 122 (2017) 249–257, https://doi.org/10.1016/j.polymer.2017.06.041.

[63] A.J. Müller, M. Ávila, G. Saenz, J. Salazar, Crystallization of PLA-Based Materials, 2015. https://www.scopus.com/inward/record.uri?eid=2-s2.0-84937402505&partnerID=40&md5=ac5324e269347aa03a860534e6bb77c1.

[64] M.J. Barthel, F.H. Schacher, U.S. Schubert, Poly(ethylene oxide) (PEO)-based ABC triblock terpolymers-synthetic complexity vs. application benefits, Polym. Chem. 5 (2014) 2647–2662, https://doi.org/10.1039/c3py01666h.

[65] N. Mulchandani, A. Gupta, K. Masutani, S. Kumar, S. Sakurai, Y. Kimura, V. Katiyar, Effect of block length and stereocomplexation on the thermally processable poly(ε-caprolactone) and poly(lactic acid) block copolymers for biomedical applications, ACS Appl. Polym. Mater. 1 (2019) 3354–3365, https://doi.org/10.1021/acsapm.9b00789.

[66] J. Bao, X. Dong, S. Chen, W. Lu, X. Zhang, W. Chen, Fractionated crystallization and fractionated melting behaviors of poly(ethylene glycol) induced by poly (lactide) stereocomplex in their block copolymers and blends, Polymer 190 (2020), 122189, https://doi.org/10.1016/j.polymer.2020.122189.

[67] Y. Wu, L. Li, S. Chen, J. Qin, X. Chen, D. Zhou, H. Wu, Synthesis, characterization, and crystallization behaviors of poly(D-lactic acid)-based triblock copolymer, Sci. Rep. 10 (2020) 3627, https://doi.org/10.1038/s41598-020-60458-9.

[68] W. Han, X. Liao, Q. Yang, G. Li, B. He, W. Zhu, Z. Hao, Crystallization and morphological transition of poly(l -lactide)–poly(ε-caprolactone) diblock copolymers with different block length ratios, RSC Adv. 7 (2017) 22515–22523, https://doi.org/10.1039/C7RA03496B.

[69] R.V. Castillo, A.J. Müller, Crystallization and morphology of biodegradable or biostable single and double crystalline block copolymers, Prog. Polym. Sci. Oxf. 34 (2009) 516–560, https://doi.org/10.1016/j.progpolymsci.2009.03.002.

[70] R.V. Castillo, A.J. Müller, J.-M. Raquez, P. Dubois, Crystallization kinetics and morphology of biodegradable double crystalline PLLA- b -PCL diblock copolymers, Macromolecules 43 (2010) 4149–4160, https://doi.org/10.1021/ma100201g.

[71] E. Weidner, S. Kabasci, R. Kopitzky, P. Mörbitz, Thermal and morphological properties of poly(L-lactic acid)/poly(D-lactic acid)-B-polycaprolactone diblock copolymer blends, Materials 13 (2020) 2550, https://doi.org/10.3390/ma13112550.

[72] R. Liénard, N. Zaldua, T. Josse, J.D. Winter, M. Zubitur, A. Mugica, A. Iturrospe, A. Arbe, O. Coulembier, A.J. Müller, Synthesis and characterization of double crystalline cyclic diblock copolymers of poly(ε-caprolactone) and poly(l(d)-lactide) (c(PCL-b- PL(D)LA)), Macromol. Rapid Commun. 37 (2016) 1676–1681, https://doi.org/10.1002/marc.201600309.

[73] E. Laredo, N. Prutsky, A. Bello, M. Grimau, R.V. Castillo, A.J. Müller, Ph. Dubois, Miscibility in poly(L-lactide)-b-poly(ε-caprolactone) double crystalline diblock copolymers, Eur. Phys. J. E. 23 (2007) 295–303, https://doi.org/10.1140/epje/i2007-10191-6.

[74] I.W. Hamley, P. Parras, V. Castelletto, R.V. Castillo, A.J. Müller, E. Pollet, P. Dubois, C.M. Martin, Melt structure and its transformation by sequential crystallization of the two blocks within poly(L-lactide)-block-poly (ε-caprolactone) double crystalline diblock copolymers, Macromol. Chem. Phys. 207 (2006) 941–953, https://doi.org/10.1002/macp.200600085.

[75] I.W. Hamley, V. Castelletto, R.V. Castillo, A.J. Müller, C.M. Martin, E. Pollet, Ph. Dubois, Crystallization in poly(L-lactide)-b-poly(∈-caprolactone) double crystalline diblock copolymers: a study using x-ray scattering, differential scanning calorimetry, and polarized optical microscopy, Macromolecules 38 (2005) 463–472, https://doi.org/10.1021/ma0481499.

[76] L. Peponi, I. Navarro-Baena, J.E. Báez, J.M. Kenny, A. Marcos-Fernández, Effect of the molecular weight on the crystallinity of PCL-b-PLLA di-block copolymers, Polymer 53 (2012) 4561–4568, https://doi.org/10.1016/j.polymer.2012.07.066.

[77] M.T. Casas, J. Puiggalí, J.-M. Raquez, P. Dubois, M.E. Córdova, A.J. Müller, Single crystals morphology of biodegradable double crystalline PLLA-b-PCL diblock copolymers, Polymer 52 (2011) 5166–5177, https://doi.org/10.1016/j.polymer.2011.08.057.

[78] I. Navarro-Baena, A. Marcos-Fernandez, J.M. Kenny, L. Peponi, Crystallization behavior of diblock copolymers based on PCL and PLLA biopolymers, J. Appl. Crystallogr. 47 (2014) 1948–1957, https://doi.org/10.1107/S1600576714022468.

[79] W. Han, S. Li, X. Liao, B. He, Q. Yang, G. Li, Confined crystallization morphology of poly(ε -caprolactone) block within poly(ε -caprolactone)–poly(l -lactide) copolymers, Polym. Int. 68 (2019) 1992–2003, https://doi.org/10.1002/pi.5911.

[80] J. Bao, X. Dong, S. Chen, W. Lu, X. Zhang, W. Chen, Confined crystallization, melting behavior and morphology in PEG- *b* -PLA diblock copolymers: amorphous versus crystalline PLA, J. Polym. Sci. 58 (2020) 455–465, https://doi.org/10.1002/pol.20190077.

[81] L. Li, Z.-Q. Cao, R.-Y. Bao, B.-H. Xie, M.-B. Yang, W. Yang, Poly(l-lactic acid)-polyethylene glycol-poly(l-lactic acid) triblock copolymer: a novel macromolecular plasticizer to enhance the crystallization of poly(l-lactic acid), Eur. Polym. J. 97 (2017) 272–281, https://doi.org/10.1016/j.eurpolymj.2017.10.025.

[82] L. Wang, C. Feng, J. Shao, G. Li, H. Hou, The crystallization behavior of poly (ethylene glycol) and poly(l -lactide) block copolymer: effects of block length of poly(ethylene glycol) and poly(l -lactide), Polym. Cryst. 2 (2019), https://doi.org/10.1002/pcr2.10071.

[83] X. Yun, X. Li, Y. Jin, W. Sun, T. Dong, Fast crystallization and toughening of poly (L-lactic acid) by incorporating with poly(ethylene glycol) as a middle block chain, Polym. Sci. Ser. A. 60 (2018) 141–155, https://doi.org/10.1134/S0965545X18020141.

[84] Y. Gong, W. Song, Y. Wu, D. Zhang, Y. Liu, Q. Zhao, M. He, X. Chen, Effect of chain segment length on crystallization behaviors of poly(l -lactide-b-ethylene glycol-b- l -lactide) triblock copolymer, Polym. Polym. Compos. 28 (2020) 77–88, https://doi.org/10.1177/0967391119863951.

[85] P. Jariyasakoolroj, N. Rojanaton, L. Jarupan, Crystallization behavior of plasticized poly(lactide) film by poly(l-lactic acid)-poly(ethylene glycol)-poly(l-lactic acid) triblock copolymer, Polym. Bull. 77 (2020) 2309–2323, https://doi.org/10.1007/s00289-019-02862-4.

[86] Y. Baimark, Y. Srisuwan, Thermal and mechanical properties of highly flexible poly(L-lactide)- *b* -poly(ethylene glycol)- *b* -poly(L-lactide) bioplastics: effects of poly(ethylene glycol) block length and chain extender, J. Elastomers Plastics 52 (2020) 142–158, https://doi.org/10.1177/0095244319827993.

[87] D. Chen, L. Lei, M. Zou, X. Li, Non-isothermal crystallization kinetics of poly (ethylene glycol)–poly(l-lactide) diblock copolymer and poly(ethylene glycol) homopolymer via fast-scan chip-calorimeter, Polymers 13 (2021) 1156, https://doi.org/10.3390/polym13071156.

[88] W. Koosomsuan, M. Yamaguchi, P. Phinyocheep, K. Sirisinha, High-strain shape memory behavior of PLA-PEG multiblock copolymers and its microstructural origin, J. Polym. Sci., Part B: Polym. Phys. 57 (2019) 241–256, https://doi.org/10.1002/polb.24775.

[89] Y. Chen, L. Wang, W. Chen, C. Zhong, S. Li, J. Shao, G. Li, H. Hou, The isothermal crystallization kinetics of poly(ethylene glycol)- *block* -poly(l -lactide) block copolymers (PEG–PLLA): effects of the block lengths of PEG and PLLA, CrystEngComm 24 (2022) 3903–3912, https://doi.org/10.1039/D2CE00448H.

[90] F. Xue, X. Chen, L. An, S.S. Funari, S. Jiang, Crystallization induced layer-to-layer transitions in symmetric PEO-b-PLLA block copolymer with synchrotron simultaneous SAXS/WAXS investigations, RSC Adv. 4 (2014) 56346–56354, https://doi.org/10.1039/c4ra09284h.

[91] S. Huang, S. Jiang, L. An, X. Chen, Crystallization and morphology of poly (ethylene oxide-b-lactide) crystalline–crystalline diblock copolymers, J. Polym. Sci., Part B: Polym. Phys. 46 (2008) 1400–1411, https://doi.org/10.1002/polb.21474.

[92] J. Yang, Y. Liang, J. Luo, C. Zhao, C.C. Han, Multilength scale studies of the confined crystallization in poly(l -lactide)- block -poly(ethylene glycol) copolymer, Macromolecules 45 (2012) 4254–4261, https://doi.org/10.1021/ma202505f.

[93] J.E.K. Schawe, S. Pogatscher, Material characterization by fast scanning calorimetry: practice and applications, in: Fast Scanning Calorim, 2016, pp. 3–80, https://doi.org/10.1007/978-3-319-31329-0_1.

[94] C. Schick, R. Androsch, New insights into polymer crystallization by fast scanning chip calorimetry, in: Fast Scanning Calorim, 2016, pp. 463–535, https://doi.org/10.1007/978-3-319-31329-0_15.

[95] Y. Cui, R. Jin, Y. Zhou, M. Yu, Y. Ling, L.-Q. Wang, Crystallization enhanced thermal-sensitive hydrogels of PCL-PEG-PCL triblock copolymer for 3D printing, Biomed. Mater. 16 (2021), 035006, https://doi.org/10.1088/1748-605X/abc38e.

[96] C.W. Tower, K. Allen, A. Carandang, R.M. Van Horn, Solubility considerations in relative block crystallization and morphology of PEO- *b* -PCL films, Polym. Cryst. 3 (2020), https://doi.org/10.1002/pcr2.10107.

[97] J.M. White, J. Jurczyk, R.M. Van Horn, Physical structure contributions in pH degradation of PEO-b-PCL films, Polym. Degrad. Stabil. 183 (2021), 109468, https://doi.org/10.1016/j.polymdegradstab.2020.109468.

[98] M. Ponjavic, M.S. Nikolic, S. Jeremic, L. Djokic, J. Nikodinovic-Runic, V. R. Cosovic, J. Djonlagic, Influence of short central PEO segment on hydrolytic and enzymatic degradation of triblock PCL copolymers, J. Polym. Environ. 26 (2018) 2346–2359, https://doi.org/10.1007/s10924-017-1130-2.

[99] N. Brigham, C. Nardi, A. Carandang, K. Allen, R.M. Van Horn, Manipulation of crystallization sequence in PEO- *b* -PCL films using solvent interactions, Macromolecules 50 (2017) 8996–9007, https://doi.org/10.1021/acs.macromol.7b02004.

[100] T.H. Le Kim, H. Jun, Y.S. Nam, Importance of crystallinity of anchoring block of semi-solid amphiphilic triblock copolymers in stabilization of silicone nanoemulsions, J. Colloid Interface Sci. 503 (2017) 39–46, https://doi.org/10.1016/j.jcis.2017.04.079.

[101] M. Ponjavic, M.S. Nikolic, S. Jevtic, J. Rogan, S. Stevanovic, J. Djonlagic, Influence of a low content of PEO segment on the thermal, surface and morphological properties of triblock and diblock PCL copolymers, Macromol. Res. 24 (2016) 323–335, https://doi.org/10.1007/s13233-016-4048-y.

[102] F.-F. Xue, X.-S. Chen, L.-J. An, S.S. Funari, S.-C. Jiang, Confined lamella formation in crystalline-crystalline poly(ethylene oxide)-b-poly(ε-caprolactone) diblock copolymers, Chin. J. Polym. Sci. Engl. Ed. 31 (2013) 1260–1270, https://doi.org/10.1007/s10118-013-1325-5.

[103] F. Xue, X. Chen, L. An, S.S. Funari, S. Jiang, Soft nanoconfinement effects on the crystallization behavior of asymmetric poly(ethylene oxide)-block-poly(ε-caprolactone) diblock copolymers, Polym. Int. 61 (2012) 909–917, https://doi.org/10.1002/pi.4158.

[104] J. Sun, C. He, X. Zhuang, X. Jing, X. Chen, The crystallization behavior of poly (ethylene glycol)-poly(ε- caprolactone) diblock copolymers with asymmetric block compositions, J. Polym. Res. 18 (2011) 2161–2168, https://doi.org/10.1007/s10965-011-9626-2.

[105] R.M. Van Horn, J.X. Zheng, H.-J. Sun, M.-S. Hsiao, W.-B. Zhang, X.-H. Dong, J. Xu, E.L. Thomas, B. Lotz, S.Z.D. Cheng, Solution crystallization behavior of crystalline-crystalline diblock copolymers of poly(ethylene oxide)-block-poly (ε-caprolactone), Macromolecules 43 (2010) 6113–6119, https://doi.org/10.1021/ma1010793.

[106] M.L. Arnal, S. Boissé, A.J. Müller, F. Meyer, J.-M. Raquez, P. Dubois, R. E. Prud'Homme, Interplay between poly(ethylene oxide) and poly(l-lactide) blocks during diblock copolymer crystallization, CrystEngComm 18 (2016) 3635–3649, https://doi.org/10.1039/c6ce00330c.

[107] M. Vivas, J. Contreras, F. López-Carrasquero, A.T. Lorenzo, M.L. Arnal, V. Balsamo, A.J. Müller, E. Laredo, H. Schmalz, V. Abetz, Synthesis and characterization of triblock terpolymers with three potentially crystallisable blocks: polyethylene-b-poly(ethylene oxide)-b-poly(ε-caprolactone), Macromol. Symp. 239 (2006) 58–67, https://doi.org/10.1002/masy.200690110.

[108] Z. Wei, F. Yu, G. Chen, C. Qu, P. Wang, W. Zhang, J. Liang, M. Qi, L. Liu, Nonisothermal crystallization and melting behavior of poly(e-caprolactone)- b-poly(ethylene glycol)-b-poly (e-caprolactone) by DSC analysis, J. Appl. Polym. Sci. 114 (2009) 1133–1140, https://doi.org/10.1002/app.30706.

[109] C. He, J. Sun, J. Ma, X. Chen, X. Jing, Composition dependence of the crystallization behavior and morphology of the poly(ethylene oxide)-poly (ε-caprolactone) diblock copolymer, Biomacromolecules 7 (2006) 3482–3489, https://doi.org/10.1021/bm060578m.

[110] W. Zhu, W. Xie, X. Tong, Z. Shen, Amphiphilic biodegradable poly(CL-b-PEG-b-CL) triblock copolymers prepared by novel rare earth complex: synthesis and crystallization properties, Eur. Polym. J. 43 (2007) 3522–3530, https://doi.org/10.1016/j.eurpolymj.2007.04.024.

[111] T. Shiomi, K. Imai, K. Takenaka, H. Takeshita, H. Hayashi, Y. Tezuka, Appearance of double spherulites like concentric circles for poly(ε-caprolactone)-block-poly (ethylene glycol)-block-poly(ε-caprolactone), Polymer 42 (2001) 3233–3239, https://doi.org/10.1016/S0032-3861(00)00597-8.

[112] H. Takeshita, K. Fukumoto, T. Ohnishi, T. Ohkubo, M. Miya, K. Takenaka, T. Shiomi, Formation of lamellar structure by competition in crystallization of both components for crystalline-crystalline block copolymers, Polymer 47 (2006) 8210–8218, https://doi.org/10.1016/j.polymer.2006.09.043.

[113] V. Karava, A. Siamidi, M. Vlachou, E. Christodoulou, A. Zamboulis, D.N. Bikiaris, A. Kyritsis, P.A. Klonos, Block copolymers based on poly(butylene adipate) and poly(l -lactic acid) for biomedical applications: synthesis, structure and thermodynamical studies, Soft Matter 17 (2021) 2439–2453, https://doi.org/10.1039/D0SM02053B.

[114] Y. Shen, J. Zhang, N. Zhao, F. Liu, Z. Li, Preparation of biorenewable poly (γ-butyrolactone)- *b* -poly(l -lactide) diblock copolyesters *via* one-pot sequential metal-free ring-opening polymerization, Polym. Chem. 9 (2018) 2936–2941, https://doi.org/10.1039/C8PY00389K.

[115] Y.-T. Yan, G. Wu, S.-C. Chen, Y.-Z. Wang, Controlled synthesis and closed-loop chemical recycling of biodegradable copolymers with composition-dependent properties, Sci. China Chem. 65 (2022) 943–953, https://doi.org/10.1007/s11426-021-1196-7.

[116] W. Huang, X. Wen, J. Zhou, X. Zhang, Understanding the hydrolysis mechanism on segments and aggregate structures: corrosion-tailored poly (lactic acid) deriving copolymers with δ-valerolactone, Int. J. Biol. Macromol. 222 (2022) 961–971, https://doi.org/10.1016/j.ijbiomac.2022.09.241.

[117] A.J. Müller, J. Albuerne, L. Marquez, J.-M. Raquez, P. Degée, P. Dubois, J. Hobbs, I.W. Hamley, Self-nucleation and crystallization kinetics of double crystalline poly(p-dioxanone)-b-poly(ε-caprolactone) diblock copolymers, Faraday Discuss 128 (2005) 231–252, https://doi.org/10.1039/b403085k.

[118] A.J. Müller, J. Albuerne, L.M. Esteves, L. Marquez, J.-M. Raquez, P. Degée, P. Dubois, S. Collins, I.W. Hamley, Confinement effects on the crystallization kinetics and self-nucleation of double crystalline poly(p-dioxanone)-b-poly (ε-caprolactone) diblock copolymers, Macromol. Symp. (2004) 369–382, https://doi.org/10.1002/masy.200451128.

[119] F. Pooch, M. Sliepen, K.J. Svedström, A. Korpi, F.M. Winnik, H. Tenhu, Inversion of crystallization rates in miscible block copolymers of poly(lactide)- *block* -poly (2-isopropyl-2-oxazoline), Polym. Chem. 9 (2018) 1848–1856, https://doi.org/10.1039/C8PY00198G.

[120] C. Jin, X. Leng, M. Zhang, Y. Wang, Z. Wei, Y. Li, Fully biobased biodegradable poly(l -lactide)- *b* -poly(ethylene brassylate)- *b* -poly(l -lactide) triblock copolymers: synthesis and investigation of relationship between crystallization morphology and thermal properties, Polym. Int. 69 (2020) 363–372, https://doi.org/10.1002/pi.5958.

[121] W. Yan, L. Fang, T. Weigel, M. Behl, K. Kratz, A. Lendlein, The influence of thermal treatment on the morphology in differently prepared films of a oligodepsipeptide based multiblock copolymer: phase Morphology of Oligodepsipeptide Based Copolyesterurethanes, Polym. Adv. Technol. 28 (2017) 1339–1345, https://doi.org/10.1002/pat.3953.

[122] M. Nerantzaki, K.-V. Adam, I. Koliakou, E. Skoufa, A. Avgeropoulos, G. Z. Papageorgiou, D. Bikiaris, Novel Castor oil-derived block copolymers as promising candidates for biological applications: biorelevant and biocompatible, Macromol. Chem. Phys. 218 (2017), 1700305, https://doi.org/10.1002/macp.201700305.

[123] S. Nojima, Y. Higaki, K. Kaetsu, R. Ishige, N. Ohta, H. Masunaga, T. Hirai, K. Kojio, A. Takahara, Effect of molecular mobility of pre-ordered phase on crystallization in microphase-separated lamellar morphology of strongly segregated crystalline-crystalline diblock copolymers, Polymer 116 (2017) 403–411, https://doi.org/10.1016/j.polymer.2017.02.086.

[124] Z. Shi, Y. Wei, C. Zhu, J. Sun, Z. Li, Crystallization-driven two-dimensional nanosheet from hierarchical self-assembly of polypeptoid-based diblock copolymers, Macromolecules 51 (2018) 6344–6351, https://doi.org/10.1021/acs.macromol.8b00986.

[125] G. Wang, M. Jiang, Q. Zhang, R. Wang, X. Qu, G. Zhou, Biobased multiblock copolymers: synthesis, properties and shape memory behavior of poly (hexamethylene 2,5-furandicarboxylate)-b-poly(ethylene glycol), Polym. Degrad. Stabil. 153 (2018) 292–297, https://doi.org/10.1016/j.polymdegradstab.2018.04.034.

[126] Y. Wei, J. Tian, Z. Zhang, C. Zhu, J. Sun, Z. Li, Supramolecular nanosheets assembled from poly(ethylene glycol)- *b* -poly(*N* -(2-phenylethyl)glycine) diblock copolymer containing crystallizable hydrophobic polypeptoid: crystallization driven assembly transition from filaments to nanosheets, Macromolecules 52 (2019) 1546–1556, https://doi.org/10.1021/acs.macromol.8b02230.

[127] Y. Zhang, Q. Zhou, Y. Liu, Controlled synthesis of polymethylene-b-poly(ethylene glycol) as well as its crystallization and self-assembly behavior, Int. J. Polym. Anal. Char. 24 (2019) 412–420, https://doi.org/10.1080/1023666X.2019.1602316.

[128] S. Bistac, M. Brogly, D. Bindel, Crystallinity of amphiphilic PE-b-PEG copolymers, Polymers 14 (2022) 3639, https://doi.org/10.3390/polym14173639.

[129] R.V. Castillo, M.L. Arnal, A.J. Müller, I.W. Hamley, V. Castelletto, H. Schmalz, V. Abetz, Fractionated crystallization and fractionated melting of confined PEO microdomains in PB-b-PEO and PE-b-PEO diblock copolymers, Macromolecules 41 (2008) 879–889, https://doi.org/10.1021/ma0718907.

[130] A. Boschetti-De-Fierro, D. Fierro, J. Albuerne, S.S. Funari, V. Abetz, Thermal monitoring of morphology in triblock terpolymers with crystallizable blocks, J. Polym. Sci., Part B: Polym. Phys. 45 (2007) 3197–3206, https://doi.org/10.1002/polb.21318.

[131] Y. Dou, N. Tian, Z. Ning, N. Jiang, Z. Gan, Facile method for the synthesis of PCL-*b* -PA6- *b* -PCL using amino-terminated PA6 as a macroinitiator and its characterization, Macromolecules 55 (2022) 10090–10099, https://doi.org/10.1021/acs.macromol.2c01662.

[132] W. Fam, J. Mansouri, H. Li, V. Chen, Improving CO 2 separation performance of thin film composite hollow fiber with Pebax®1657/ionic liquid gel membranes, J. Membr. Sci. 537 (2017) 54–68, https://doi.org/10.1016/j.memsci.2017.05.011.

[133] T. Nakaoki, J. Yasui, T. Komaeda, Biosynthesis of P3HBV-b-P3HB-b-P3HBV triblock copolymer by Ralstonia eutropha, J. Polym. Environ. 27 (2019) 2720–2727, https://doi.org/10.1007/s10924-019-01555-3.

[134] L. Shi, W. Hu, Y. He, Y. Ke, G. Wu, M. Xiao, L. Huang, S. Tan, Preparation and characterization of poly(ethylene glycol)-block-Poly(3-hydroxybutyrate-co-3-hydroxyvalerate)-block-Poly(ethylene glycol) triblock copolymers, Macromol. Res. 28 (2020) 310–318, https://doi.org/10.1007/s13233-020-8005-4.

[135] Y. Wang, A. Chung, G.-Q. Chen, Synthesis of medium-chain-length polyhydroxyalkanoate homopolymers, random copolymers, and block copolymers by an engineered strain of *Pseudomonas entomophila*, Adv. Healthc. Mater. 6 (2017), 1601017, https://doi.org/10.1002/adhm.201601017.

[136] J.K. Palacios, H. Zhang, B. Zhang, N. Hadjichristidis, A.J. Müller, Direct identification of three crystalline phases in PEO-b-PCL-b-PLLA triblock terpolymer by in situ hot-stage atomic force microscopy, Polymer 205 (2020), 122863, https://doi.org/10.1016/j.polymer.2020.122863.

[137] E. Matxinandiarena, A. Múgica, M. Zubitur, V. Ladelta, G. Zapsas, D. Cavallo, N. Hadjichristidis, A.J. Müller, Crystallization and morphology of triple crystalline polyethylene-b-poly(ethylene oxide)-b-poly(ε-caprolactone) PE-b-PEO-b-PCL triblock terpolymers, Polymers 13 (2021) 3133, https://doi.org/10.3390/polym13183133.

[138] E. Matxinandiarena, A. Múgica, M. Zubitur, B. Zhang, V. Ladelta, G. Zapsas, N. Hadjichristidis, A.J. Müller, The effect of the cooling rate on the morphology and crystallization of triple crystalline PE -*b*- PEO -*b*- PLLA and PE -*b*- PCL -*b*- PLLA triblock terpolymers, ACS Appl. Polym. Mater. 2 (2020) 4952–4963, https://doi.org/10.1021/acsapm.0c00826.

[139] E. Matxinandiarena, A. Múgica, A. Tercjak, V. Ladelta, G. Zapsas, N. Hadjichristidis, D. Cavallo, A. Flores, A.J. Müller, Sequential crystallization and multicrystalline morphology in PE- *b* -PEO- *b* -PCL- *b* -PLLA tetrablock quarterpolymers, Macromolecules 54 (2021) 7244–7257, https://doi.org/10.1021/acs.macromol.1c01186.

[140] J.K. Palacios, J. Zhao, N. Hadjichristidis, A.J. Müller, How the complex interplay between different blocks determines the isothermal crystallization kinetics of triple-crystalline PEO-b-PCL-b-PLLA triblock terpolymers, Macromolecules 50 (2017) 9683–9695, https://doi.org/10.1021/acs.macromol.7b02148.

[141] J.K. Palacios, A. Tercjak, G. Liu, D. Wang, J. Zhao, N. Hadjichristidis, A.J. Müller, Trilayered morphology of an ABC triple crystalline triblock terpolymer, Macromolecules 50 (2017) 7268–7281, https://doi.org/10.1021/acs.macromol.7b01576.

[142] J.K. Palacios, A. Mugica, M. Zubitur, A. Iturrospe, A. Arbe, G. Liu, D. Wang, J. Zhao, N. Hadjichristidis, A.J. Müller, Sequential crystallization and morphology of triple crystalline biodegradable PEO-b-PCL-b-PLLA triblock terpolymers, RSC Adv. 6 (2016) 4739–4750, https://doi.org/10.1039/c5ra25812j.

[143] V. Ladelta, G. Zapsas, Y. Gnanou, N. Hadjichristidis, A new tricrystalline triblock terpolymer by combining polyhomologation and ring-opening polymerization. synthesis and thermal properties, J. Polym. Sci. Part Polym. Chem. 57 (2019) 2450–2456, https://doi.org/10.1002/pola.29492.

[144] V. Ladelta, G. Zapsas, E. Abou-hamad, Y. Gnanou, N. Hadjichristidis, Tetracrystalline tetrablock quarterpolymers: four different crystallites under the same roof, Angew. Chem. Int. Ed. 58 (2019) 16267–16274, https://doi.org/10.1002/anie.201908688.

[145] J. Zhao, D. Pahovnik, Y. Gnanou, N. Hadjichristidis, Sequential polymerization of ethylene oxide, ε-caprolactone and l-lactide: a one-pot metal-free route to tri- and pentablock terpolymers, Polym. Chem. 5 (2014) 3750–3753, https://doi.org/10.1039/c4py00429a.

[146] N. Hadjichristidis, H. Iatrou, M. Pitsikalis, S. Pispas, A. Avgeropoulos, Linear and non-linear triblock terpolymers. Synthesis, self-assembly in selective solvents and in bulk, Prog. Polym. Sci. Oxf. 30 (2005) 725–782, https://doi.org/10.1016/j.progpolymsci.2005.04.001.

[147] N. Hadjichristidis, M. Pitsikalis, H. Iatrou, Synthesis of block copolymers, Adv. Polym. Sci. 189 (2005) 1–124, https://doi.org/10.1007/12_005.

[148] Y.-W. Chiang, Y.-Y. Hu, J.-N. Li, S.-H. Huang, S.-W. Kuo, Trilayered single crystals with epitaxial growth in poly(ethylene oxide)-block-poly(ε-caprolactone)-block-poly(l-lactide) thin films, Macromolecules 48 (2015) 8526–8533, https://doi.org/10.1021/acs.macromol.5b02042.

[149] P.C. Hiemenz, T.P. Lodge, Polymer Chemistry, second ed., CRC Press, Boca Raton, FL, USA, 2007.

[150] X. Leng, Y. Ren, Z. Wei, Y. Bian, Y. Li, Synthesis of star-comb double crystalline diblock copolymer of poly(ε-caprolactone)- *block* -poly(l -lactide): effect of chain topology on crystallization behavior, Macromol. Chem. Phys. 218 (2017), 1700178, https://doi.org/10.1002/macp.201700178.

[151] H. Tsuji, K. Tamura, Y. Arakawa, A versatile strategy for the synthesis and mechanical property manipulation of networked biodegradable polymeric materials composed of well-defined alternating hard and soft domains, RSC Adv. 9 (2019) 7094–7106, https://doi.org/10.1039/C9RA00255C.

[152] X. Yan, J. Li, T. Ren, Synthesis of well-defined star, star-block, and miktoarm star biodegradable polymers based on PLLA and PCL by one-pot azide–alkyne click reaction, RSC Adv. 8 (2018) 29464–29475, https://doi.org/10.1039/C8RA06262E.

[153] S. Xiang, D.-D. Zhou, L.-D. Feng, X.-C. Bian, G. Li, X.-S. Chen, T.-C. Wang, Influence of chain architectures on crystallization behaviors of PLLA block in PEG/PLLA block copolymers, Chin. J. Polym. Sci. 37 (2019) 258–267, https://doi.org/10.1007/s10118-019-2202-7.

[154] J. Wei, L. Wu, H. Zhu, Y. Li, Z. Wang, Formation of well-organized, concentric-ringed spherulites of four-arm star symmetric PEO- *b* -PCL *via* confined evaporative crystallization, CrystEngComm 22 (2020) 7016–7024, https://doi.org/10.1039/D0CE01183E.

[155] J. Zhang, Q. Zhang, S. Zhou, Y. Liu, W. Huang, Synthesis and characterization of amphiphilic miktoarm star polymers based on sydnone-maleimide double cycloaddition, Polym. Chem. 9 (2018) 203–212, https://doi.org/10.1039/C7PY01476G.

[156] M. Brogly, S. Bistac, C. Delaite, C. Alzina, Influence of semi-crystalline poly(ε -caprolactone) and non-crystalline polylactide blocks on the thermal properties of polydimethylsiloxane-based block copolymers, Polym. Int. 69 (2020) 1105–1112, https://doi.org/10.1002/pi.5964.

[157] N. María, Y. Patil, G. Polymeropoulos, A. Peshkov, V. Rodionov, J. Maiz, N. Hadjichristidis, A.J. Müller, (PVDF)2(PEO)2 miktoarm star copolymers: synthesis and isothermal crystallization leading to exclusive β-phase formation, Eur. Polym. J. 179 (2022), 111506, https://doi.org/10.1016/j.eurpolymj.2022.111506.

[158] C. Nikovia, L. Theodoridis, S. Alexandris, P. Bilalis, N. Hadjichristidis, G. Floudas, M. Pitsikalis, Macromolecular brushes by combination of ring-opening and ring-opening metathesis polymerization. Synthesis, self-assembly, thermodynamics, and dynamics, Macromolecules 51 (2018) 8940–8955, https://doi.org/10.1021/acs.macromol.8b01905.

[159] M. Zhang, J. Gu, X. Zhu, L. Gao, X. Li, X. Yang, Y. Tu, C.Y. Li, Synthesis of poly (butylene terephthalate)- block -poly(ethylene oxide)- block -poly(propylene oxide)- block -poly(ethylene oxide) multiblock terpolymers via a facile PROP method, Polymer 130 (2017) 199–208, https://doi.org/10.1016/j.polymer.2017.10.010.

[160] O. Jeon, S.H. Lee, S.H. Kim, Y.M. Lee, Y.H. Kim, Synthesis and characterization of poly(L-lactide)-poly(ε-caprolactone) multiblock copolymers, Polymer 53 (2012) 3780–3790.

[161] M. Huang, X. Dong, L. Wang, L. Zheng, G. Liu, X. Gao, C. Li, A.J. Müller, D. Wang, Reversible lamellar periodic structures induced by sequential crystallization/melting in PBS- *co* -PCL multiblock copolymer, Macromolecules 51 (2018) 1100–1109, https://doi.org/10.1021/acs.macromol.7b01779.

[162] M. Ponjavic, S. Jevtic, M.S. Nikolic, Multiblock copolymers containing poly (butylene succinate) and poly(ε-caprolactone) blocks: effect of block ratio and length on physical properties and biodegradability, J. Polym. Res. 29 (2022), https://doi.org/10.1007/s10965-022-03144-w.

[163] R. D'Ambrosio, R. Michell, R. Mincheva, R. Hernández, C. Mijangos, P. Dubois, A. Müller, Crystallization and stereocomplexation of PLA-mb-PBS multi-block copolymers, Polymers 10 (2017) 8, https://doi.org/10.3390/polym10010008.

[164] Y. Huang, J. Liu, A. Zhang, T. Zhou, Crystallization behavior of poly (tetramethylene oxide) influenced by the crystallization condition of poly (butylene succinate) in their copolymers, J. Wuhan Univ. Technol.-Materials Sci. Ed. 34 (2019) 496–506, https://doi.org/10.1007/s11595-019-2079-x.

[165] Y. Shang, Z. Jiang, Z. Qiu, Synthesis, thermal and mechanical properties of novel biobased, biodegradable and double crystalline Poly(butylene succinate)-b-Poly (butylene sebacate) multiblock copolymers, Polymer 214 (2021), 123248, https://doi.org/10.1016/j.polymer.2020.123248.

[166] S. Naghavi Sheikholeslami, M. Rafizadeh, F. Afshar Taromi, H. Shirali, Crystallization and photo-curing kinetics of biodegradable poly(butylene succinate- *co* -butylene fumarate) short-segmented block copolyester: poly (butylene succinate- *co* -butylene fumarate) copolymer, Polym. Int. 66 (2017) 289–299, https://doi.org/10.1002/pi.5264.

[167] X.-M. Zhou, W.-J. Xie, Synthesis and characterization of poly(ester ether urethane)s block copolymers based on biodegradable poly(butylene succinate) and Poly(ethylene glycol), Polym. Degrad. Stabil. 140 (2017) 147–155, https://doi.org/10.1016/j.polymdegradstab.2017.04.023.

[168] C.-S. Feng, Y. Chen, J. Shao, G. Li, H.-Q. Hou, The crystallization and melting behaviors of PDLA-b-PBS-b-PDLA triblock copolymers, Chin. J. Polym. Sci. 38 (2020) 298–310, https://doi.org/10.1007/s10118-020-2361-6.

[169] A.J. Müller, R.M. Michell, A.T. Lorenzo, Isothermal crystallization kinetics of polymers, in: Polym. Morphol. Princ. Charact. Process., 2016, pp. 181–203, https://doi.org/10.1002/9781118892756.ch11.

[170] A.T. Lorenzo, M.L. Arnal, J. Albuerne, A.J. Müller, DSC isothermal polymer crystallization kinetics measurements and the use of the Avrami equation to fit the data: guidelines to avoid common problems, Polym. Test. 26 (2007) 222–231, https://doi.org/10.1016/j.polymertesting.2006.10.005.

[171] R.A. Pérez-Camargo, I. Arandia, M. Safari, D. Cavallo, N. Lotti, M. Soccio, A. J. Müller, Crystallization of isodimorphic aliphatic random copolyesters: pseudo-eutectic behavior and double-crystalline materials, Eur. Polym. J. (2018) 233–247, https://doi.org/10.1016/j.eurpolymj.2018.02.037.

[172] B. Wu, X. Zeng, L. Wu, B.-G. Li, Nucleating agent-containing P(LLA-mb-BSA) multi-block copolymers with balanced mechanical properties: article, J. Appl. Polym. Sci. 134 (2017), https://doi.org/10.1002/app.44777.

[173] Y. Cao, P. Zhu, Z. Wang, Y. Zhou, H. Chen, A.J. Müller, D. Wang, X. Dong, Influence of soft block crystallization on microstructural variation of double crystalline poly(ether- *mb* -amide) multiblock copolymers, Polym. Cryst. 1 (2018), https://doi.org/10.1002/pcr2.10012.

[174] I. Flores, A. Basterretxea, A. Etxeberria, A. González, C. Ocando, J.F. Vega, J. Martínez-Salazar, H. Sardon, A.J. Müller, Organocatalyzed polymerization of PET- *mb* -poly(oxyhexane) copolymers and their self-assembly into double crystalline superstructures, Macromolecules 52 (2019) 6834–6848, https://doi.org/10.1021/acs.macromol.9b01110.

[175] C. Zhang, R.A. Pérez-Camargo, L. Zheng, Y. Zhao, G. Liu, L. Wang, D. Wang, Crystallization of poly(hexamethylene carbonate)-co-poly(hexamethylene urethane) segmental block copolymers: from single to double crystalline phases, Polymer 222 (2021), 123675, https://doi.org/10.1016/j.polymer.2021.123675.

[176] L. Wang, X. Dong, P. Zhu, X. Zhang, X. Liu, D. Wang, High elasticity and corresponding microstructure origin of novel long chain poly(amide-block-ether) filament fibers, Eur. Polym. J. 90 (2017) 171–182, https://doi.org/10.1016/j.eurpolymj.2017.02.047.

[177] Y. Baimark, W. Rungseesantivanon, N. Prakymoramas, Improvement in melt flow property and flexibility of poly(l-lactide)-b-poly(ethylene glycol)-b-poly(l-lactide) by chain extension reaction for potential use as flexible bioplastics, Mater. Des. 154 (2018) 73–80, https://doi.org/10.1016/j.matdes.2018.05.028.

[178] M.P. Arrieta, L. Peponi, Polyurethane based on PLA and PCL incorporated with catechin: structural, thermal and mechanical characterization, Eur. Polym. J. 89 (2017) 174–184, https://doi.org/10.1016/j.eurpolymj.2017.02.028.

[179] F. Noormohammadi, M. Nourany, G. Mir Mohamad Sadeghi, P.-Y. Wang, H. Shahsavarani, The role of cellulose nanowhiskers in controlling phase segregation, crystallization and thermal stimuli responsiveness in PCL-PEGx-PCL block copolymer-based PU for human tissue engineering applications, Carbohydr. Polym. 252 (2021), 117219, https://doi.org/10.1016/j.carbpol.2020.117219.

[180] M. Ochoa, N. Collazos, T. Le, R. Subramaniam, M. Sanders, R.P. Singh, D. Depan, Nanocellulose-PE-b-PEG copolymer nanohybrid shish-kebab structure via interfacial crystallization, Carbohydr. Polym. 159 (2017) 116–124, https://doi.org/10.1016/j.carbpol.2016.12.028.

[181] T. Le, R. Subramanian, O. Ajala, P. Pellegrin, D. Depan, The mobility of PEG chains versus micellar stability towards the formation of PE-b-PEG nanohybrid

shish-kebab on carbon nanotubes, Polym. Adv. Technol. 30 (2019) 1796–1806, https://doi.org/10.1002/pat.4612.
[182] X. Zhang, P. Dang, B. Deng, X. Xia, K. Wang, Y. Li, T. Xia, Controlled crystallization of diblock copolymers on carbon materials: effect of block length, Appl. Surf. Sci. 583 (2022), 152487, https://doi.org/10.1016/j.apsusc.2022.152487.
[183] S. Xia, Y. Shen, Y. Zhou, P. Yao, Q. Liu, B. Deng, Biodegradable multiblock copolymers containing poly[(3-hydroxybutyrate)-co-(3-hydroxyvalerate)], poly (ε-caprolactone), and polyhedral oligomeric silsesquioxane: synthesis, characterization, and tensile property, Colloid Polym. Sci. 296 (2018) 1667–1677, https://doi.org/10.1007/s00396-018-4389-5.
[184] G. Yin, X. Yang, Q. Li, Influences of terminal POSS on crystallization and degradation behavior of PCL-PLLA block copolymer, Polym. Cryst. 1 (2018), https://doi.org/10.1002/pcr2.10019.
[185] L.C.E. da Silva, T.S. Plivelic, M. do Carmo Gonçalves, Morphological investigation of ternary and semicrystalline organic–inorganic hybrid nanocomposite, J. Mater. Sci. 57 (2022) 6196–6211, https://doi.org/10.1007/s10853-022-07003-3.
[186] Z. Jing, X. Shi, G. Zhang, J. Gu, Synthesis and properties of poly(lactide)/poly (ε-caprolactone) multiblock supramolecular polymers bonded by the self-complementary quadruple hydrogen bonding, Polymer 121 (2017) 124–136, https://doi.org/10.1016/j.polymer.2017.06.019.
[187] X. Shi, Z. Jing, G. Zhang, Y. Xu, Y. Yao, Fully bio-based poly(ε-capolactone)/poly (lactide) alternating multiblock supramolecular polymers: synthesis, crystallization behavior, and properties: article, J. Appl. Polym. Sci. 134 (2017), 45575, https://doi.org/10.1002/app.45575.
[188] Z. Jing, J. Li, W. Xiao, H. Xu, P. Hong, Y. Li, Crystallization, rheology and mechanical properties of the blends of poly(l -lactide) with supramolecular polymers based on poly(d -lactide)–poly(ε-caprolactone- *co* -δ-valerolactone)–poly(d -lactide) triblock copolymers, RSC Adv. 9 (2019) 26067–26079, https://doi.org/10.1039/C9RA04283K.
[189] X. Li, W. Xu, W. Yuan, K. Liu, J. Zhou, G. Shan, Y. Bao, P. Pan, Separate crystallization and melting of polymer blocks and hydrogen bonding units in double-crystalline supramolecular polymers, Polymer 222 (2021), 123670, https://doi.org/10.1016/j.polymer.2021.123670.
[190] Z. Jing, X. Huang, X. Liu, M. Liao, Y. Li, Poly(lactide)-based supramolecular polymers driven by self-complementary quadruple hydrogen bonds: construction, crystallization and mechanical properties, Polym. Int. 72 (2023) 39–53, https://doi.org/10.1002/pi.6445.
[191] H. Wu, Y. Higaki, A. Takahara, Molecular self-assembly of one-dimensional polymer nanostructures in nanopores of anodic alumina oxide templates, Prog. Polym. Sci. 77 (2018) 95–117, https://doi.org/10.1016/j.progpolymsci.2017.10.004.
[192] G. Liu, A.J. Müller, D. Wang, Confined crystallization of polymers within nanopores, Acc. Chem. Res. (2021) 3028–3038, https://doi.org/10.1021/acs.accounts.1c00242.